1990

Tubular roof bit design, and evaluation of roof drag-bits

Zhichun (Trent) She
University of Wollongong

TUBULAR ROOF BIT DESIGN, & EVALUATION OF ROOF DRAG-BITS

A thesis submitted in fulfilment of the requirements
for the award of the degree of

MASTER OF ENGINEERING (Honours)

from

THE UNIVERSITY OF WOLLONGONG

by

ZHICHUN (TRENT) SHE
BE, MAUSIMM, GRADUATE MIEAUST

DEPARTMENT OF CIVIL AND
MINING ENGINEERING
1990

Acknowledgements

The author wishes to express his sincere gratitude to his supervisor, Professor L.C. Schmidt for his invaluable guidance and continuous encouragement during the course of this investigation. Especially, his constructive criticisms and fruitful discussions during the writing of the thesis are greatly appreciated.

The support provided by Dr. P.N. Standish during the various stages of this work are also acknowledged sincerely by the author. The current work by the author is a contribution to the Rapid Face Bolting Program carried out in the Department of Civil and Mining Engineering at the University of Wollongong. This work was carried out while assisting Dr. P.N. Standish as part of the team working on the Rapid Face Bolting Project.

He wishes to thank Associate Professor R.W. Upfold and Dr. E.Y. Baafi for their stimulating advice.

A word of gratitude is also extended to all the technicians of the Department of Civil and Mining Engineering, in particular Mr. A. Grant for assistance in the laboratory work.

The author also wishes to acknowledge Mr. A.B. Yu and Mr. D.W. Xu for their suggestions and discussions.

The author is indebted to all members of his family, special acknowledgement being due to his parents and his wife for the constant support and encouragement throughout all the years, and to his dear son for the fun and happiness he brought to the rather long period of the study.

Finally, the author would like to extend his appreciation to all those who are not named here, but have contributed to the completion of this thesis.

Declaration

I hereby declare that the work presented in this thesis was carried out by me in the Department of Civil and Mining Engineering, the University of Wollongong, unless specified otherwise in the text, and that any part of it has not been submitted to any other university or institution for a degree.

.....

ZHICHUN (TRENT) SHE

Abstract

The method of supporting excavated roof in coal mines by conventional roof bolting systems is challenged due to its shortcomings of the time-consuming installation and the increased number of accidents attributable to the work under unsupported roofs. Though a few alternatives have been considered, the ultimate and most efficient bolting method has often been conceived as the one called a self-drilling roof bolt, or a Rapid Face Bolting System. The on-going Rapid Face Bolting project undertaken by the University of Wollongong includes a special drilling bit design, and the principal design considerations for this tubular roof bit are high efficiency and low cost. Through review of the physical properties of different cutting materials, considering the special needs of the project and establishing a series of special criteria for a tubular roof bit design, two kinds of tubular roof bolts are proposed to suit hard and soft rock formations, respectively.

Most of the currently used drag-bits for bolthole drilling are different versions of the drag-bit recommended by Fish et al. in 1956, and their configurations, especially the cutting tips, substantially have remained unchanged since they first were proposed. The cutting tip has an obtuse angle in its front face, which introduces an sharp point on its cutting edge. The result of the finite element analysis shows that the top point possesses a much greater stress concentration than any other parts of the tip, and is in a very adverse condition when load is imposed on the bit. The stress at the top point of the tip exceeds the critical stress even under

the load applied in normal drilling conditions, and this part of the tip is likely to fail. With the increase of the loads, modelling severe drilling conditions, the area with the stress reaching the critical stress is expanded, which implies that the failure region would be extended.

An extensive series of experiments, which model the process of underground bolthole drilling, has been conducted in the laboratory. The operating parameters and the specific energy have been generated as the outcome of the test with the aid of a Keithley Data Acquisition System connected to the drilling operation unit. The experimental results are in general agreement with the outcome of the finite element analysis. The results show that the performance of a bit is determined by the condition of the cutting tips of the bit, which is reflected in the values of the specific energy generally. By linear regression analysis on the size distribution of the cuttings, a simple empirical method to predict the drag-bit performance is also proposed.

Table of Contents

List of Figures

List of Tables

Notation

α	Rear angle of a drill bit.
β	Rake angle of a drill bit.
δ	Cutting angle of a drill bit.
e_r	Rotary component of specific energy.
e_t	Thrust component of specific energy.
E_{50}	Tangent modulus at 50% ultimate compressive strength.
E_i	Initial tangent modulus at zero load.
E_s	Secant Modulus for a particular point (Chapter Four).
E_s	Specific energy (Chapter Six).
E_t	Tangent modulus at a particular point on the stress -strain diagram for a specified stess.
γ	Tool angle.
h_0	Cutting depth of a bit.
h_1	Height desired to allow cuttings and drilling fluid to pass.
H	Bottom exposure of a drill bit.
M_R	Rock modulus ratio.
P_x	Thrust force.

P_y	Rotary force.
r	correlation coefficient.
SS_x	Sum of squares for deviations of x_i from X_m.
SS_{xy}	Sum of products of deviations of x_i and y_i from X_m and Y_m respectively.
SSR	Sum of squares for regression.
$\sigma_1, \sigma_2, \sigma_3$	Principal normal stresses.
σ_{max}	Maximum principal normal stress.
σ_{min}	Minimum principal normal stress.
σ_{ult}	Uniaxial ultimate compressive strength.
x_i	Mean cutting size of sample i.
X_m	Mean of all x_i.
y_i	Percentage of cutting size of sample i.
Y_m	Mean of all y_i.

Chapter One

Introduction

1.1 General Remarks

During the last few decades, the use of rockbolts for reinforcing and stabilizing mine roofs has been increasing steadily. Today rockbolting has become a primary support system and is recognized to be so in the mining industry, especially, in coal mines. Nearly all of the underground coal mines are mined under bolted roofs in the United States (Peng, 1986) and other major coal-producing western countries. During this period, the use of rockbolts has resulted in a great reduction in the number of fatal and non-fatal accidents in coal mines (Smelser et al., 1982). Moreover, productivity has been increased, cost decreased, and ventilation improved under the bolted mine roof which provides an unobstructed opening with minimum maintenance. Rockbolting stands out as the most effective and the most economical technique among the various methods of rock reinforcements (Hoek, 1982 and Bieniawski, 1987).

Despite its widespread usage and continuous development, there still remains disadvantages in the currently used rockbolting systems, especially in the installation procedures of the rockbolts, which need to be overcome to improve safety and productivity.

In currently used rockbolting systems, the installation procedures require that a drill rod be withdrawn after the completion of a bolthole, and then a rockbolt be inserted into the hole. These operations expose the operator to the unsupported roof for a fairly long period, as well as prolong the dead time during bolt installation. It is believed that if the installation procedures are properly modified, both safety and productivity of rockbolting systems can be greatly improved.

However, what are called self-drilling rockbolts have always been conceived as the ultimate and most efficient bolting method, in which the bolt drills its own hole and remains in the rock once the hole is drilled. Consequently, the operation of extracting the drill rod and inserting the bolt is eliminated from the process of installation of self-drilling rockbolts.

Robertson et al. (1986) envisage that the successful development of self-drilling bolts would have to include low cost drill bits for one hole only, and the bolt itself as well as the method and the equipment for installation would need to be low in cost.

The University of Wollongong started developing a Rapid Face Bolting System in 1986 so as to improve the excavation rate of continuous miners and the safety of working conditions. The so-called Rapid Face Bolting System virtually is a self-drilling bolting system using a 'single-pass' bolt for rockbolt installation in underground coal mines.

1.2 Objectives of Study

The main theme of this thesis is to design a special kind of tube bit, and to evaluate the widely used roof drag-bit.

The tube bit designed for the Rapid Face Bolting System is a one-hole-only bit used to drill a bolthole to accommodate a 'single-pass' bolt, and is not retrievable after the completion of the hole. Different from that of the coring bit employed in geological site investigations, the principal design considerations for the tubular roof bit are high efficiency and low cost.

Aimed at the low cost consideration, the material choice of the cutting tips for the special tubular roof bits is based on reviewing the drilling requirement for the bit and the physical properties of different cutting materials, especially the hardness of the materials. A series of special criteria for a tubular roof bit design has been established to guide the design of the bits used in this particular circumstance. Eventually, two kinds of single-pass tubular roof bits are proposed to suit hard and soft rock formations respectively.

Most of the currently used drag-bits for the bolthole drilling are different versions of the drag-bit recommended by Fish et al. in 1956, and their configurations, especially the cutting tips, substantially remain unchanged since they were proposed. Some bits are subject to severe damage on their cutting tips even immediately after starting drilling in certain circumstance due to the aggressive sharp front point of the cutting tips. It seems that there may be alternative shapes of the cutting tips which may be able to provide better performance than the existing

cutting tips under certain operating conditions . To verify this point of view, it is necessary to evaluate the currently used drag-bit. It is also required to catalogue the drag-bits with different specifications for different usages according to their performance (Cutifani, 1983). For instance, the drag-bits used for conventional bolthole drilling may require a constant penetration rate with a reasonably long life, whereas the drag bits employed for single-pass bolthole drilling may require a penetration rate as high as possible without much concern for the bit life. Different configurations of cutting tips can be suggested to suit different drilling environments, and efficiently to fulfil all types of drilling targets.

To describe the drag-bit wear feature, a three dimensional (3D) finite element method is applied to analyse the stress condition at the cutting tip of a drag-bit. By introducing a 3D finite element analysis package, STRAND5, the full tip of a drag-bit is modelled, and three load patterns, representing three kinds of drilling conditions, are applied. It is revealed through the computations that a severe stress concentration exists along the front cutting edge with a peak value at the top point. Even under the load applied under normal drilling conditions, the top point of the tip is likely to fail. The failure region extends from that point with the increase of the load applied on the tip.

An extensive series of experiments, which model the process of underground bolthole drilling, has been conducted at the laboratory. The operating parameters and the specific energy have been generated as the outcome of the test with the aid of a Keithley Data Acquisition System connected to the drilling operation unit. In addition, by linear regression analysis on the size distribution of

the cuttings, a simple empirical method to predict the drag-bit performance is proposed.

Chapter Two

Rockbolting and the Rapid Face Bolting System

2.1 Strata Control and Rockbolting

Effective strata control means attaining stability of underground openings in rock masses, and therefore leads to successful mining engineering. For example, unless the excavations are stable, access to a mine cannot be gained, and mining production will be impossible. In this context, the importance of strata control becomes obvious when one considers the importance of mining in mineral and energy development. The interaction of mining with other branches of mineral engineering is depicted in Fig. 2.1 (Bieniawske, 1987).

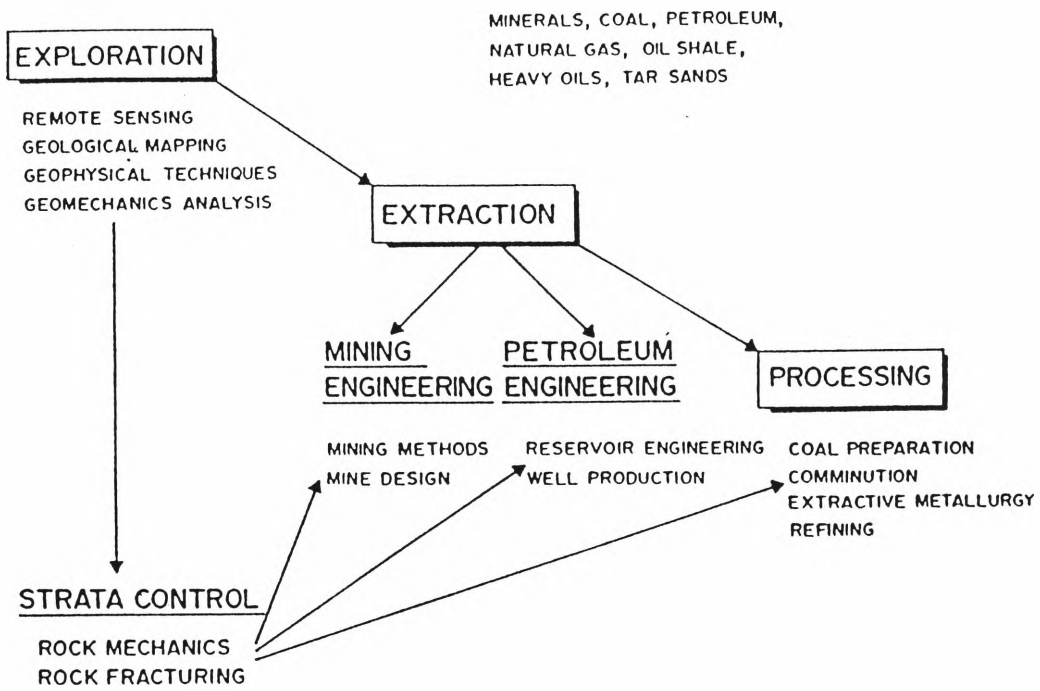

Fig. 2.1 The Scope of Mineral Engineering

Strata control is a fundamental aspect of mining engineering, being concerned with controlling the movement of the underground openings such as are found in mineral, tunnel, or petroleum operations. Without effective strata control, mineral and fuel production is impossible within the bounds of economic reality.

Strata control is the science that studies the behaviour of rock mass in transition from one state of equilibrium to another. It provides a basis for the design of support systems to prevent or control the collapse or failure of a roof, floor, and ribs both safely and economically. In essence, strata control means maintaining rock mass stability. This control is an engineering field of specialty which is important because the design of underground excavations is, to a large extent, the design of underground support systems, that is, rock reinforcement.

These systems may range from no support, in the case of temporary mining excavations, in good rock to heavy support, needed for large permanent underground excavations, in less competent rock strata. Note that in coal mining, strata control is often termed 'ground control' and involves the selection of roof support, pillar sizing, and prevention of floor heave. In hard rock (metal) mining, strata control is concerned with rockburst control, drift stability and stope support.

The design of strata control systems in mines is a basic requirement for the mining engineer; it is the first step toward effective roof control (Gale and Fabjanczyk, 1986).

While there are many methods of external roof supports with steel, timber, or concrete, the external roof support is aimed at controlling the immediate zone around an opening, and does little to improve overall ground stability. For example, steel sets or shotcrete support systems, which do not form part of the rock mass, restrict movements of the rock mass and support it externally. On the other hand, internal roof support systems, using rockbolts, actually form part of the rock mass, and reinforce and mobilize the inherent strength of the rock mass.

Among the various methods of rock reinforcement, rock bolting stands out as the most effective technique. Rockbolts can be promptly installed after blasting and mucking, that is very important from a rock mechanics point of view. In addition, rockbolts can easily be combined with other support systems such as wire mesh, shotcrete or concrete lining, that are frequently required by local rock mass conditions. In the last four decades, internal roof reinforcement by rockbolting has improved to such a degree that it has become an almost universal

control method against ground movement, and for the prevention of rockfalls in mine excavations.

2.2 Roof Support by Rockbolting

The history of rockbolting dates from the end of 19th century. However, roof-bolts were not used extensively until forty to fifty years later. Since then, the use of rockbolts in mining as well as in underground excavations for civil engineering applications has become world-wide, and hundreds of millions of bolts are installed annually (Stillbory, 1986). In 1951, BHP Co. Ltd. began introducing rockbolts into its mines in NSW, Australia (Hii, 1985).

The United States are credited with pioneering the use of rockbolts in underground excavations as early as 1930. Although the first use of rockbolts is lost in antiquity, it was not until 1943 that their systematic use on a planned basis was described by Weigel in the Engineering and Mining Journal. He described a system introduced by the St. Joseph Lead Company in 1936 in Missouri (Panek 1973). Rockbolting first became popular in 1947 in the United States where it was promoted by the US Bureau of Mines in an attempt to reduce the number of accidents caused by roof falls. In less than two years, it had come into general use in the US mining industry. In 1949, the method was in use at over 200 mines and by 1952 annual consumption had reached 25 million bolts. In recent years, the range of application of rockbolts has widened due to advances in rock mechanics and the increasing use of rock reinforcement in underground excavations as an

alternative to more traditional forms of support. Also, the development of new rockbolt concepts has led to the use of roof-bolts in non-traditional applications.

Growth of rockbolting was rapid. In 1968, the US bureau of Mines reported that 912 coal mines used 55 million rockbolts annually and 60% of underground coal production was mined under bolted roofs. By 1984, over 90% of American underground coal production was mined under bolted roofs (Bieniawski, 1987). The consumption of rockbolts in USA was increased to over 100 million per year in 1985 from 75 million in 1982 (Scott, 1983; Singh et al., 1984; Peng, 1986) with an incremental ratio of over 10% per annum. According to Daws (1987), there are similar tendencies towards the use of roof-bolts in Australia, South Africa, Canada and other major coal-producing countries.

Roof-bolting is not suitable for all strata conditions, but where it can be applied, a cheap and effective support is provided. Moreover, as the bolted mine roof can provide an unobstructed opening with minimum maintenance, productivity has been increased, and ventilation improved. Rockbolting has thus been accepted as the most effective but also a relatively cheap method of support.

Rockbolting also has the advantage that it reduces storage and handling requirements, decreases the size of the openings that must be excavated to achieve a given clearance, provides greater freedom of movement for trackless vehicles without risk of dislodging supports, and offers negligible maintenance of installed supports.

Rockbolts are the most commonly used system for rock mass stabilization, particularly in the coal mining industry. In summary, the main reasons for the widespread use of rockbolt reinforcement systems are as follows:

1) prompt installation, improving safety
2) versatile, being able to be used in any excavation geometry,
3) usually simple to install,
4) low resistance to air flow, improving ventilation,
5) no posts, girders and the other obstructions, free passage way,
6) less influenced by the shock waves of explosives,
7) relatively inexpensive, and
8) installation can be fully mechanized.

2.2.1 Rockbolting theory and mechanisms

Rock reinforcement must utilize the structural properties of the rock mass to improve the stability of underground excavations. The principal objective in the design of underground support is to help the rock mass support itself. This concept applies to all rock reinforcement systems.

The behaviour of an opening and the performance of the support system depend upon the load-deformation characteristics of the rock and of the support, as well as on the manner and timing of the support installation. The interaction between the support and the rock mass is qualitatively illustrated by the the ground reaction curve (refer to Fig. 2.2), which was developed in detail by

Deere et al. (1970) but was discussed by R. Fenner in Austria as early as 1938. Most recently, the concept was studied by Brown et al. (1983).

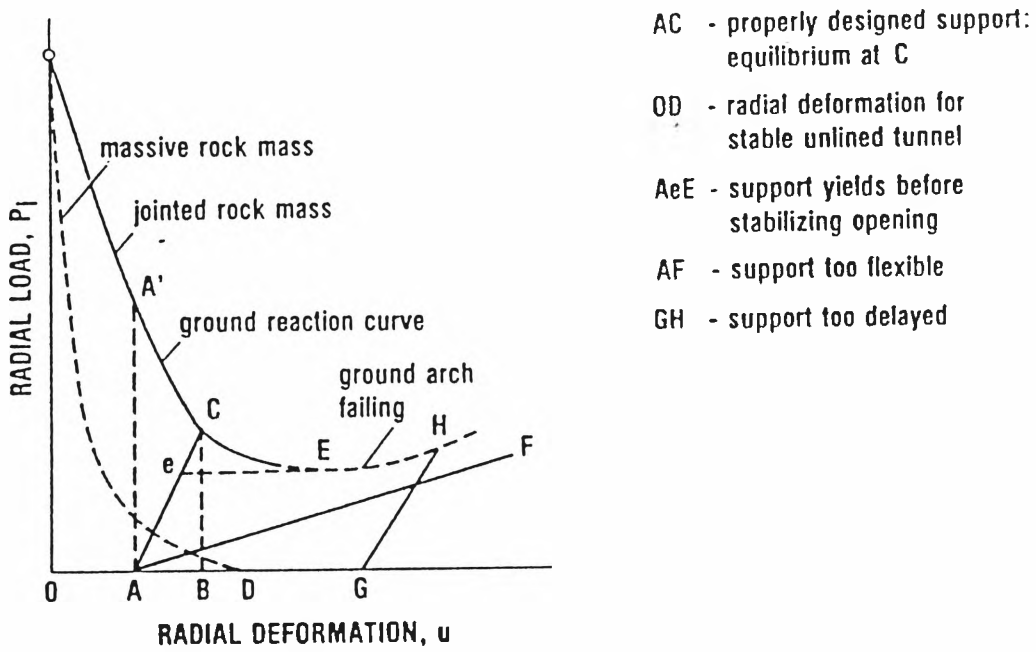

Fig. 2.2 Concept of Ground Reaction Curve for Rock Tunnels

Bieniawski (1987) explained the ground reaction curve in details as follows:

When a tunnel is excavated, the rock moves inwards. The ground reaction curve displays the load that must be applied to the roof or the walls of the tunnel to prevent further movement. If the support were perfectly incompressible, the load of the support would be represented by the ling AA'. Support, however, deforms and, with the walls of the tunnel also deforming, an equilibrium is attained

at point C at a radial displacement of the walls equal to OB and a support deformation equal to AB, at which stage the support load is BC.

However, the equilibrium at point C is only reached if the support is properly designed and placed timely. Line AeE in Fig. 2.2 depicts support which yields before stabilizing the opening, line AF represents support which is too flexible, while line GH is support too delayed in installation, hence ineffective. Accordingly, it is important to note that support should be installed as soon as possible so that the early rock-deformation could stress the support at the same time as the rock mass is generating the arching movement and shear stress in an attempt to be self-supporting. Furthermore, the less competent the rock, the earlier the support should be installed. Thus, active rock reinforcement will be more effective and will require less capacity than passive support but installation must take place as soon as possible after each face advance. Active rock reinforcement will require less support because the ability of the rock to support itself is being utilized while with passive support the full weight of the rock is being supported.

Although the concept of the ground reaction curve has been studied extensively by Deere et al. (1970), Rabcewicz (1964), Pacher (1977), and by Brown et al.(1983), the ground reaction curve cannot as yet be theoretically defined for rock masses, though some attempts have been made (Detourney & Vardoulakis 1985). Furthermore, even if the theory could be used to predict the curve, Deere believes that the large local variations in construction procedures would inhibit the usefulness of the curve for the practical design of supports, not to mention that the load-deformation characteristics of some supports are also not clearly understood. The only possibility of of obtaining quantitative data on the required support

resistance and ground deformation behaviour lies in measurements in-situ. From measurements of the radial displacement of excavation surfaces and of the displacement inside the rock mass as a function of time during mining, the stabilization process as well as the loading of the support can be established (Bieniawski 1984).

The mechanics of rock reinforcement by rockbolting includes the concept of rock-support interaction as the main principle. The design of rock reinforcement systems with rockbolts depends on the geotechnical properties of the discontinuities and of the intact rock, the size and shape of the excavations, the magnitudes of redistributed stresses and the degree of deformation acceptable in the completed excavation. The mechanisms of rock reinforcement by tensioned rockbolts and by untensioned rockbolts are different.

1. Mechanisms of the Tensioned Point-anchored Rockbolt

The main function of the tensioned rockbolt is to bind together a discontinuous rock mass, such as a sedimentary rock which is made up of a series of bedding planes, or a rock containing natural joints and fractures, or the outer layer of blasted rock around an opening excavated with explosives.

It is established that there are tension zones in a roof, especially at the 'entries' of underground mines. The roofs in these entries act like beams supported on both sides with layers separated from each other. The designer of the roadway supports must take the weight of such separated beds (immediate roof) into consideration (Biron etc., 1983).

Suppose there are two separated roof layers, one of which can split on the other under bending stress, with thicknesses of $\mathbf{h}_1$ and $\mathbf{h}_2$, and widths of **b** as shown in Fig. 2.3 (Biron et al., 1980). If the span of the opening is **l** and the uniform load per unit length is **q**, there will be a maximum bending stress σ in the extreme fibre in the middle of the span (refer to Fig. 2.3a) as follows:

$$\sigma = 0.75 \frac{\mathbf{ql}^2}{\mathbf{bh}_1^2 + \mathbf{bh}_2^2} \qquad \mathbf{2.1}$$

where $\mathbf{h}_1$ the thickness of the lower roof layer,

$\mathbf{h}_2$ the thickness of the upper roof layer.

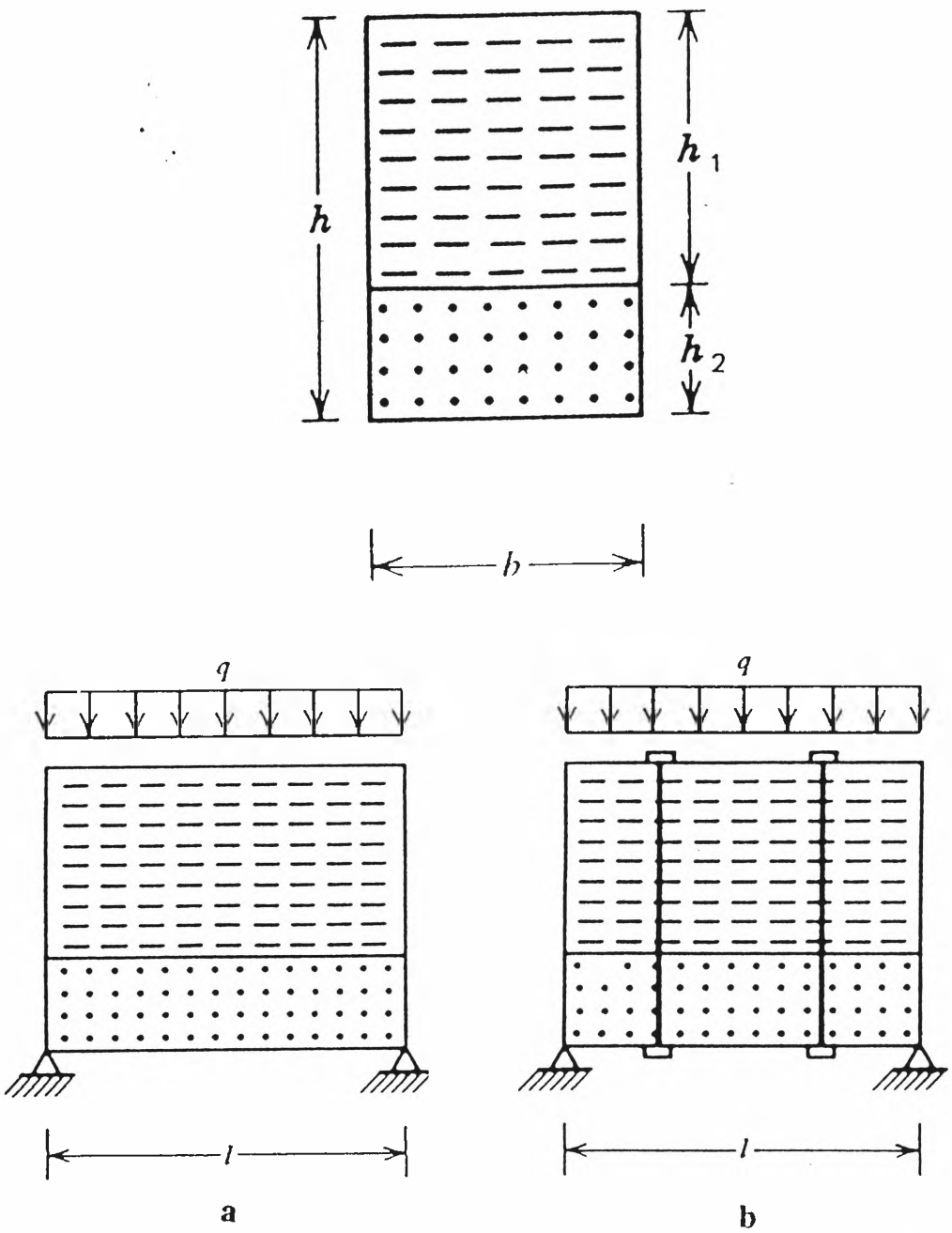

Fig. 2.3 Principle of Tensioned Point-anchored Rockbolt

If these two layers were tied together by means of bolts so as to prevent interfacial slip (refer to Fig. 2.3b), the bending stress σ' in the extreme fibre in the middle of the span would be:

$$\sigma' = 0.75 \frac{ql^2}{b(h_1 + h_2)^2} \qquad 2.2$$

It can be seen that the value of σ' is much less than σ. If

$h_1 = h_2 = h_0$, the ratio of two cases is as follows:

$$\frac{\sigma}{\sigma'} = \frac{0.75(ql^2/2bh_0^2)}{0.75[ql^2/b(2h_0^2)^2]} = 2 \qquad 2.3$$

Therefore, by binding the two layers, the bending stress can be reduced to half in this case. Moreover, the tensile stress in the roof can be carried by the 'steel' rods which are resistant to tensile stresses. The binding of the layers can be effected as soon as the roadway is opened,without much bed separation.

The other mechanisms by which tensioned rockbolt reinforce the mine roof include the suspension effect (Obert et al, 1967; Panek 1961, 1962 & 1964), arching action (Cox, 1974) and the keying effect (Karabin et al., 1976).

2. Mechanisms of the Untensioned Grouted Rockbolt

The untensioned grouted resin bolts reinforce the mine roof in a different manner from that for the tensioned mechanical anchored bolts. Because they are not tensioned during installation, they usually offer a passive support in that they first take up the load when the roof strata begin to deform.

As a fully grouted resin bolt provides complete bonding between the steel bolt, resin and the hole wall for the full length of the bolt, the frictional or

shear resistance is the major mechanism for preventing strata separation. Because the bore hole is completely filled with resin and contains a steel bar, the lateral movement of the roof strata or strata slippage is minimized. The major mechanisms by which fully grouted resin bolts reinforce the mine roof are frictional resistance (Karabin etc, 1976) and strata rigidity (Peng etc, 1985) produced by the full-length bonding between bolt, resin and the hole wall.

In summary, despite a large amount of research carried out to investigate the theories of rockbolting and the widespread usage of rockbolts, the real mechanisms by which the rockbolts reinforce the immediate roof of an underground mine entry are still relatively unknown. The mechanisms by which rockbolts reinforce the mine roof can be classified into six types: the suspension effect, the beam-building effect, the frictional resistance effect, the strata rigidity effect, the arching action, and the keying effect. The common practice of rockbolting is largely based on some empirical rules (Peng,1986).

2.2.2 Overview of typical rockbolting systems

A large number of different rockbolts are now used world-wide. Many rockbolt types show only minor differences in their design and are basically varieties of the same concept. In general, there are two major types of roof bolts commonly used in underground mines. One is the tensioned point anchored bolt and the other is the nontensioned full-length anchored bolt. The point-anchored bolt, ususally known as a mechanical bolt, is a tensioned bolt anchored at its extreme end with a mechanical device. The bearing plate inserted between the bolt

head and the roofline at the mouth of the borehole serves as the other anchor point. In the full-length-anchored bolt, the annulus between the holt and the hole wall is grouted with resin or cement throughout the full length of the hole while no tension is applied during installation. In addition to these two major types of bolts, the other types of rockbolts used are principally the friction anchored bolts.

It is estimated that the most popular type is the mechanical anchored bolt which is used in about 60% followed by the grouted bolt used for 30% of installations. The remaining 10% includes other methods of rockbolting, mainly the friction stabilizer (Bieniawski, 1987). Following is an overview of typical rockbolt systems, in which only the most widely used rockbolt type from each group will be highlighted as the group representative.

1. Mechanical Point-anchored Bolts

Although there are various types of mechanical bolts, all of them generally consist of three common elements (refer to Fig. 2.4, Lang et al., 1979):

1) a solid steel bar or shank,
2) an anchoring device at the top end of the bar, and
3) a tensioning device at the lower end of the bar.

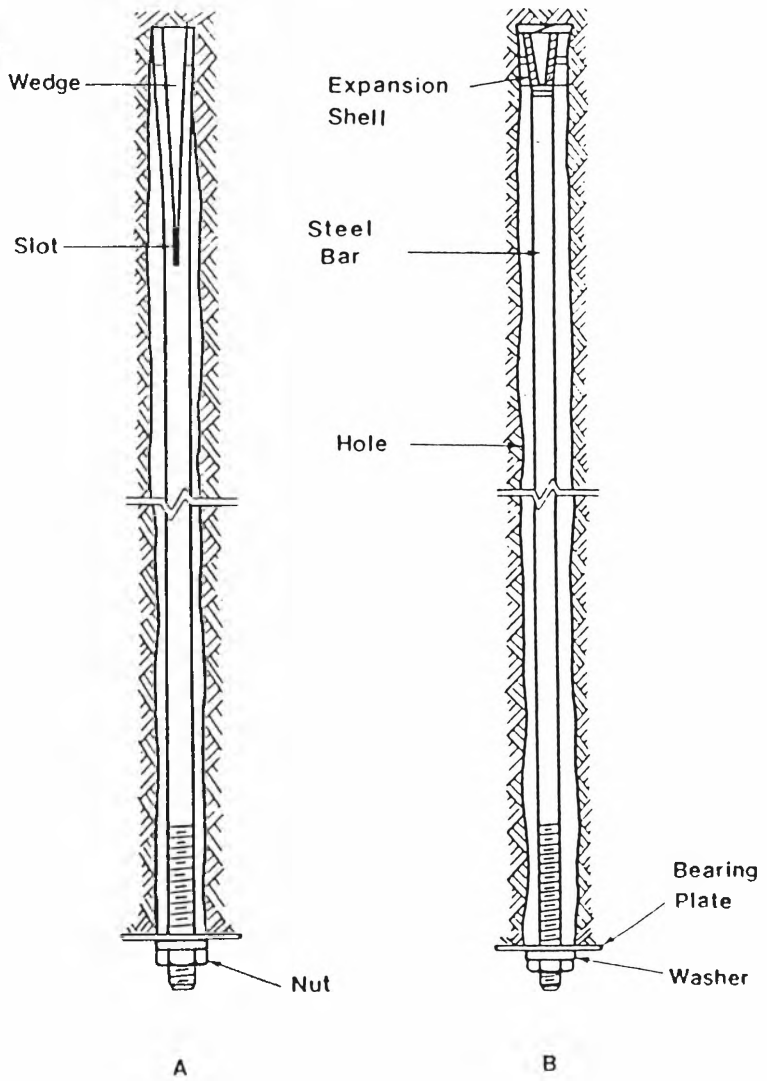

Fig. 2.4 Typical Mechanical Rockbolts.

A, slot-wedge bolt B, expansion shell bolt

The mechanical-anchored bolt operates basically in this manner, so that a wedge attached to the bolt shank is driven into a conical expansion shell or a slot at the top end of the bolt. This action forces it to expand against and into the wall of the borehole.

The procedure of installing the expansion-shell point-anchored bolt is generalized by Peng (1986) as follows:

1) drill the hole to the desired length,
2) insert the bolt with the washer (if any), bearing plate, and expansion shell facility assembled in that order,
3) rotate the bolt by the hydraulic-driven motor,
4) pull down the plug to anchor the bolt, and
5) tighten the nut to build up tension in the bolt.

The advantages of the mechanical point-anchored bolt are:

1) relatively inexpensive,
2) immediate support action after installation,
3) able to serve as permanent reinforcement by post-grouting,
4) high bolt loads available in hard rock, and
5) versatile for rock reinforcement, assuming hard rock conditions.

2. Grouted Bolts

A schematic view of grouted bolts is given in Fig. 2.5 (Biron, 1983), where grout is put into part or the full length of the hole. A tap is used to stop the grout from running down. Fine plastic tubing is placed to drain the air while inserting the deformed steel rod. After the grout sets, it has high adherence and keeps the bolt in place. Cement or resin are used as grouting agents. Rebar or threaded bar are usually used as the bolt bodies. The rebar used with resin creates a system commonly used for tensioned rockbolts, while rebar or threaded bar with cement grout is usually used for untensioned bolts.

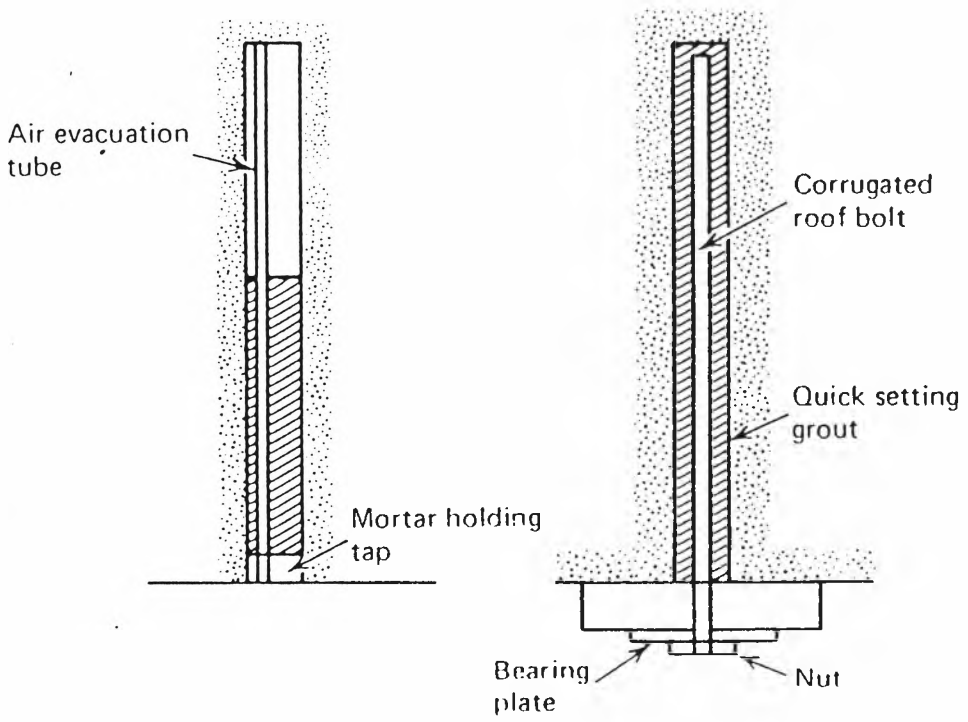

Fig. 2.5 Schematic View of Grouted Bolts

A standard procedure of installing rebar and resin cartridges is described as follows by Karabin etc. (1976):

1) drill the hole to the desired length,
2) insert the proper number of resin cartridges into the hole, and insert a plug to hold the cartridges in the hole,
3) push the rebar through the resin cartridges to the bottom of the hole,
4) rotate the rebar for manufacturer's recommended mixing time,
5) apply full machine thrust to the rebar head, hold for 20 to 30 sec, and release, and
6) complete the fully grouted resin bolt installation.

The advantage of grouted bolts can be summarized as follows:

1) under normal conditions anchorage is virtually guaranteed and independent of the strata type,
2) if properly installed, the system will turn to be a competent and durable reinforcement system,
3) the bolts do not need to be tensioned, which saves on both time and labour,
4) if fully grouted, the bolt can absorb blast vibrations without reductions of the bolt load with time, and
5) high corrosion resistance is obtained in permanent installations.

3. Friction Anchored Bolts

Friction anchored bolts represent the most recent development in rock reinforcement techniques. Two friction anchored rockbolt types are available, the split set and the swellex. The frictional resistance to sliding of the rock on the steel (for the swellex combined with mechanical interlock) is generated by a radial force against the borehole wall over the length of the bolt.

The split set consists of a long steel tube with a slot cut through its whole length as shown on Fig. 2.6 (Scott, 1977). When the tube is forced into a hole with a smaller diameter, it closes inside the hole and creates a frictional (shear) stress between the rock and tube wall and a radial stress against the rock, which in turn reinforces the surrounding roof rock. Therefore, the anchoring mechanism of the split set bolt arises from frictional forces. The load generated approaches the ultimate load bearing capacity of the bolt.

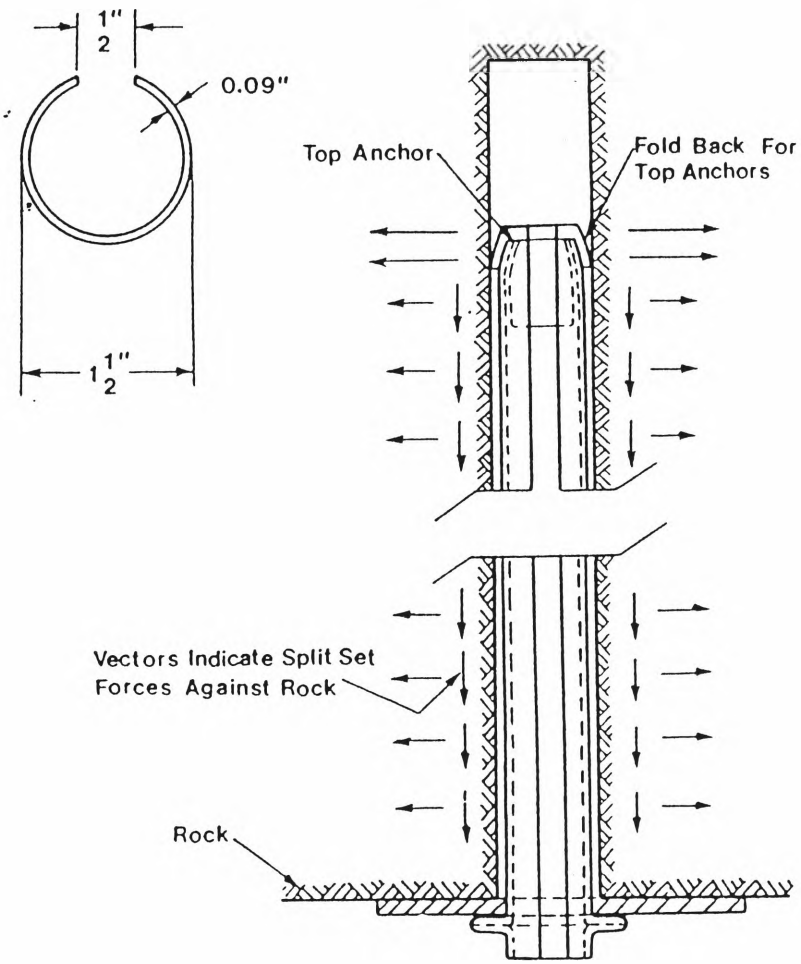

Fig. 2.6 Schematic View of Split Set Bolt

The advantages of the split set bolt are (1) simple installation, (2) immediate support action after installation, (3) no hardware other than a jackleg or jumbo boom needed for installation, and (4) easy application of wire mesh.

The swellex bolt system consists of a bolt, an installation rod with chuck, and a high pressure water pump (Atlas Copco, 1982). The bolt is made of a steel tube with a diameter smaller than that of the hole. When setting a swellex bolt

(refer to Fig. 2.7, Stillborg, 1986), water is pumped at high pressure into the tube through a connection at the lower sleeve. This causes the tube to swell in the hole and to fill it completely. The anchoring of the swellex bolt is provided by frictional forces to a load which approaches the ultimate load bearing capacity of the bolt. Mechanical interlock between the bolt and the rock prevents the bolt from sliding.

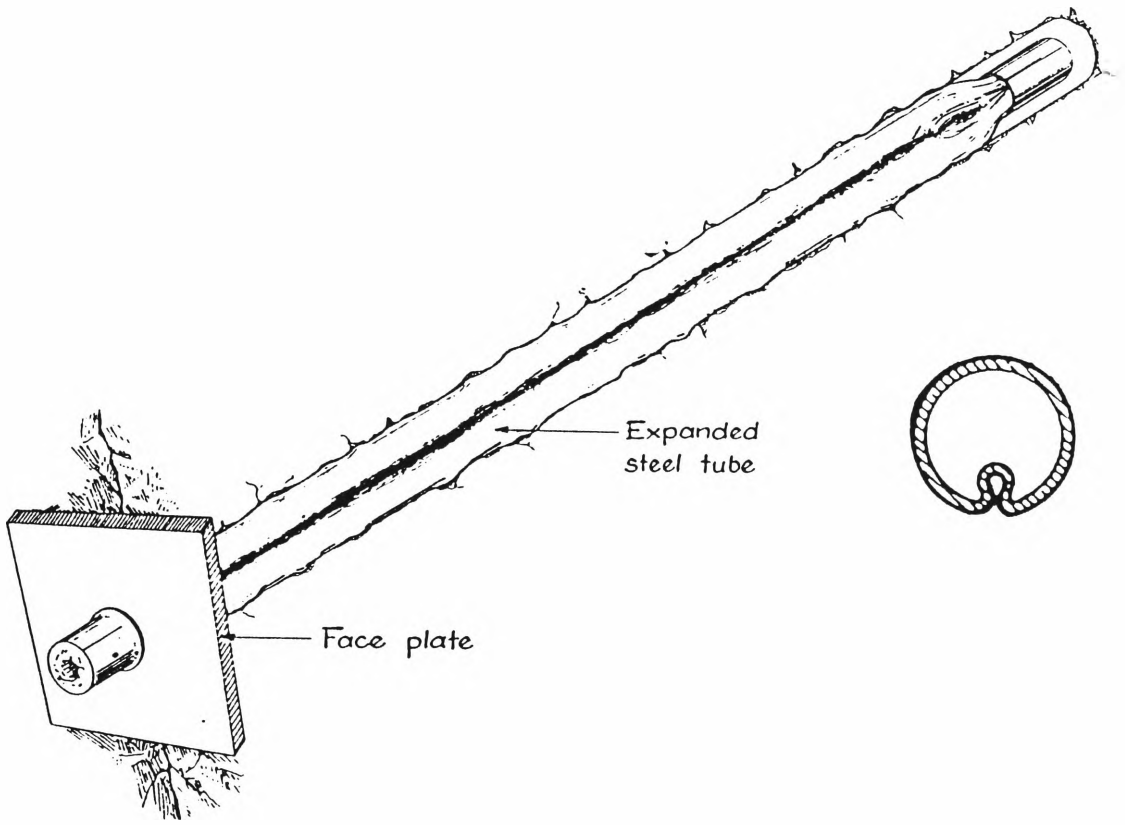

Fig. 2.7 Schematic View of Swellex Bolt

The major advantages of the swellex bolt system are (1) rapid and simple installation, (2) no rotation, high torque or feed force required, (3) versatile usage in terms of ground conditions and good resistance against vibrations, and (4) full contact and holding force in water-bearing ground where grout agents may be washed out.

4. Comparison of Mechanical Bolts and Grouted Bolts

The mechanical point-anchored bolt and the grouted bolt are two major types of rockbolts commonly used in underground mines. Their mechnisms, consitution, installation and advantages have been anlysed in previous parts of this section. Table 2.1 compares the other characteristics, which have not mentioned before, of the mechanical bolt and grouted bolt so as to draw a full picture of these two bolting systems.

Table 2.1 Comparison of Mechanical and Grouted Bolts

Item	Mechanical Bolts	Grouted Bolts
Anchor agent	slot/wedge or expansion device	grout
Anchorage	friction of top part of bolt and surrounding rocks	bonding of full length of bolt and surrounding rocks by grout
Initial anchorage	pre-tensioned, & immediate support after installation	nontensioned, passive support
Strata applicable	moderately hard to hard rocks	independent of strata
Durability	not serving as permanent reinforcement	used as permanent reinforcement
Rigidity	low rigid behaviour	high rigid behaviour
Stress concentration induced	very high at the area of rocks where anchor is set	no stress concentration induced
Bolting expense	comparatively low	comparatively high
Reliability	losing bearing capacity or creeping	resisting both vertical/

	with time as result of blast vibration, lateral movements, & or when rock spalls off around bore- hole collar due to high rock stresses induced around anchor	very reliable

2.3 Rapid Face Bolting System

The engineer who must design a rock reinforcement system today is faced with an increasing demand to optimize his design with respect to both safety and economic considerations. Among the various methods of rock reinforcement, rockbolting stands out as the most effective and economic technique.

By analysing the installation procedures of currently and commonly used rockbolting systems, it is found that there is always an operation manually to pull out drill rods from, and to insert a rockbolt into, the drill hole. This operation lengthens the installation period, which means that less productivity is achieved. Moreover, the operation exposes a miner under an unsupported roof condition for a certain period, which implies that the miner is subject to unsafe working conditions.

With the increasing use of rockbolting for support in conjunction with production operations there has been a distinct increase in attributable accidents. It seems that the accident frequency is increasing in proportion to rockbolting activities. According to Findlay (1984), Hoerndlein (1985), and Carr (1985), the statistics for 1982-1983 revealed that roof-bolting was responsible for 25% of all the lost-time accidents incurred during coal face activities. Whereas in

the year 1983-1984 26% of the serious body injury accidents reported involved some aspect of installing roof-bolts or handling or testing roof-bolting machines. Currently used rockbolting systems, therefore, are not perfect methods for achieving rock reinforcement. Some shortcomings exist in these rockbolting systems, especially in the installation procedures of rockbolts, and these need to be overcome urgently to improve safety and productivity.

2.3.1 Birth of Rapid Face Bolting System

For the purpose of reducing accidents from rockbolting, the US Bureau of Mines has developed some technology which can lead to reduced accidents from roof falls in the operations of rockbolting in underground mining. As a result of the research, remote manual roof bolters (Hill et al., 1983), a fibreglass epoxy-resin pumpable roof-bolting system (Soloman et al., 1983) and automated bolter modules have been developed. But the projects have not been successful commercially. Safety for miners has instead been solved by the use of hydraulic temporary roof supports, and the bolt installation procedure still remains unimproved.

However, the ultimate and most efficient bolting method has often been conceived as a method called the self-drilling roof bolt, where the bolt drills its own hole and remains in the rock once the hole is drilled. Consequently the procedure of withdrawing the drill rod and inserting a bolt is eliminated (Stillborg, 1986). This procedure not only reduces the dead time during bolt installation, but

also reduces the exposure of the operators to the unsupported roof, thus improving safety (Peng, 1986).

In 1979, Engineers International developed three kinds of self-drilling bolts, i.e. the spring actuated bolt, the resin anchor bolt, and the slot-and-wedge bolt (Fig. 2.8), which were operated successfully in the laboratory (Engineers International, 1979).

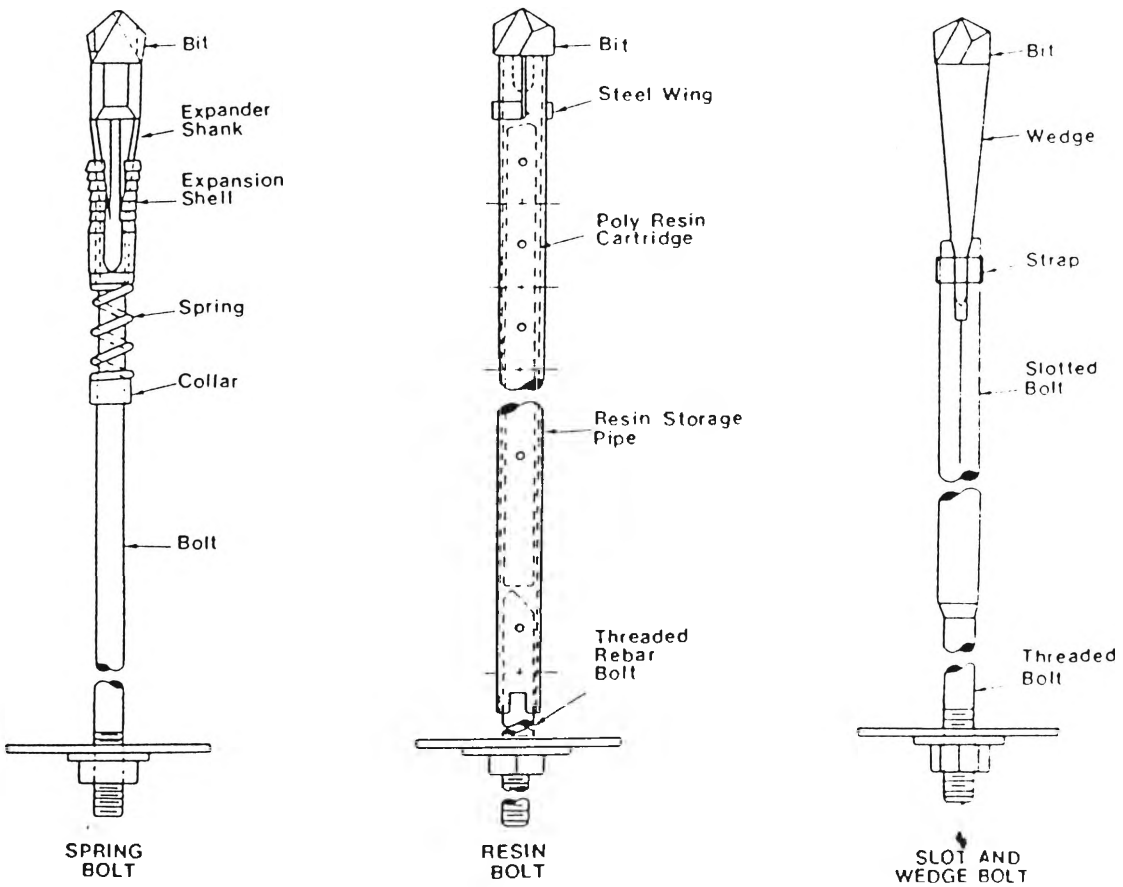

Fig. 2.8 Developed Concepts in Self-drilling Rockbolts

It is apparent that the structure of the bolt itself is rather complicated, and would add to the cost of bolt. So the advantage of time-saving for installing the

bolts may not be able to compensate for the cost added for manufacturing the bolts. Up till now, there has not been any further development of the system reported.

To improve the excavation rate of continuous miners and the safety of working conditions, the Joint Coal Board (NSW) and six other coal mining companies approached the University of Wollongong, with a view to developing what is called a Rapid Face Bolting System. In the following review and also Chapters 3, 5 and 6, the references have been made to the Reports for Rapid Face Bolting Project Nos. 1, 2, 3, and 4 (Standish, 1987, 1988 and 1989, see References A1 to A5) and Consultant Report for Sandvik (Upfold, and Standish 1989, see Reference A6).

2.3.2 General concept of the Rapid Face Bolting System

The Rapid Face Bolting system is a self-drilling bolting system using a 'single-pass' bolt for roof bolt installation in the coal field. The basic idea of the system is to develop a special drill bit/rockbolt kit which will be employed as a drill bit/rod set during the bolt hole drilling operation, and as a rockbolt be set after completion of the hole. With this system, the bolt installation procedure can still adopt that employed for the traditional rockbolting systems, but exclude the operation of the traditional rockbolting system, withdrawing the drill rod/bit from, and inserting a rockbolt into, the bolt hole. Subsequently, the procedure of rockbolt installation is simplified, and the time for miners to be exposed under the unsupported roof is greatly reduced, furnishing better productivity and higher safety.

It was envisaged that the use of the Rapid Face Bolt would involve a number of steps similar to those employed by more traditional systems. These steps would include:

1) preparation of bolt/steel for drilling, including mounting bolt/steel in the drill chuck,
2) drilling of the hole to the required depth,
3) chemical grouting of bolt/steel into ground, spin to mix and hold to set,
4) torqueing of the nut on to the holding plate to tension bolt, and
5) move on to next bolt position.

By comparison of the procedure with that described for the traditional bolting systems in the Section of the overview of typical rockbolting systems, the steps for the Rapid Face Bolting allow for a reduction in the time required to install each of the roof bolts, with the removal of the 'double handling' step of replacing the drill steel with the roof bolt. In addition, by applying the special drill bit/bolt kit to an automated bolting system, the withdrawal of the operation of swaping a drill rod for a bolt will enhance the performance of the system.

The Rapid Face Bolt will be installed by existing techniques used for installation of grouted rockbolts. Either the chemical 'sausages' or pumpable resin/hardener will be used as the grouting agents.

2.3.3 Key factor for Rapid Face Bolting project

The key to the success of the Rapid Face Bolting project is to develop a special drill bit/bolt kit (i.e. a 'single-pass' bolt), which is able to drill its own hole and to be fixed in the hole at the completion of drilling.

During a drilling operation, the drill rod/bolt is acting as a drill column carrying significant torsional and axial loads. The material used for the special 'single-pass' bolt, therefore, has to possess greater ultimate tensile and shear strengths than the materials purely employed as rockbolts. The cross-section of the drill rod/bolt, also, must provide a high stiffness to avoid excessive deformation during the drilling operation. For this reason, a number of cross-sections of drill rod/bolt have been proposed:

1) a round bar with slot or grove on side, or a hole at the centre, for the passage of water/grout in the drilling/bolt system, or
2) tube or pipe.

The selection or design of a drill bit used in the Rapid Face Bolting system has to be determined according to the drill rod/bolt chosen. In general, if a round bar is chosen as the drill rod/bolt in the Rapid Face Bolt system, the traditional rockbolt drag bit is most likely to be used. The reason for this is that traditional rockbolt drag bit can be well adapted to the drill rod/bolt system. Also, that the bit is commercially available, and is not too expensive, even when being used as a single-pass bit, and it allows a wide range of choices.

If a tube or a pipe is selected as the drill rod/bolt, a special tubular bit has to be designed for the Rapid Face Bolting system, as there is no tubular bit

commercially available which can offer such a low price that is economically acceptable as a 'single-pass' bit for the self-drilling rockbolting system.

The design of the 'single-pass' tubular roof bit is centred on a low cost, and must meet the following criteria:

1) is able to complete a bolt hole, i.e. with a bit life of approximate 2-3 m,
2) uses the the tube or the pipe as selected as the bit body,
3) chooses as cheap material as possible for the cutting tips of the bit, and
4) simplifies the configuration of the bit to its ultimate degree.

Chapter Three

Tubular Roof Bit Design

3.1 General Remarks

A tube bit, more often called a coring bit, has long been used for geological site investigations. It is a ring-like bit; its front face, professionally named the kerf in drilling engineering, is armed with cutting tools or special cutting material, a typical example of which is shown on Fig. 3.1.

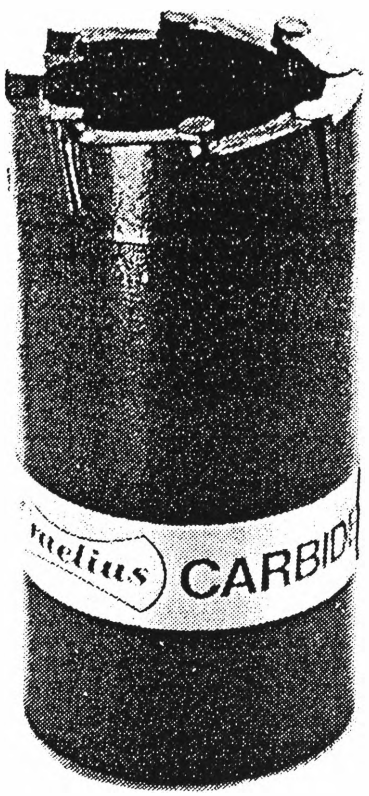

Fig. 3.1 Typical Coring Bit (Source: Craelius, 1986)

Core drilling mechanics, similar to that of any other rotary drilling, perform two actions: rotation of the drill rod and exertion of axial force on the bit so as to feed and advance it into the rock. Core drilling requires that the bit will rotate and cut out a cylindrical core of the rock through which it passes, instead of cutting off all rock in front of the bit, as in the case of full face rotary drilling or non-core drilling.

The major use of core drilling has always been geological site investigations, for example: sampling ore bodies, testing geological structures and rock defects, etc. For these purposes, the requirement for core drilling to reach a depth of over a thousand metres is not considered uncommon. Consequently, a reliable and long-life bit is desirable, especially in deep-hole drilling, and the cutting material for a core bit has to be of high strength and wear resistance.

For many years, diamond has been widely used as the principal cutting material for a coring bit because of its extreme hardness. There are three quite different types of diamond coring bits which have been used since the middle of the 19th century. The first diamond coring bit, introduced as early as 1862, was a surface bit set by hand with processed natural diamond. The second type of coring bit, consisting of finer diamond impregnated in a sintered metallic matrix, appeared around 1940 (Industrial Diamond Review, 1984). The introduction of polycrystalline diamond cutters for rock drilling has formed a third type of coring bit and was introduced in the early 1980's (Clark, 1987).

The tube bit for the rapid face bolting system, on the other hand and as stated before, is a one-hole pass bit, which is used to drill a hole for the installation of a 'single pass' bolt, and is not retrievable after the completion of the hole. Therefore, the basic consideration of a single-pass roof tube-bit design is low cost. In other words, the design of the configuration of the bit has to be simple, and the cutting material has to be cheap, in order to reach a minimum cost and to enable the rapid bolting system to compete with other conventional roof bolting systems. This design concept is contrary to that of the coring bit for geological site investigations, in which case the bit life is the primary consideration.

A comparison of the design targets and technical requirements is made between the coring bit for geological site investigations and the tube bit for a rapid face bolting system in Table 3.1.

Table 3.1 A Comparison Between Two Tube-Bits

Item Compared	Tubular Roof Bit	Geological Coring Bit
Bit life	one bolt hole (1.5 m or so)	the longer, the better*
Rock drilled	sedimentary rocks mainly	any possible kind of rock
Coring required	not at all	high quantity and quality
Direction of hole	upward	downward
Cutting material	sufficient to complete a hole	high hardness and wearability
Bit configuration	as simple as possible	as required
Bit cost	to a minimum level	not of great importance

* **The length a coring bit can drill depends on many factors, mainly including the material of the cutting tips, the rock drilled, and so on.**

Obviously, the aims and technical requirements of the two types of bits are widely different. Therefore, the design principles for a geological coring bit are definitely not applicable to the single-pass tubular roof bit. The design considerations for the latter should be reassessed and special effort should be centred on the cutting material choice and the bit configuration.

3.2 Material Choice for a Tubular Roof Bit

The cutting material used for a coring bit in the field of geological investigations has passed through mainly five principal stages: carbon tool steel hardened by quenching in water followed with a tempering treatment, hand-set natural diamond, tungsten carbide, fine diamond sintered in a metallic matrix, and polycrystalline diamond. The development is towards a material which has mechanical properties of high hardness, resistance to abrasive wear, toughness and strength, thermal stability, long service life and is suitable for a variety of rock type conditions.

On the other hand, the ideal cheap material for the one-hole tubular roof tube bit would be of a certain level of hardness and toughness to cut sandstone, but the wearing resistance would not necessarily be very large, for the bit performance is only needed to be efficient up to a depth of about two meters. Obviously, the current development of rock cutting materials for geological investigations is too sophisticated for the cutting tools of a tubular roof bit. Even the well developed, comparatively cheap materials, such as tungsten carbide inserts,

seem to be luxury materials for the purpose because of their cost. Therefore, as the cutting materials used in a conventional coring bit possibly are not economical for the tubular roof bits, the material selection may be subdivided into several categories of metal drilling materials. But, first the hardness of cutting tool materials and its measurement test should be examined, as it is considered as an effective quality control test, and is useful as a first indication of the properties of tool materials (Boyer, 1987).

3.2.1 Hardness of cutting materials and its measurement

Hardness at room temperature is much the most commonly measured property of tool materials. It is an effective quality control test and useful as a first indication of the properties of tool material (Trent, 1984 and ASM, 1975). The concept of hardness as it relates to the tool industry can be thought of as resistance to permanent deformation. The scope of hardness properties includes such varied attributes as resistance to abrasives, resistance to plastic deformation, high yield point, high strength, absence of elastic damping , brittleness, and lack of ductility. Hardness is easily measured and offers some insight to the suitability of a cutting material for a given application.

The hardness test is, by far, the most valuable and most widely used mechanical test for evaluating the properties of cutting materials. The hardness of a material usually is considered as resistance to permanent indentation. In general, an indenter is pressed into the surface of the metal to be tested under a specific load for

a definite time interval, and a measurement is made of the size or depth of the indentation.

The reason to test hardness of a material is that there exists a relation between hardness and other properties of a material. Therefore, the results of different properties of a material may closely parallel each other. The hardness test is preferred, because it is a simple, easy and relatively staight-forward nondestructive test. Hardness is not a fundamental property of a material. Hardness values are arbitrary, and there are no absolute standards of hardness. Hardness has no quantitative value, except in terms of a given load applied in a specified manner for a specified duration and a specified penetrator shape (Boyer, 1987).

The hardness test is generally divided into two categories: macrohardness and microhardness. Macrohardness refers to testing with applied loads on the indenter of more than 1 kg and covers, for example, the testing of tools, dies, and sheet and sheet material in heavier gages. On the other hand, microhardness designates testing with applied loads of 1 kg and less on very thin material, and only covers extremely small parts.

The macrohardness test includes three basic testing methods, i.e. Brinell Testing, Rockwell Hardness Testing and Vickers Hardness Testing. The macrohardness is evaluated by the amount of permanent deformation or plastic flow of the material. This amount of flow may be determined by measuring the depth of the indentation, or by measuring the area. As the test material becomes softer, the

depth of penetration becomes greater. Likewise, the projected area increases as the test material becomes softer.

1. Rockwell Hardness Test

The Rockwell hardness test is one of the most common methods of hardness testing, by which the hardness is determined by the depth of the indentation in the test material resulting from application a given force on a specific indenter. The reasons that the Rockwell hardness testing is the most widely used method for determining hardness are:

1) it is simple to perform and does not require highly skilled operators,
2) by using different loads and indenters, Rockwell hardness testing can be used to determine the hardness of most metals and alloys, ranging from the softest bearing materials to the hardest steels,
3) a reading can be taken in a matter of seconds with conventional manual operation and in even less time with automated setups, and
4) optical measurements are not required (all readings are direct).

Although a number of different indenters are used for Rockwell hardness testing, the most commonly one used for testing hard materials, such as

hardened steels and cemented carbides, is a diamond ground to a 120° cone with a spherical apex that has a 0.2 mm radius as shown in Fig. 3.2 (ASM, 1985).

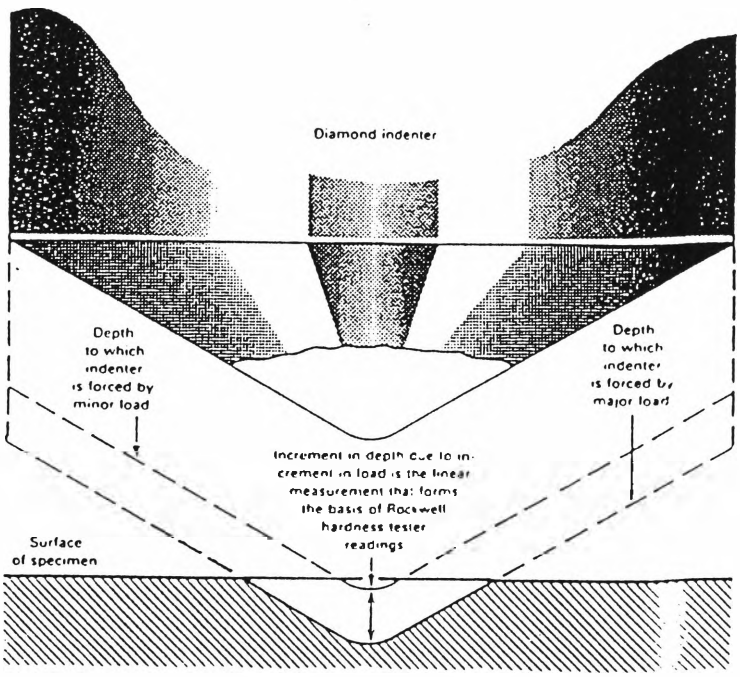

Fig 3.2 Indenter of Rockwell Hardness Testing

While there are many Rockwell hardness scales due to the combination of loads applied in the test, and sizes and materials of indenters, the most widely used scales for hard material tests are the Rockwell hardness C (HRC) and the Rockwell hardness A (HRA). Table 3.2 shows HRC and HRA scale designations and their typical applications.

Table 3.2 Designations and Applications of Rockwell Hardness A & C Scales

Scale Designation	Indenter Type	Applied Load (kg)	Application
C	Brale diamond	150	steel, hard cast irons, titanium, deep case-hardened steel & metal harder than HRB 100
A	cone indenter	60	cemented carbides, thin steel & shallow case-hardened steel

2. Brinell Testing

In the Brinell test, hardness is evaluated by the area of the impression created by forcing a specific indenter, a 10 mm diameter hardened steel or tungsten carbide ball, into the test material under a specific force for a given length of time. However, in highly automated Brinell testing systems, hardness is evaluated by the depth of the impression, which makes it similar to the Rockwell test in basic principle.

The practical limits of hardness measurement by the Brinell method are determined by the fact that highly hardened steel or other extremely hard materials cannot be tested by a hardened steel ball, because the ball itself can flatten and become permanently deformed under the applied load. A value of 450 HB (equals approximately 46 HRC) of Brinell hardness is considered as the top range of the Brinell test in practice, although the use of a tungsten carbide ball extends the

range to about 600. Therefore Brinell testing is not suitable for the materials with a high hardness, such as high speed steel and cemented carbide materials.

3. Vickers Hardness Testing

The principle of the Vickers hardness test is the same as that of the Brinell test. An indenter, made of diamond with the form of a square-based pyramid with an angle of 136° between faces (refer to Fig. 3.3), is pressed into the material to be tested, the load is removed, the diagonals of the resulting indentation are measured, and the hardness number is calculated by dividing the load by the surface area of indentation. The loads applied vary from 1 to 120 kg with the standard values of 5, 10, 20, 30, 50, 100 and 120 kg. For most hardness testing, 50 kg is the maximum value, because loads of more than 50 kg are likely to fracture the diamond indenter, particularly when used on hard materials.

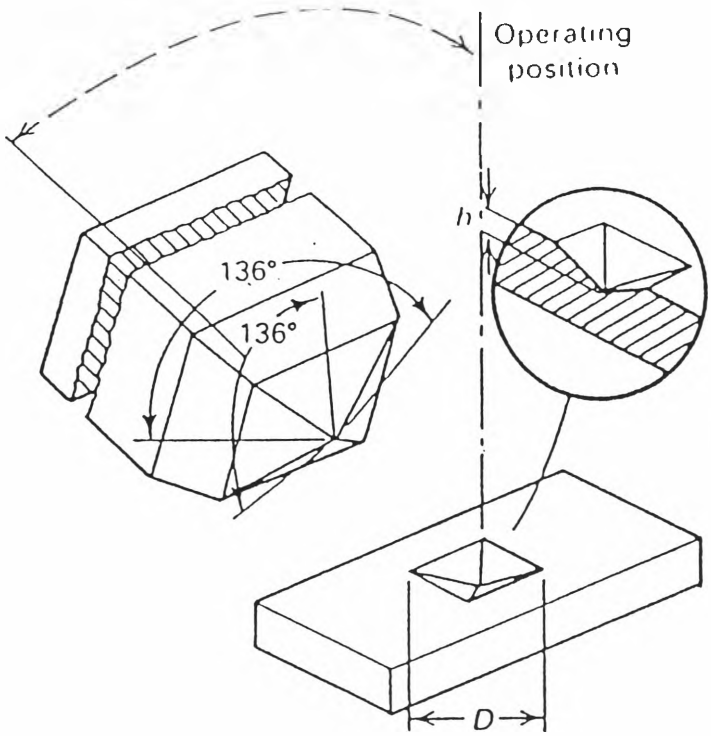

Fig. 3.3 Diamond Pyramid Indenter Used for Vickers Testing and Resulting Indentation in the Workpiece

The Vickers hardness number (HV) in a uniform material is practically independent of the test load, as the impressions under varying loads are geometrically similar (Angus, 1976).

As the Brinell test is rarely employed for hardnesses above 450 HB, the Vickers test can be regarded as a direct extension of the Brinell scale for hardnesses above 400 HB, and is practically coincident with it for hardnesses below 350.

The Vickers test is suitable for a wide range of hardness testing and is especially useful in the situation where the direct comparison of a great variety of hardnesses for various materials to a consistent scale is demanded.

4. Hardness Conversion

From a practical stand-point, it is important to be able to convert the results of one type of hardness test into those of a different test. Because a hardness test does not measure a well-defined property of a material, and because all tests in common use are not based on the same types of measurements, it is not surprising that universal hardness-conversion relationships have not been developed.

Hardness conversions are empirical relationships. Table 3.3 can be used for conversion among Rockwell scales C and A, and Vickers Diamond Pyramid hardness, and are found in Metals Handbook, Mechanical Testing (ASM,

1985), and is applicable to all alloy steels, tool steels and cemented carbide materials.

Table 3.3 Approximate Comparison of Hardness Scales

Vickers (HV)			940	900	860	820	780	740	700	660
Rock. C (HRC)			68.0	67.0	65.9	64.7	63.3	61.8	60.1	58.3
Rock. A (HRA)			85.6	85.0	84.4	83.8	83.0	82.2	81.3	80.3
620	580	560	540	520	500	480	460	440	420	400
56.3	54.1	53.0	51.7	50.5	49.1	47.7	46.1	44.5	42.7	40.8
79.2	78.0	77.4	76.7	76.1	75.3	74.5	73.6	72.8	71.8	70.8

3.2.2 High speed steels (HSS)

Metal drilling materials most widely used for production machining are high speed steels, while carbide drills of several designs are used for drilling certain ceramic and plastic materials and for metallic materials of high hardness. However, the number of holes drilled with carbide drills is still a small percentage of the total (Kennedy et al., 1975). The other main groups of cutting tool materials are carbon (and lower alloy) steel, cast cobalt-based alloys, ceramics, and diamond (Trent, 1984).

In the 1970's the greatest percentage of HSS used for the manufacture of drills was composed of those grades exhibiting the highest strength

and toughness, notably M1, M2, M10 and T1 (Kennedy, 1975) . These four standard types of high speed steel are used in the majority of high-speed drills because they furnish the necessary combination of strength, toughness and hot hardness (Eagle & Globe, 1981).

The hot hardness or red hardness is the ability of a material to retain hardness and strength at high and elevated temperature (Fritzlen, 1975). Generally speaking, the hardness of a cutting material will reduce with the increase of cutting temperature, but the reduced rate of hardness with temperature varies from material to material. The lower the reduced rate of hardness with the elevated temperature, the better hot hardness will a material be considered to have. In terms of rock drilling, the hot hardness of a cutting material is also a very important property of the material, for the temperature generated between the cutting edge and the rock face by the drilling action during the drilling process can easily reach several hundred degrees (°C) if the cutting tools are not promptly cooled. With such high temperatures, the hardness of a cutting material can be sharply weakened immediately, that will result in the failure of the cutting tools.

Fig. 3.4 shows the hardness of carbon steel and HSS versus temperature (Trent, 1984). The fact of the linear decrease of hardness in a carbon steel with the increase of temperature implies that the carbon steel does not possess a good hot hardness. On the other hand, the hardness of a HSS is a relatively stable and varies in a limited range before the temperature reaches up to 400°C. Afterwards, the hardness falls sharply with further rise of temperature. Those phenomena suggest that the HSS furnishes a high hot hardness and would be a suitable cutting material for temperatures less than 400°C.

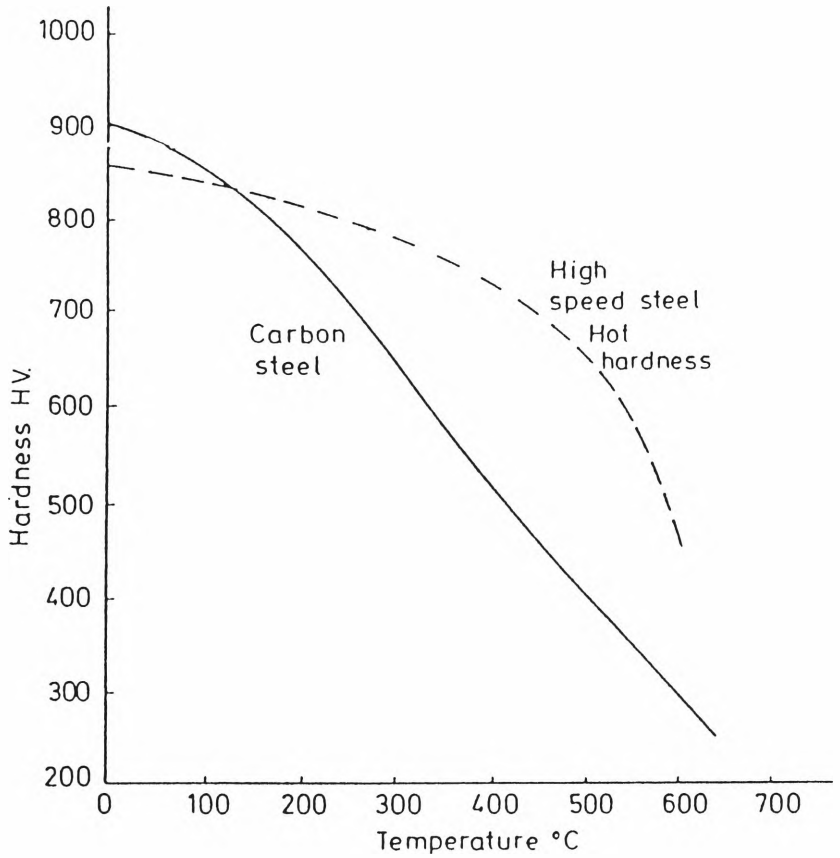

Fig. 3.4 Hardness of Carbon Steel & HSS vs. Temperature

The chemical compositions of HSS are principally carbon (C), tungsten (W)/molybdenum (Mo), cobalt (Co), chromium (Cr), vanadium (V) and iron (Fe). The detailed chemical compositions of the above-mentioned HSS T1, M1, M2 and M10 are listed on Table 3.4 (Trent, 1984 & ASM, 1975).

Table 3.4 Detail Compositions of T1, M1, M2 & M10

Designation	Chemical Composition (%)				
	C	Cr	Mo	W	V
T1	0.75	4.0	non	18.0	1.0
M1	0.8	4.0	8.5	1.5	1.0
M2	0.85	4.0	5.0	6.5	2.0
M10	0.85	4.0	8.0		2.0

Tungsten HSS, Group T1, contains the principal alloy elements of tungsten, chromium, vanadium, cobalt and carbon. The steel is characterized by high hot hardness and wear resistance. High alloy and high carbon contents produce a large number of hard wear-resistant carbides. The presence of many wear-resistant carbides in a hard heat-resistant matrix makes the steel suitable for cutting tool application.

Molybdenum high speed steels, Group M, are similar in properties to the tungsten high speed steels, but with two advantages: slightly greater toughness at the same hardness, and lower initial cost with the equivalent performance, being almost 30% less than similar grades of the Group T steel. However, the Group M steels are somewhat more sensitive than Group T steels to hardening conditions, particularly to temperature and atmosphere. They will decarbonize and overheat easily under adverse treatment conditions. This condition is especially true of the high molybdenum grades. It is estimated that approximately 85% of all high speed tool steels produced in the USA in the 1970's are in this group. Their typical uses are for cutting tools of all kinds (ASM, 1975).

Tungsten high speed steels are all deep hardening when quenched from their recommended hardening temperatures. The maximum hardness of Group T steels varies with the alloy content and especially the carbon content. A Rockwell hardness measure of C 64.5 is obtained on all steels of this group.

Molybdenum high speed steels possess the hardenability similar to that of the tungsten steels because of the similarity between the two groups. When properly hardened, all Group M steels will test to at least one-half to one point Rockwell C harder than comparable Group T steels. This increase is the another advantage of M steels over T steels.

Table 3.5 lists the typical values of mechanical properties of HSS T1, M1, M2 and M10.

Table 3.5 Mechanical Properties of HSS T1, M1, M2 &M10

Code of HSS	Transv. Rupture Stress (GPa)	Fract. Toughness (M $Nm^{2/3}$)	Impact Strength (mN)	Hardness (HV)	Rockwell (C)
T1	4.6	18	15	835	65.1
M1	4.8	18	24	835	65.1
M2	4.8	17	25	850	65.6
M10	4.0	15	13	880	66.4

A further trend has been noted toward greater use of vanadium in high speed steels because of the better wear-resistance and longer tool life imparted by the hard vanadium carbides.

3.2.3 Tungsten carbide alloy (WC alloy)

The first successful application of tungsten carbide as a cutting material was made in Germany in 1920's (Shaw, 1989).

Tungsten carbide is one of a group of compounds, carbides, nitrides, borides and silicides of transition elements of groups IV, V and VI of the Periodic Table (Goldschmidt,1967). Of these, the carbides are important as cutting tool materials, and the dominant role has been played by the mono-carbide of tungsten, WC. The rigid and strongly bonded hexagonal structure of tungsten carbide undergoes no major structural changes up to its melting point, which is over 2500°C, and its properties are therefore stable and unaltered by heat treatment, unlike steels which can be softened by annealing and hardened by rapid cooling (Schwarzkopf, 1960).

Tungsten carbide has a diamond indentation hardness of over 2000 HV at room temperature, which is much higher than that of steel. The hot hardness of tungsten carbide is not very great, and drops rapidly with increasing temperatures as shown on Fig. 3.5 (Trent, 1984). Even then it still remains much harder than steel under almost all conditions. The very high hardness, and the stability of the

properties when subjected to a wide range of thermal treatments, are favourable to the use of tungsten carbide as a cutting material.

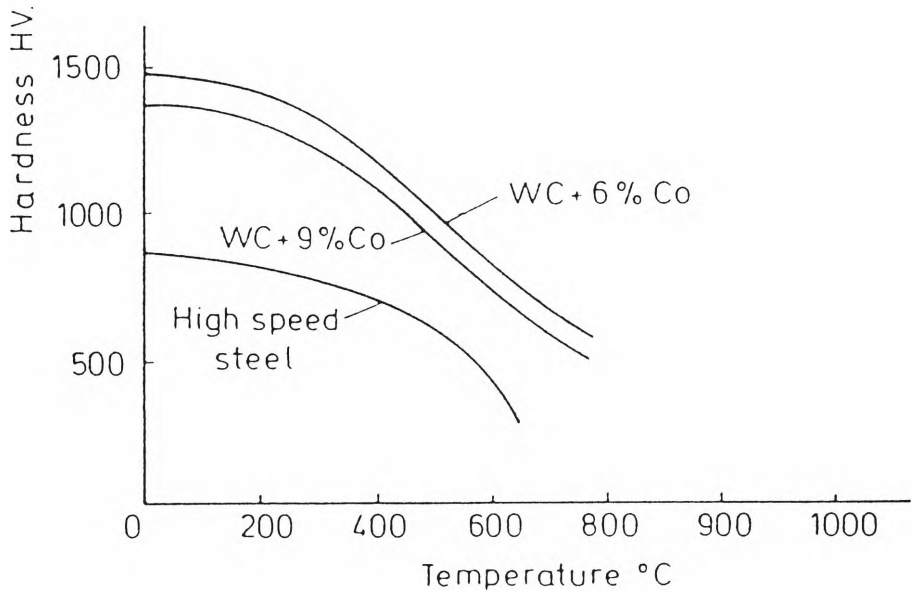

Fig. 3.5 Comparison of Hardness of HSS & WC Alloy

The performance of carbide cutting tools is very dependent upon the composition and grain size in addition to the general quality of the product. The WC alloy used for cutting normally contains at least 80% carbide by volume and 4% to 15% cobalt by weight, with the carbide grains varying in size between 0.5 μm to 10 μm across. Table 3.6 gives the properties of a range of WC-Co alloys in relation to their composition and grain size, and Fig. 3.6 shows graphically the influence of cobalt content on some of the mechanical properties. Both hardness and compressive strength are highest with alloys of low cobalt content and decrease continuously as the cobalt content is raised. For any composition, the hardness is

higher the finer the grain size, and over the whole range of compositions used for cutting the tungsten carbide is march harder than the hardest steel.

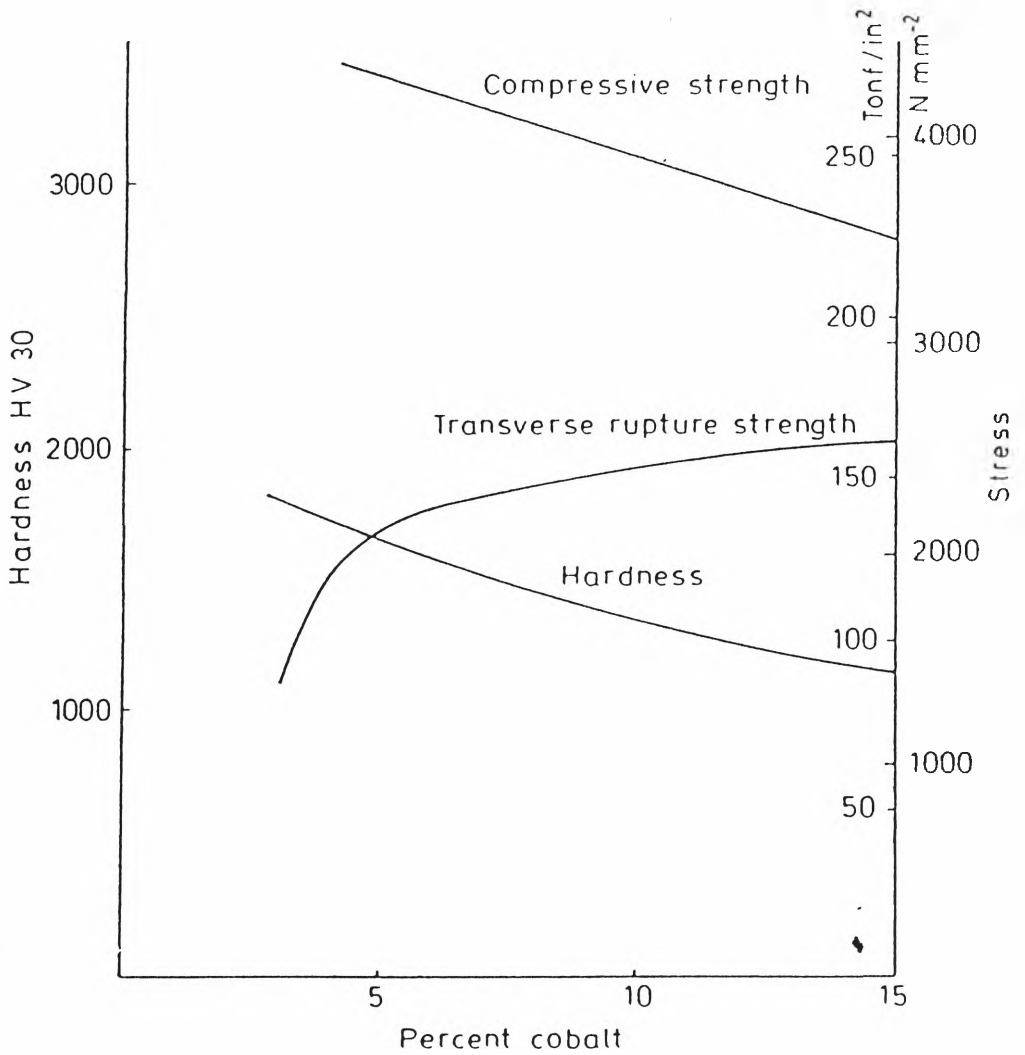

Fig.3.6 Influence of Cobalt Content on Mechanical Properties of Tungsten Carbide Alloy

Table 3.6 Influence of Composition and Grain Size of WC Alloy on Some of its Mechanical Properties

Co	Mean WC	Hardness	Trans. Rupture	Comp. Strength	Young's Modulus	Density
%	μm	HV	MPa	MPa	GPa	g/cm^3
3	0.7	2020	1000			
	1.4	1820				
6	0.7	1800	1700	4550		
	1.4	1575	2300	4250	630	14.95
9	1.4	1420	2400	4000	588	14.75
	4.0	1210	2770	4000		
15	0.7	1400	2770		538	
	1.4	1160	2600	3500		1400

Fig.3.7 (Trent, 1968) shows a comparison between the compressive strengths of HSS and WC Alloy at a higher temperature range and lower stress level. Both hardness and compressive strength of tungsten carbide decrease as the temperature is raised (refer to Figs. 3.5 and 3.7). The comparison of compressive strength at elevated temperatures with that of high speed steel (ref. to Fig. 3.7) shows that a WC alloy with 6% Co withstands a stress of 750 MPa at 1000°C, while the corresponding temperature for HSS is 750°C. With tungsten carbide the temperature, at which this stress can be supported, drops if the cobalt content is raised or the carbide grain size is increased (Aschan, 1975).

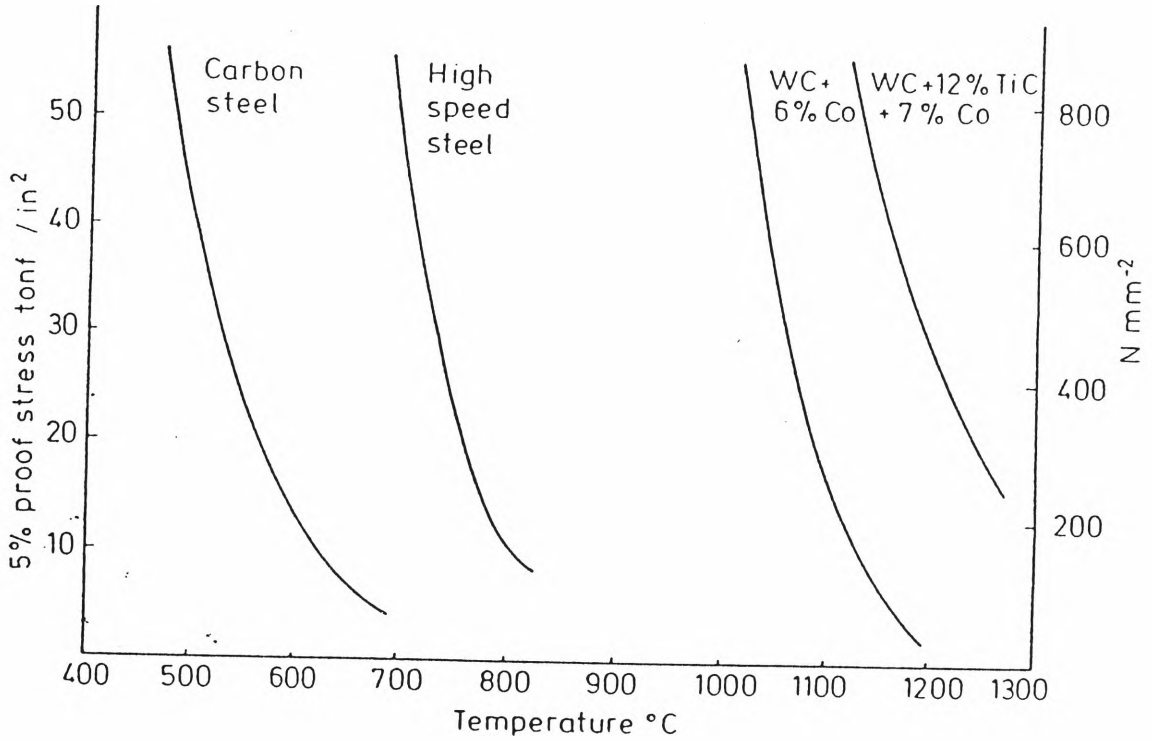

Fig. 3.7 Compressive Strengths of HSS and WC Alloy at a Higher Temperature Range and Lower Stress Level

The ASM Committee on Sintered Carbides (1975) suggests that the high hardness and wear resistance of tungsten carbide make it well suited for rock drilling and mining applications. Various types of specialized rock bits for drilling in extremely hard and abrasive rock formations utilize carbide inserts instead of other conventional cutting materials. Carbide insert bits are almost mandatory for drilling rocks harder than limestone, and their use has all but made the steel bit for drilling hard rock obsolete, both on a basis of performance and economics.

Table 3.7 (ASM, 1975) lists mechanical properties of five tungsten carbides potentially used for rock cutting tools. The cobalt contents of these carbides are between 6.5 and 15%.

Table 3.7 Mechanical Properties of WC for Rock Drilling

WC Grade Number	Rockwell A Hardness	Trans.Rupture (MPa)	Comp.Strength (MPa)	Y's Modulus (GPa)	Density (g/cm^3)
1	90.5	2068	4440	565.4	14.6
2	89.2	2827	4433	558.5	14.6
3	89.1	2827			14.5
4	89.0	2827	4158	572.3	14.5
5	86.3	2482	3482	551.6	14.1

3.2.4 Summary

According to the mechanical properties of HSS and its competitive prices, it seems that some types of high-speed steels, e.g. M1, M2, M10 and T1, could be used as the cutting material for the low-cost single-pass tubular bit, and are well worthy of investigation as cutting materials for the self-drilling bolting bit.

Tungsten carbide is a little more costly, but it can drill the hard rock formations which cannot be handed by the tools made from steels. Consequently, tungsten carbide may have to be used as the cutting material for the roof tubular bit in some extreme cases.

3.3 Criteria for a Tubular Roof Bit Design

The shape and material of a cutting tool are two important points which largely affect the cutting efficiency, but they are not the only points. The other factors, including the body structure of a tube bit and the arrangement of the cutting tools on the bit face, may significantly affect the bit performance too. A bit with sharp tools of high strength material may perform poorly if the bit body is not properly designed or the cutting tools are improperly arranged, while a bit with comparatively blunt cutting tools may furnish a higher efficiency and longer bit life if it is of a good design.

Basically, the design of the body-structure of a tube bit includes the thickness of the bit face, the number, area and shape of waterways, water slot and the arrangement of the cutting tools on the bit face. Also included are the cutting tool exposures, the rake angle and the number of cutting tools. All these factors, which affect the drilling efficiency, will be individually detailed.

3.3.1 Cutting tool exposures

All cutting tools project from the bit body. These projections of the cutting tools are generally called the cutting exposure. According to the positions of projection, the cutting exposures are divided into three types, i.e. the inner, outer or the bottom exposure. Fig. 3.8 is a diagram showing these exposures. The purpose of designing exposures is to let the tools fluently cut into the rock, to allow the drilling water to flow freely, and to lessen the wearing of the bit body.

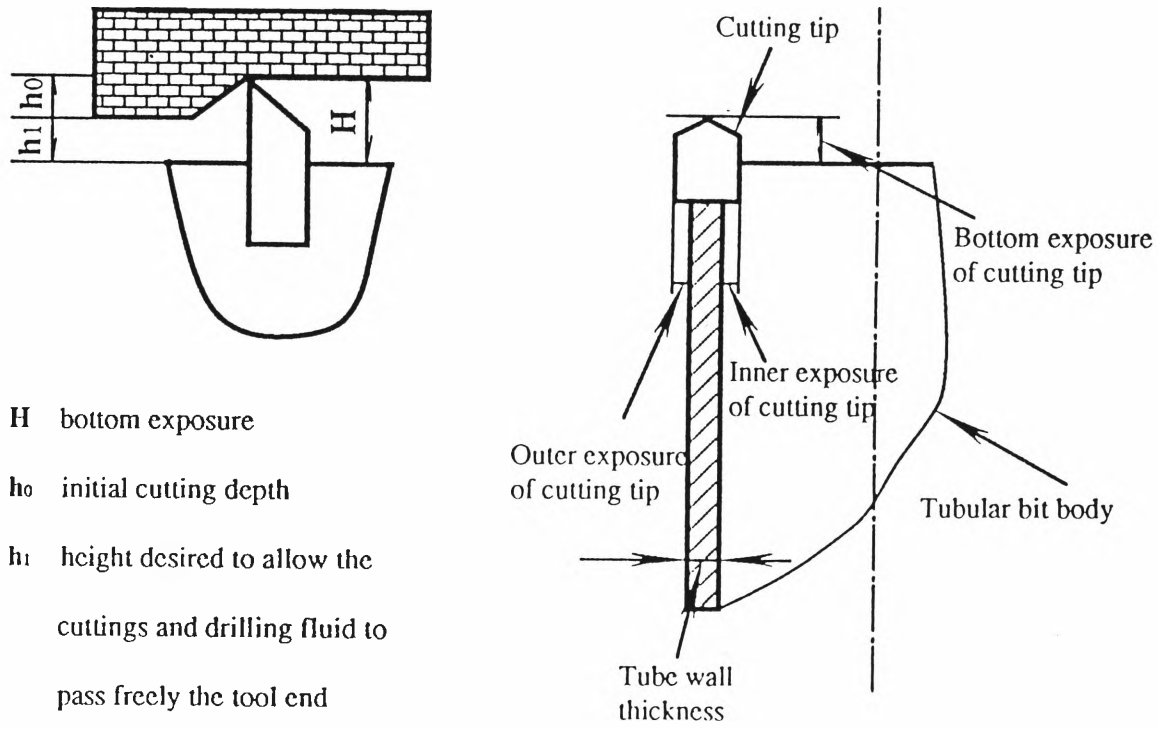

Fig. 3.8 Exposures of Cutting Tip

1. Inner and Outer Exposures

Inner exposure and outer exposure are rulers which set the diameters of a drilling hole and core size, i.e. the annulus between the core and the bit inner wall, as well as the annulus between the bit outer wall and the hole wall.

If these exposures are too big, the cutting tools are less supported and weakened. Moreover, the annulus of the cutting area is extended, and this will lead to an increment of cutting resistance, and hence to an increase of power consumed. On the other hand, if the inner and outer exposures are very small, the resistance to the flush flow will be great, and as a result, core jam will occur.

The decision about the value of an inner and outer exposures mainly depends on the drilled strata. Usually, a small value of the exposure is selected in a hard rock formation, as a small volume of flush flow is demanded because of the stable hole wall, the low drilling speed, and the small amount of drilling debris produced. A comparatively large value of exposure is desirable in the condition of a soft rock formation, because of the high penetration rate and the large quantity of cuttings created during the drilling process.

According to exploratory core drilling experience, the arrangement of inner and outer exposures is about 2 -3 mm in soft formations and approximately 1-1.5 mm in medium hard rocks. (Centre Laboratory, 1979)

2. Bottom Exposure

The purpose of having a bottom exposure on a drilling bit is to let tools easily cut into the rock and allow the drilling fluid and rock cuttings to be flushed out. Consequently, the value of the bottom exposure should not be smaller than the summation of the values of the cutting depth $\mathbf{h}_0$ and the gap required for the clearance of drilling fluid and debris $\mathbf{h}_1$, i.e.:

$$\mathbf{H} = \mathbf{h}_0 + \mathbf{h}_1.$$

where $\mathbf{H}$ bottom exposure.

$\mathbf{h}_0$ initial cutting depth of a tool

h_1 height desired to allow the cutting debris and drilling fluid to flow pass the tool end.

In medium hard rocks, the cutting depth and the flow outlet height are small. Therefore, the bottom exposure **H** should be also small, but it cannot be too small, otherwise the bit will have a very short life because of the easily worn-out bottom exposure. Normally, a value of 2-3 mm for a bottom exposure is suitable in medium hard rocks.

A large value of bottom exposure is required to drill soft rocks, as the cutting depth is high and more rock cuttings are produced. But this exposure does not mean that the greater the value, the better the performance the bit will show. Considering the fact that the bending moment of a cutting tool increases with the bottom exposure, a value of bottom exposure of around 3-5 mm in soft formations will enable efficient drilling and prevent breaking of tools.

3.3.2 Rake angle and other cutting tool angles

Fig. 3.9 is a diagram showing the angles of a cutting tool on a bit body and their relations.

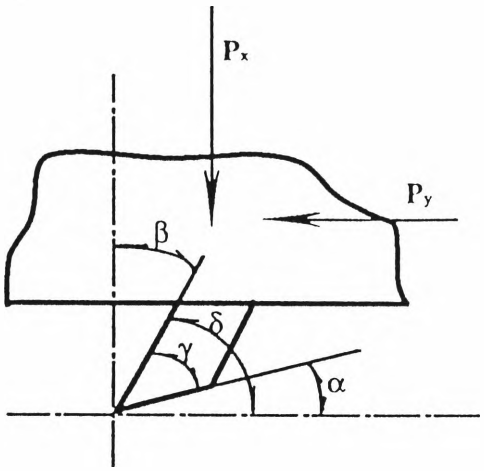

β Rake angle

γ Tool angle

α Rear angle

δ Cutting angle

P_x Thrust force

P_y Rotary force

Fig. 3.9 Angles of Cutting Tool

Rake angle β is the angle between the front face of a cutting tip on a drill bit and the vertical line. The rake angle is provided to give a cutting tool a wedge like action and to affect the direction of the flow of cuttings.

Different rake angles of the cutting tools on a bit body will result in a different cutting angle towards the cut rock, hence lead to a different effect on rock cutting.

The value of the tool angle γ determines if it is easy or not for a tool to cut into rock, and also determines the wearability and the bending strength of a cutting tool. Obviously, the smaller the tool angle, the easier it will be for a tool to cut into rock, to wear out and to chip off, and vice-versa. In actual drilling, the wear-out and chip-off of a cutting tool turns out to be a basic consideration, so a small tool angle is adopted in soft rocks while a large tool angle is used in hard rocks.

The value of the rear angle α affects the contact and wear between the rear of a tool and the rock surface. A certain degree of rear angle must be introduced to guarantee no contact and less wear between a tool rear and the rock surface. It is unnecessary to have a great rear angle, for the increased rear angle will reduce tool angle. Sometimes, an angle called the cutting angle and denoted by δ, which equals α plus γ, is adopted to describe a tool specification. The cutting angle δ is correlated with the rake angle β, i.e.:

$$\delta = 90^0 - \beta.$$

When $\delta = 90^\circ, \beta = 0$ called neutral rake

$\delta < 90^\circ, \beta > 0$ called positive rake

$\delta > 90^\circ, \beta < 0$ called negative rake

The cutting angle is decided again according to the rock drilled. Generally, the harder the rock, the greater the cutting angle.

In hard rocks, the principal problem to be solved for cutting tools is the wearrate due to chipping of the cutting tips. It is found that both positive rake and neutral rake bits are liable to lose their cutting edge rapidly. To provide the greatest possible support to the cutting tips , a negative rake angle is preferred , although this reduces the effective cutting force for a given magnitude of thrust (Fish etc., 1956). But the rake angle cannot be too small, or else the rock cutting speed and the removal of cuttings will become a problem. Usually, a rake angle of not smaller than -10^o is required.

In soft rock conditions, the wearing of cutting tools by the rock is not so severe and the strength of the rock is not so high as in that of hard rock, therefore a positive rake is used to achieve a high penetration rate. Normally, a value of 3°-5° is a suitable rake angle for a drill bit used in soft rock conditions.

In summary, the rake angle of a cutting tool should suit the nature of the rock to be cut: a positive rake angle is very often adopted in soft or lowly abrasive rocks, but positive angles are not usually used in hard or highly abrasive rocks.

3.3.3 Waterways on a bit body

Water-ways of a tubular roof bit are the access on a bit body for drilling fluid to be ejected up to the top of a drill hole from the inside of the drill tube and flow down to the ground in order to cool the cutting tool and to remove chips. Whether a design of a waterway is suitable will directly affect the tool cooling and rock cutting removal, and hence will affect the drilling efficiency and the tool wear. The waterway cannot be ignored in tubular bit design.

1. Number and Area of Waterways

In a hard metal alloy tube bit, each cutting tool normally has its associated waterway, so that each tool will have a fair chance to be cooled. Therefore, the number of waterways is equal to the number of cutting tools. To

guarantee the prompt removal of cuttings and the swift cooling of tools, a waterway is usually arranged close to the cutting tool. The area of a waterway very much depends on the rock formation to be drilled. In soft rock, a high drilling speed and a great amount of cuttings are expected, and the waterway should be large. In hard rock, on the other hand a small waterway is all that is needed.

In order to reduce the loss of water head, the waterway should not be too small, or else the small cross section of water access will create a high resistance to the flush flow. But the area of waterway cannot be too large either, for the large cross-sectional area of the waterway will reduce the flow speed, hence affecting the cutting carrying capacity and the tool cooling. In a compromise, the ideal total area of the waterways should be slightly greater than the annular area between the inner wall of the bit and core, or the annular area between the hole wall and the outer wall of the bit.

2. Waterway Shapes

A basic rule for waterway design is to meet the drilling requirement and to consider the manufacturing process not to weaken the strength of a bit body. Its design should give the flush flow a smooth easy outlet with a simple shape. Waterway shapes are mainly designed as rectangles, triangles, half circles or even isosceles trapezoids as shown on Fig. 3.10. Usually, the shapes of half circle and trapezoid are preferred.

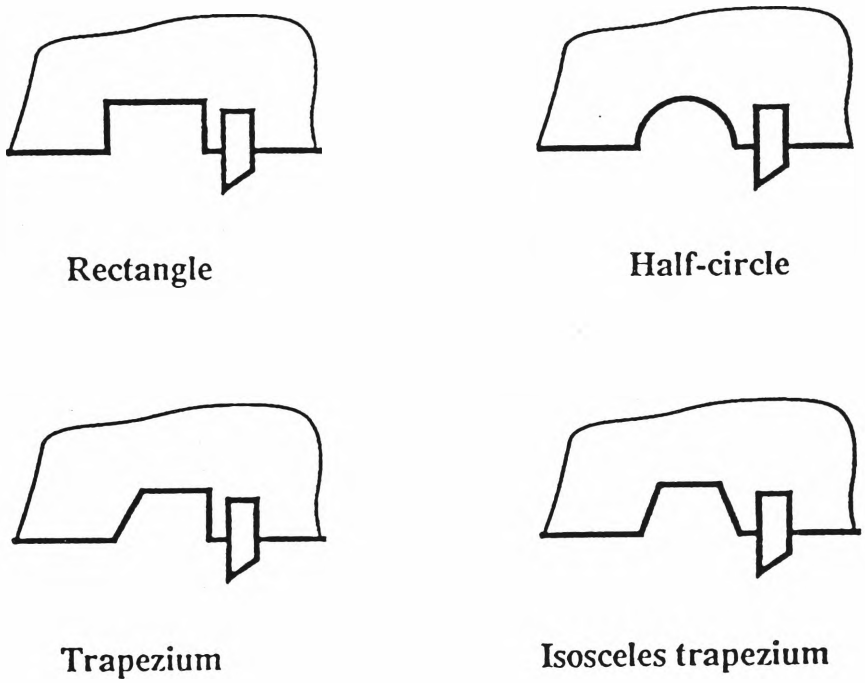

Fig. 3.10 Shapes of Commonly Used Waterways

3.4 Proposed Tubular Roof Bit

As has been analysed, different rock formations require different cutting material and bit configurations. Basically, two kinds of single-pass tubular roof bits are designed to suit the hard and soft rock formations respectively. The determination of the hard and soft rocks may have to be by a trial-and-error method first, and later on modified by the experience collected from use.

3.4.1 Tubular roof bit for hard rock formations

For hard rock, the cutting materials with a high hardness and wear resistance is desirable, therefore tungsten material should be used.

In hard rock drilling, a smaller amount of flushing water is needed due to the fewer rock cuttings produced than for soft rock drilling. The waterway may be eliminated in order to simplify the configuration of the single-pass tubular roof bit, so as to minimize the cost. Instead, the bottom exposure is designed to outlet the flushing fluid, thereby demanding a large bottom exposure to fulfil the function. But on the other hand, comparatively large thrust and shear forces are desirable in hard rock drilling. The increased thrust causes the instability of, and increases the compressive force on, the cutting tips, and the extra shear creates a high bending moment on the cutting tips. All of these factors are prone to lead to fracture of the cutting tips; hence a small bottom exposure is favourable for improving the stability of, and reducing the chance of fracture. In a compromise, a bigger bottom exposure than **H** (refer to formula 3) is suggested with a value of 2.5-4 mm.

A small diameter and a thin kerf of drill bit is required in hard rock drilling to minimize the volume of rock to be cut. In a particular rock condition, a certain strength of rock bolt is needed, which means that the diameter and wall thickness of a tubular bolt cannot be changed. The only way to minimize the removal of rock by cutting is to reduce the outer and inner exposures of the cutting tips to their smallest possible values. Meanwhile, the elimination of waterways in the bit design requires the compensation for the loss of water access, therefore large inner and outer exposures are needed. As a result of compromise, the inner and

outer exposures are given a value of 2 mm, which is slightly greater than the suggested value in the previous section on "Bit Design Criteria".

The rake angle determines the drill speed of a bit and the wearability of a cutting tool, and therefore the life of a bit. But the life of the single-pass tubular roof bit is not a very important factor in the design consideration, so a neutral rake angle instead of a negative rake angle is chosen to simplify the design and to obtain a reasonably high penetration rate. Fig. 3.11 is the configuration of the proposed tubular roof bit for hard rock formation.

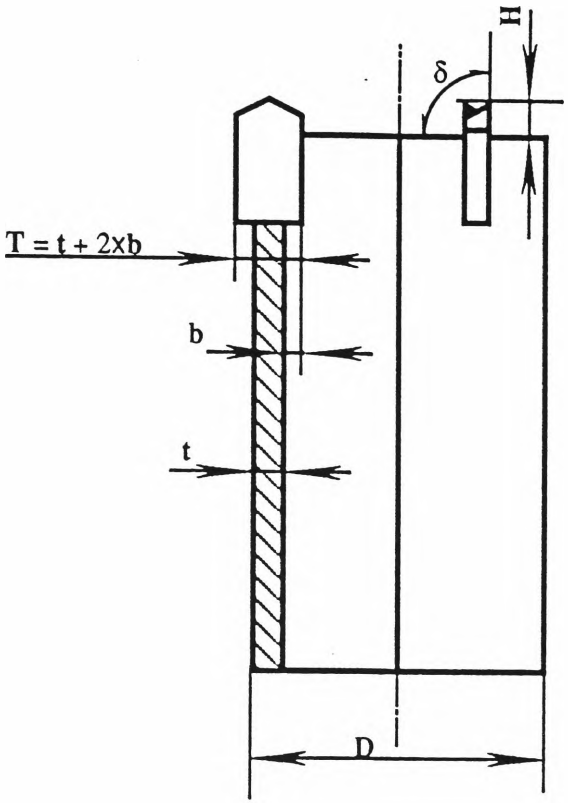

Elevation

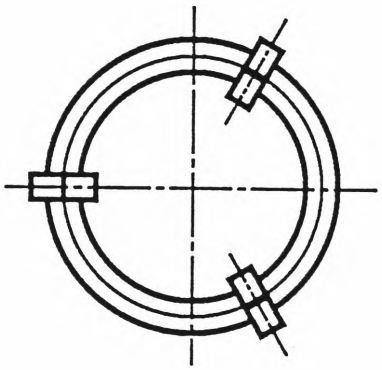

Plan

D outside diameter of tube

t thickness of tubular bolt

T width of cutting tip

H bottom exposure of cutting tools

b outer or inner exposure

δ cutting angle, 90°

Fig. 3.11 Tubular Roof Bit Designed for Hard Rock Formations

3.4.2 Tubular roof bit for soft rock formations

Soft rock formation generally is of less strength and abrasiveness than hard rock. Therefore, the demands of the hardness and wear resistance of cutting materials for a bit used in soft rock conditions are not so high as in the case of a bit for hard rock drilling. The mechanical properties of HSS materials can meet the demands in this case.

The main consideration for design of a soft rock drill bit is to achieve a high drilling speed. So a sharp cutting tool and positive rake is introduced in the design. Correspondingly, larger exposures of the cutting tool are adopted to allow the larger flushing flows needed to cool the cutting tools and to remove rock cuttings. The inner and outer exposures are suggested with a value of 3 mm, whereas a value of 4 mm is given to the bottom exposure. A positive rake with a value of 4° is introduced for the bit used in a soft rock condition to gain a high penetration rate. Waterways are needed on the bit body for a large volume of flushing flow to pass through. An easily manufactured shape, a rectangle, for the waterways is used in this instance. Fig. 3.12 is the diagram of the proposed tubular roof bit to be used for the condition of soft rock formations.

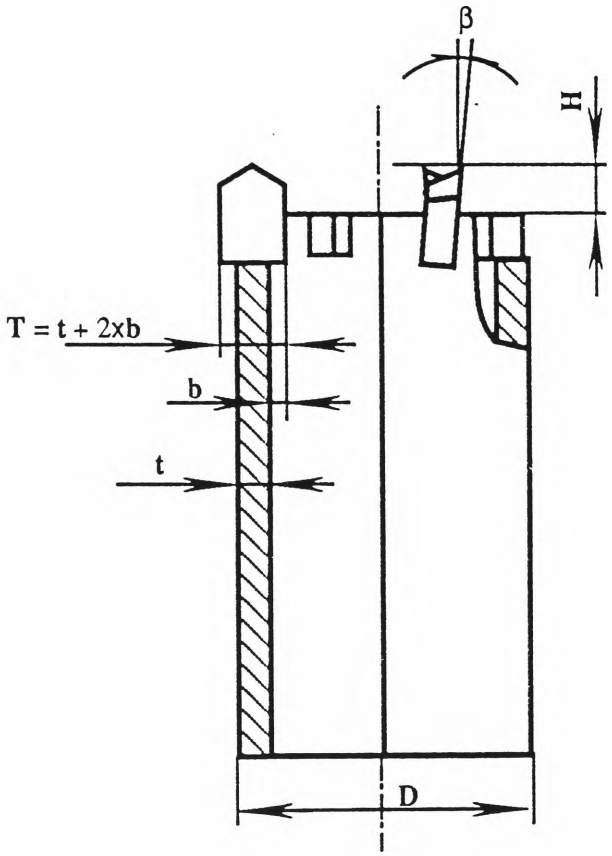

Elevation

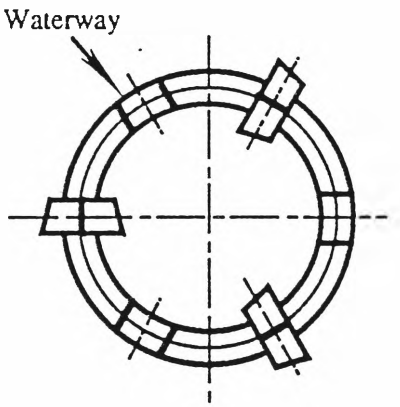

Plan

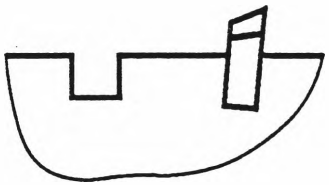

Side elevation of unfolded tube

D outside diameter of tube

t thickness of tubular bolt

T width of cutting tip

H bottom exposure of cutting tools

b outer or inner exposure

β rake angle of cutting tool, 4°

Fig. 3.12 Tubular Roof Bit Designed for Soft Rock Formations

3.4.3 Other factors considered

There are a few other factors affecting the tubular roof bit design which have been considered, but have not been extensively reasoned in the above section due to their lesser importance or flexibility. They are discussed briefly as follows:

1. Configuration of cutting tips

Generally speaking, the symmetrical configuration of the cutting tip shown on Fig. 3.13 is adopted for the tubular roof bit. The reason for this is that the configuration is well accepted and extensively used in drag bits, as well as in exploration coring bit designs, and is readily and commercially available.

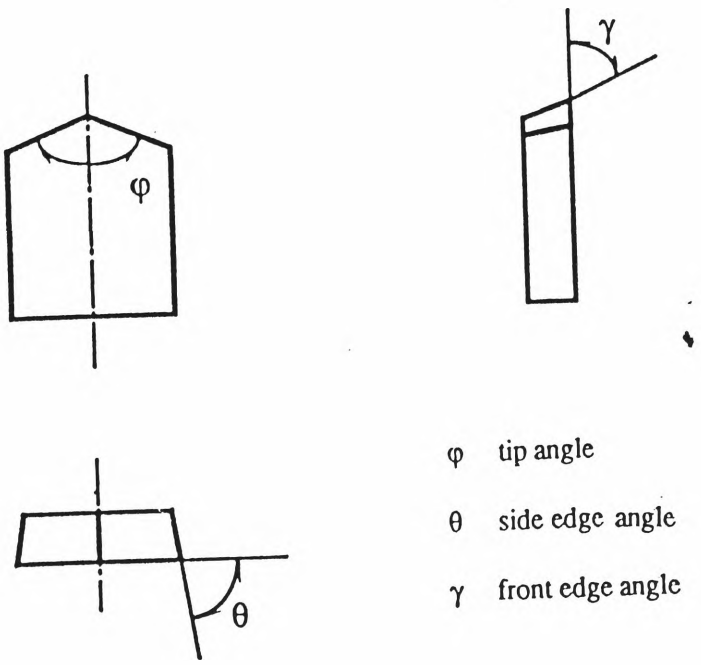

Fig. 3.13 Symmetric Configuration of Cutting Tip

Angles φ, γ and θ are the key parameters of the cutting tip. These values determine whether it is easy or not for the tip to cut into, and to be worn out by, the rock to be drilled.

According to geological coring bit and drag bit design experience (Centre Laboratory, 1979; Fish etc, 1956 and Seco-Titan, 1988), Table 3.8 lists the approximate ranges of these geometrical angles of the cutting tip.

Table 3.8 Range of Geometrical Angles of a Cutting Tip

Designation	φ	γ	θ
Value Range (°)	120 -140	60 -75	70 -90

As stated before, the principal problem to be solved for bits used in hard rock drilling is the wear rate of the cutting tips due to their chipping off, whereas the main consideration for a soft rock drill bit is to achieve a high drilling speed. It is obvious that the smaller these angles, the sharper the tip will be; and the larger the angles, the lower the wear rate of the tip will be. Therefore, the values of the geometrical angles of a cutting tip are given accordingly: the harder the rock to be drilled, the greater the values of the angles adopted.

The other alternative for the configuration of a cutting tip is an off-set shape as shown on Fig. 3.14. The proper positioning of the top points of the tips on a bit body will improve the efficiency of the bit. This situation can be achieved by a bit with off-set tips, as it is able to cut more than one slot on the

bottom of the hole, instead of only one slot as in the case of the bit with a symmetric configuration of cutting tips. But the complicated procedure of the bit manufacture makes the adoption of the off-set tips in the single-pass tubular roof bit uneconomic.

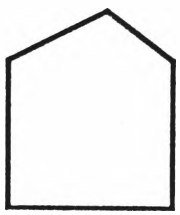

Fig. 3.14 Off-set Configuration of Cutting Tip

2. Rear angle, α

The rear angle, α, is illustrated in Fig. 3.9. Its value depends on both the configuration of the cutting tips (tool angle, γ) and the rake angle, β, and is determined by the formula:

$$\alpha = 90^\circ - (\beta + \gamma)$$

As β varies from 0° to 4°, and γ varies from 60° to 75° in the case of the tubular roof bit, α probably falls in the range of 10° - 25°.

3. Backing up of a cutting tip

The purpose of backing up a cutting tip is to reinforce the cutting tip and to improve its bending strength. The methods to support the tip can be by welding or by ribbed reinforcement, as shown in Fig. 3.15.

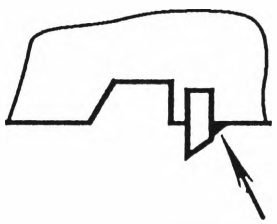

Fig. 3.15 Backing up of Cutting Tip

But the backing up of the cutting tip will greatly complicate the procedure of the manufacture of the bit, that is not economical for the design of the single-pass tubular roof bit. Moreover, the bit life is not of great importance to the tubular roof bit, and the bit without the backing up of cutting tips is still able to furnish the 'single pass' hole. Therefore, the backing up structure has not been adopted in the tubular bit design.

4. Number of cutting tips

The penetration rate V of a drill bit is determined by the following formula (Gao, 1979):

$$V = h_0\ m\ n$$

where: h_0 cutting depth of a tip

m number of cutting tips

n rotary speed of drill rig

From this relationship, it is apparent that the more cutting tips the higher the penetration rate, provided that the cutting depth of a tip and rotary speed of the drill rig are maintained constant. On the other hand, however, the more tips that are set on a bit, the more the costly bit. This trend contravenes the basic design concept of the single-pass tubular roof bit, which requires a bit with a simple configuration and a low cost. As a compromise, three cutting tips are suggested to be set on a tubular roof bit to furnish the design target and also to provide the bit with a reasonable penetration rate. In some extremely hard formations, either more cutting tips or harder cutting material may have to used to overcome the short life of the tips.

5. Water slots

Water slots are the slot along the axis of a drill bit on the inner or outer wall of the bit body as shown in Fig 3.16. They have similar functions to waterways. In order to simplify the design of, and to minimise the cost of a tubular roof bit, water slots have not been adopted, as the inner and outer exposures of cutting tips have already provided sufficient access for the drilling flow.

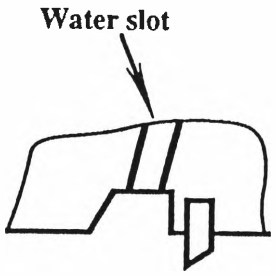

Fig. 3.16 Water Slot on a Bit Body

Chapter Four

Rock Mechanics and Drillability

4.1 General Remarks

Bolthole drilling is one of the most important procedures in rock reinforcement by the rockbolting method. Without making a suitable bolthole, a rockbolt cannot be properly installed in a rock-mass, therefore it will not be able effectively to support the rock-mass. For example, expansion-shell bolts are adversely affected by oversize boltholes, which causes the contact area between the shells and the hole wall to be reduced, thus decreasing the anchorage capacity. In addition, the efficiency of bolthole drilling will largely affect the economy of a rockbolting system, as a high penetration rate for drilling a bolthole not only saves the time spent on the individual hole drilling, but also reduces the period of the whole rock reinforcement project. The latter means that a quick and safe working condition is furnished for the following mining processes, and is of great importance in terms of economy.

Generally speaking, most methods employed for rock comminution in the rock drilling field are catalogued into mechanical areas, like rotary, percussive, down-the-hole, rotary-percussive drilling and so on. The common factors in all these methods are: to exert some mechanical forces on the rock to be drilled through some sort of cutting tool, and to spall the rock off from its original

mass. In other words, rock drilling substantially is a process of breaking rock into small chips by some mechanical means. Consequently, the improvement and consummation of rock drilling methods and their efficiency, to a large extent, depends on an understanding of the mechanical properties of rocks, especially those properties related with rock comminution by mechanical means.

In this chapter, the general rock classification and rock mechanical properties related to rotary drilling are outlined, and rock drillability will be discussed.

4.2 Rock Classification and Its Mechanical Properties (Beavis, 1985)

Rock materials may be classified in a number of ways, depending on the purpose for which the classification is required. In a geological classification, the main considerations are the mineral composition of the rock, the physical and chemical interaction between the mineral grains, and the processes which have affected the rock during and after its formation. In an engineering classification of rock material, emphasis is placed on those aspects which influence engineering behaviour. Geological classifications, although only having a very limited application in engineering geology, cannot be ignored, as often an engineering meaning is attached to a rock name; the classifications do highlight some features of a rock which can be important to the engineer.

4.2.1 Geological classification of rocks

Geological classifications include the processes involved in rock formation, the mineral composition, texture and fabric. Fundamentally, the main geological classes are genetic, so that rocks are classified according to their origin and method of formation, and are placed in one of three categories:

1. **Igneous Rocks** which are formed by the solidification of molten silicates injected upwards towards the Earth's surface and sometimes poured out at the surface. The molten silicate magma may, or may not, reach the surface, but in any event the igneous rock body may be exposed later after the removal of overlying rock by processes of erosion and denudation.

2. **Sedimentary Rocks** are derived from the weathering and denudation of older rocks. Water, wind, ice and other agents result in the breakdown of rock materials at the Earth's surface. The products of rock disintegration may be left in place or may be transported, later to be laid down elsewhere as sedimentary deposits. Under increasing loads resulting from continued deposition, earlier deposited sediments become dewatered, compacted and consolidated into sedimentary rocks. Such rocks occur in beds which have a definite order of superposition. Older beds, laid down during earlier episodes, will always underlie younger beds laid down during later episodes of deposition unless there has been some structural upheaval causing beds to be folded, contorted and overturned. Within sedimentary rocks are contained fossil debris representing the remains of earlier forms of animal and plant life. Such fossil or palaeontological

data are of great value in determining the relative ages of different sedimentary deposits.

3. **Metamorphic Rocks** are formed from pre-existing igneous and sedimentary rocks by the action of great heat and pressure or by chemical alteration, all resulting from major processes acting within the crust of the Earth. These metamorphic rocks exhibit all the indications of such drastic mechanisms. Metamorphic rocks of an earlier metamorphic epoch may be altered (metamorphosed) further by a later episode.

4.2.2 Mechanical classification of rocks

Because the geological classifications of rock have such limited applications in engineering, many attempts have been made to develop a mechanical, or engineering, classification. No such classification, which would meet all requirements, has yet been formulated.

Tables 4.1 & 4.2 are the engineering classification of *intact* rock (Deere etc, 1966), which has received a wide acceptance in the field of rock engineering.

Table 4.1 Engineering Classification of Intact Rock on the Basis of Uniaxial Compressive Strength

Class	Description	Uniaxial Compressive Strength psi	Uniaxial Compressive Strength MN/m^2	Rock Material
A	Very high strength	> 32,000	~ 220	Quartzite; diabase; dense basalts
B	High strength	16,000–32,000	~ 110 to ~ 220	Majority of igneous rocks; strong metamorphic rocks; weakly cemented sandstones; hard shales; majority of limestones; dolomites
C	Medium strength	8,000–16,000	~ 55 to ~ 110	Many shales; porous sandstones and limestones; schistose varieties of metamorphic rocks
D	Low strength	4,000–8,000	~ 28 to ~ 55	Porous low-density rocks; friable sandstone; tuff; clay shales; weathered and chemically altered rocks of any lithology
E	Very low strength	< 4,000	< 28	

Table 4.2 Engineering Classification of Intact Rock on the Basis of Uniaxial Modulus Ratio

Class	Description	Modulus ratio, E_{t50}/σ_{ult}
H	High	> 500
M	Average (medium)	200–500
L	Low	< 200

The classification system pertains to intact rock and to rock in-situ. Intact rock classification presupposes rock testing. The classification is based on two important engineering properties of rock, namely: the uniaxial compressive strength and the tangent modulus of elasticity. Table 4.1 shows the engineering classification of intact rock on the basis of uniaxial compressive strength, and the rock strength classes follow a geometric progression.

Table 4.2 shows the engineering classification of intact rock on the basis of modulus ratio M_R:

$$M_R = E_{t50} / \sigma_{ult}$$

where E_{t50} tangent modulus at 50% ultimate compressive strength of the rock, and

σ_{ult} uniaxial ultimate compressive strength.

Based on this classification, rocks are classified both by strength and modulus ratio as AM, BL, BH and CM, for example.

Beavis (1985) suggests that the classification of rock material for engineering purposes requires a statement on the following criteria, apart from what has been established by Deere's classification:

1. Petrography

Petrography basically includes the composition, texture and fabric of a rock, and the degree of weathering.

2. Homogeneity

Such an assessment is largely qualitative and subjective. In homogeneous material, the mineral constituents are so distributed that a small sample cut from any part of the material will have the same constituents in the same proportions, and will have the same properties as the material as a whole, although it may not be isotropic.

3. Isotropy

Anisotropy is a measure of the directional properties of the rock. Statistically, the rock will be isotropic if all mineral grains have random orientation of both dimensional and crystallographic parameters. Isotropy also requires that a plane of equal dimensions intersecting the rock in any direction exposes an equal number of grains. It is necessary, if there is any anisotropy, to specify its nature and orientation.

4.2.3 Rock mechanical properties

Generally, the mechanical properties of a material characterize its reaction to the effect of the force field of its environment. Particularly, the mechanical properties of rocks depend upon:

1) the nature of the rock substance,

2) the stratigraphy of the rock in situ,

3) rock defects, and

4) testing methodology.

According to Yang (1979), the most important mechanical properties that are closely correlated with rock drilling are hardness, strength, elasticity, plasticity and abrasiveness .

1. Rock hardness

Hardness of rock is the resistance to abrasion. Every rock has a range of hardness that ultimately depends on the strength of the chemical bonds.

To rate hardness of rocks, the empirical Mohs' hardness scale is used (refer to Table 4.3, after Jumikis, 1983). This method was originally used for assessing minerals, and was adopted to grade rock hardness later. Rocks of a higher Mohs' number scratch those of a lower number. This scale, being arbitrary, does not provide an absolute measure of hardness. The interval between any two successive minerals on the scale are similar, with the exception of the corundum-diamond interval. This method is recommended to be used to assess homogeneous rock. Rocks like sandstone with relatively weak cementation could give a false hardness value. They contain hard grains of quartz, and when scratched these particles could be torn from the matrix, thus giving a false measure of hardness. This method has the advantage of simplicity and cheapness, and may be carried out on site.

Table 4.3 Mohs' Scale of Hardness of Minerals

Number of relative hardness scale or rating *H*	Mineral	Chemical composition	Remarks
1	2	3	4
1	Talc	$Mg_3Si_4O_{10}(OH)_2$	Softest; can be scratched by fingernail.
2	Gypsum	$CaSO_4 \cdot 2H_2O$	Can be scratched by fingernail.
3	Calcite	$CaCO_3$	A copper penny or a brass pin can scratch calcite.
4	Fluorite	CaF_2	Fluorspar. May be scratched easily by a steel point.
5	Apatite	$Ca_5F(PO_4)_3$	Any of the calcium phosphate minerals. Can be scratched by a knife. A window glass may be rated as $H = 5.5$ on the hardness scale.
6	Orthoclase (feldspars)	$KAlSi_3O_8$	Can be scratched by a knife blade of a good-quality steel; a hardened steel file may be rated as $H = 6.5$
7	Quartz	SiO_2	Scratches steel, glass, and all of the minerals whose $H < 7$.
8	Topaz	$Al_2SiO_4(F, OH)_2$	Great hardness. A valuable jewelry stone.
9	Corundum	Al_2O_3	Harder than any other natural mineral except diamond. An important industrial abrasive and refractory. Has many gem varieties, among them ruby and sapphire.
10	Diamond	C	The hardest substance known; not all diamonds are of the same hardness, however.

The other types of tests which have been used to measure the hardness of rocks include indentation tests, such as the Knoop (Winchell, 1946) and Vickers (Das, 1974) tests which determine the microhardness of individual rock minerals, and dynamic or rebound tests, such as the Shore scleroscope and the Schmidt impact hammer tests. The dynamic or rebound tests employ a moving indenter to strike the test rock specimen, and any plastic or yielding material behaviour produced by the impact will reduce the elastic energy available to

rebound the indenter. The height of rebound is taken as a measure of the hardness of the material (Int. Soc. of Rock Mechanics, 1978).

2. Strength of Rock Material

In a mechanical sense, the strength of rock material is defined as the ability to resist stress without large scale failure. Small scale failure with the development of microfractures occurs under stresses well below the strength of the rock as a whole. As in rock, large scale failure only occurs beyond the elastic stress limit, which is the most commonly used parameter, especially for brittle rocks.

Among the various strength types of rock material, uniaxial or unconfined compressive strength is the most commonly used parameter in evaluating drillability. The uniaxial strength is defined as the failure of the rock specimen subjected to a compressive stress in one direction. Depending upon the constraint offered by the load-bearing platens of the compression testing machine, as well as upon the quality of the parallel end surfaces (smooth or rough), rock core specimens tested for their unconfined compression strength fail either in tension or in shear. Fig. 4.1 shows some of the modes of failure, and the stress-strain diagrams, of rock in unconfined compression (Jumikis, 1983).

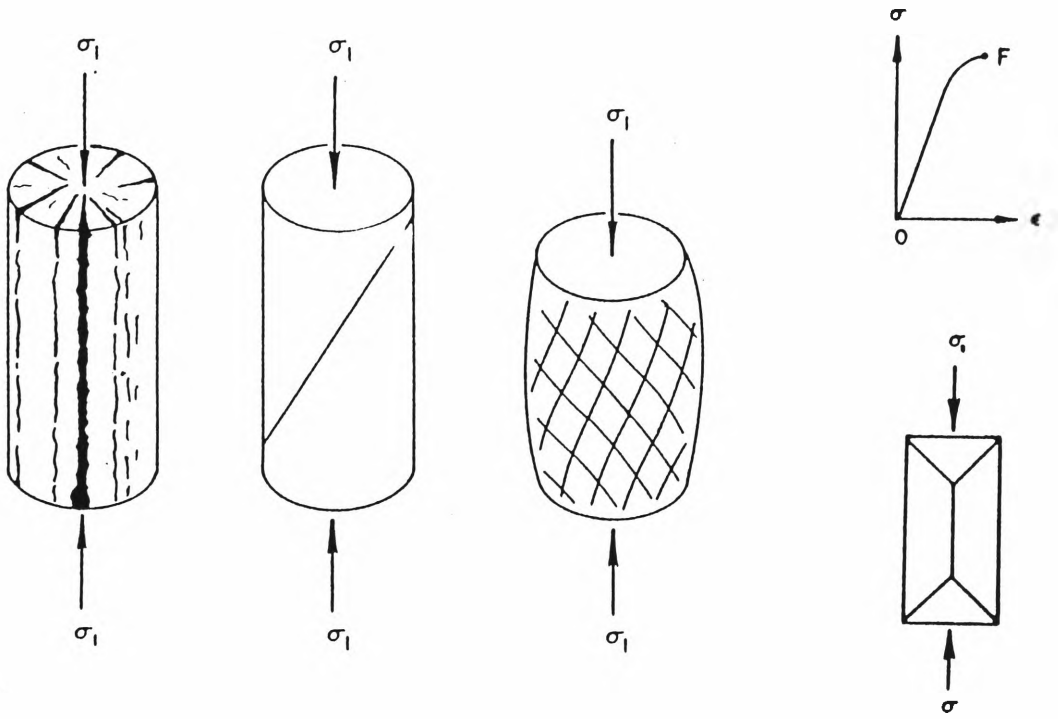

Fig. 4.1 Some Modes of Failure, & Stress-Strain, of Rock in Unconfined Compression

3. Elasticity

Under normal temperatures and pressures, rocks usually tend to exhibit a brittle kind of rupture of failure mechanism. The term 'fracture' is used here in the sense of brittle fracture or failure; this implies a complete loss of cohesion across a surface.

For most rocks, the stress-strain diagrams take an approximately linear course, like that of a perfectly elastic solid where stress is proportional to strain and where there is no yield point, ending abruptly in failure at point F on the

diagram, as in Fig. 4.2. If the relationship $\sigma = E\,\varepsilon$ for such a material holds strictly, the material is referred to as linear-elastic. Generally, rocks under ordinary compression loads deform very little before they break.

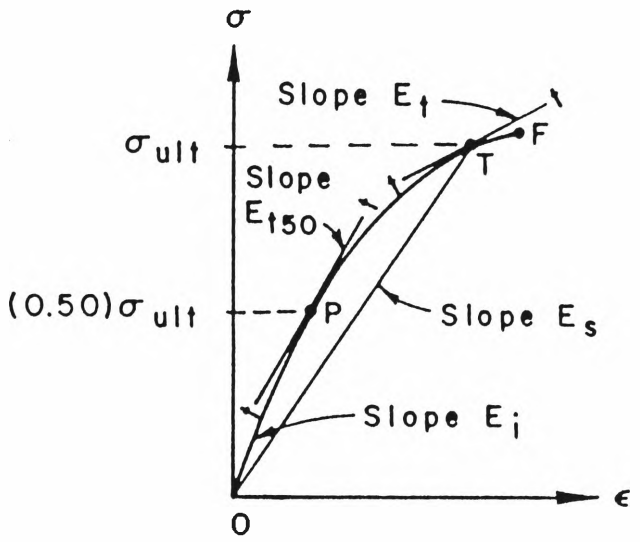

Fig. 4.2 Stress-strain Diagram of Most Rocks

Fig. 4.2 illustrates a stress-strain diagram for a perfectly elastic material. Because of its nature, the diagram shows three kinds of modulus of elasticity, namely:

1) E_i the initial tangent modulus at zero load,

2) E_t the tangent modulus at a particular point **T** on the stress-strain diagram for a specified stress (also shown is the 50% tangent at point **P**), and

3) E_s the secant modulus for a particular point **T**.

For rock, normally the initial tangent modulus E_i is referred to because it is the most accurately obtained under test conditions.

Because of many factors involved in rock strength, in rock engineering practice, when designing in rock and performing stability analyses of rocks, certain idealizations and assumptions as to the nature of rock as a construction material are usually made. The following are some of the most important and most frequently made idealizations (Jumikis, 1983):

1) The rock is assumed to be a continuous, homogeneous, isotropic, linear-elastic material.
2) This material obeys Hooke's law of proportionality between stress and strain; that is, the strains are linear functions of stresses.
3) The deformations (strains) of the loaded rock material are so small that they may be neglected in setting up equilibrium conditions.

These assumptions are supported to a sufficient degree for most practical applications by measurements of the observed strains within the elastic range in metals and rocks, with some exceptions of porous solids and other materials.

In certain rock mechanics analyses, one thus usually adheres to the fundamental theory of elasticity, to the basic elasticity constants such as Young's Modulus of elasticity **E**, and Poisson's ratio $\mu = 1/\mathbf{m}$, where $\mathbf{m} = 1/\mu$ is the Poisson's number.

4. Plasticity

Plasticity of a solid material is its property to be continuously and permanently deformed, that is, a property to change shape in any direction without rupture under a stress equal to or exceeding the yield value of the material. The plastic deformation of a material is the permanent deformation after complete unloading of the material, assuming the unloading to be elastic. In the plastic state, permanent deformation of a material may occur without fracture. The term 'fracture' implies the appearance of distinct surfaces of separation in the material.

The conditions prevailing in the deeper strata of rock, such as long duration of small differences in principal stresses, elevated temperatures, and high average pressure, all contribute to plastic deformations of rocks.

The plastic state of matter is of considerable interest to many branches of science and of engineering, among them rock mechanics and soil mechanics. The changes in minerals and rocks brought about by plastic deformation are in many respects analogous to certain phenomena observed in the changes in the structure of metals.

5. Abrasiveness

Rock abrasiveness is the abrasive effect of the rock on other materials (e.g. the cutting tools of a drill bit) as a result of contact with the rock. The abrasiveness of a rock, to a certain degree, depends on the composition and structure of the rock, especially the quartz content and the size of the rock-forming minerals.

Fig. 4.3 is a the result of an experiment (Yang, 1979), showing the volume worn out of a cutting tool under certain conditions by rocks containing various percentages of quartz. It is apparently from this experiment that the abrasiveness of a rock to a cutting tool is in proportion with the quartz content of the rock.

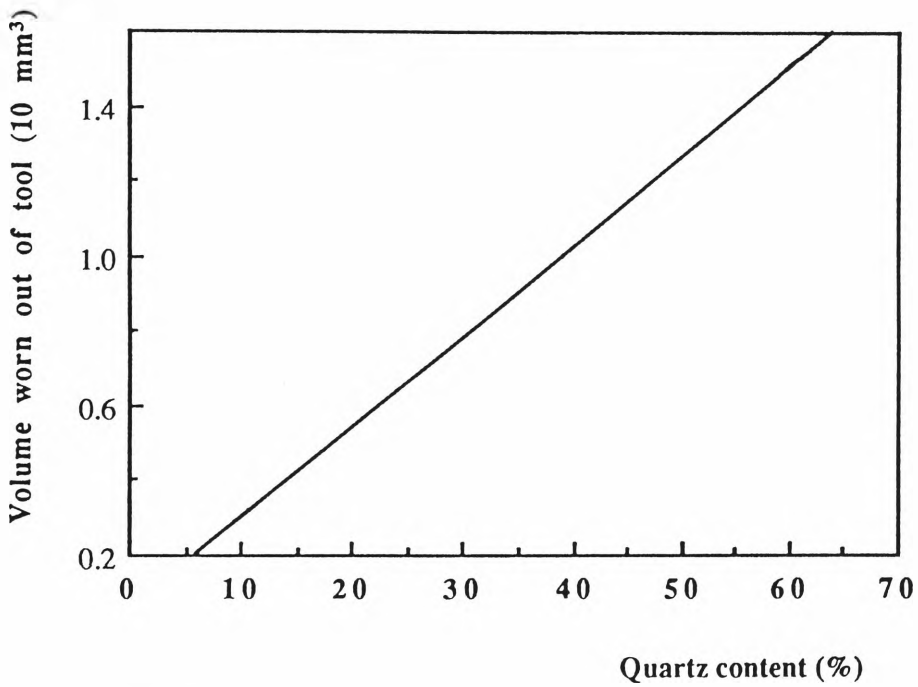

Fig. 4.3 Wearing Quantity of a Cutting Tool by Rocks with Different Quartz Contents

The size of the rock-forming minerals is macroscopically displayed by the roughness of a rock surface. Generally speaking, the larger the minerals in a rock, the rougher the rock appears, thus the higher the abrasiveness of the rocks.

The rock abrasiveness tests can be grouped in three categories:

1) Abrasive Wear Impact Tests, including Los Angeles abrasion test (ASTM, 1977), sand blast test (ASTM, 1977) and Burbank test (Burbank, 1955).
2) Abrasive Wear with Pressure Test, including the Dorry test (Obert etc, 1946) and bit wear test (Selmer-Olsen etc, 1970; White, 1969; & Goodrich, 1961), and
3) Attrition Tests (Int. Soc. of Rock Mechanics, 1978).

4.3 Rock Drillability

Drilling is a considerable item of the total rockbolting costs. An engineering geologist is often asked to indicate parameters which may serve to assess the resistance of rocks to a bolt-hole drilling machine. Nevertheless, drillability may be adopted for the purpose.

Rock drillability in a broad sense can refer to the ease with which rock can be drilled, it is a comprehensive index measuring the ability of a rock to resist being comminuted by cutting tools during the drilling process.

A rock drillability index is expressed in different ways in different fields rather than in a unique way. For instance, penetration rate (meters drilled per unit time) is used in core drilling for geological exploration, the drillability is expressed with the index of time between penetration speed and footage drilled in oil field work, and in impact drilling the drillability is explained as an index of the amount of work consumed per unit of rock crushed.

4.3.1 Factors affecting drillability

There are many factors which may affect the drillability of a rock. First of all, the rock physical properties are the factors which dominantly influence the rock drillability, followed by the factors like: the comminution method, the structure and quality of the cutting tools, drilling parameters, and so on.

1. Rock Mechanical Properties

According to McGregor (1967), the rock properties which influence drillability include hardness, toughness, abrasiveness, and grain size.

The hardness of a rock depends not only upon the hardnesses of the individual minerals concerned, which can be assessed in terms of Moh's scale, but also upon the bond strength that exists between the mineral grains. For instance, rock like sandstone with relatively weak cemetation could gives a false hardness value when hard grains of quartz contained in are scratched in a test. The harder the rock the stronger the bit which is required for drilling since higher pressures need to be exerted. Indeed, Furby (1964) suggested that rock drillability could be correlated with the results obtained by testing with a Schmidt hammer.

Toughness is related to hardness and has been defined by Deere and Miller (1966) as the ability of a material to absorb energy during plastic deformation

and represents the work required to bring about fracture. It can be assessed by an impact test.

With respect to drilling, abrasiveness may be regarded as the ability of a rock to wear away drill bits. This property is also closely related to hardness and in addition, is influenced by particle shape and texture. Bit wear is a more significant problem in rotary drilling than percussive drilling. The size of the fragments produced during drilling operations influence abrasiveness. For example, large fragments may cause scratching but comparatively little wear whereas the production of dust in tougher but less abrasive rock causes polishing. This may lead to the development of high skin hardness on tungsten carbide bits which in turn may cause them to spall. Even diamonds lose their cutting ability upon polishing. Generally coarse grained rocks can be drilled more quickly than can fine grained varieties or those in which the grain size is variable.

2. Rock Mass Properties

Rock mass properties which may affect the drillability include the bedding or schistosity planes and discontinuities existing in the rock mass to be drilled.

The ease of drilling in rocks in which there are many discontinuities is influenced by their orientation in relation to the drillhole. Drilling over an open discontinuity means that part of the energy controlling drill penetration is lost. Where a drillhole crosses discontinuities at a low angle then this may cause the bit to stick. It may also lead to excessive wear and to the hole going off line. Drilling

across the dip is generally less difficult than drilling with it. If the ground is badly broken then the drillhole may require casing. Where discontinuities are filled with clay this may penetrate the flush holes in the bit, causing it to bind or deviate from alignment. As a consequence the rate of drilling is generally quicker if the hole runs at a high angle to the discontinuities.

3. Other Factors

The rock comminution method affects the efficiency of cutting to a great extent. The so-called comminution method actually means the way by which a cutting tool acts on a rock to be cut, e.g. the nature of load or force, energy consumed and the structure of the cutting tools. The same rock indicates different drillability when different methods of drilling using diverse rock-breaking tools are employed, and also when different designs of equipment of the same category are used. This comparative study based on the drillability factor of the respective rock helps in a comparative assessment of different methods and equipment as applied to the particular rock. Drilling parameters which influence the drilling productivity include the thrust imposed on a drill bit, rotary torque and rotary rate, impact load and impact frequency.

It is apparent, from the above analysis, that rock drillability is correlated with many factors, and it is also difficult and complicated to find out the quantitative interrelation between these factors and drillability. Therefore, rock drillability is usually only determined by experiment under certain comminution methods and drilling parameters.

4.3.2 Classification of rock drillability

There are many methods to determine and classify rock drillability, but the most common acceptable means is according to the rock penetration rate. The pure penetration rate is used as the index of drillability which is obtained by drilling with certain equipment and tools, and according to a fixed technical specification. By this method, the index has to be revised from time to time, at least once in a few years, as the absolute and correlative indexes between rocks are changed with the updating of drilling techniques and equipment. For every revision, a large quantity of work has be to put into testing and statistics.

The classification depending on pure penetration rate has a few disadvantages in practice:

1) It is impossible to determine the drillability index of certain rocks in the field by a scientific means to guide drilling production, but depends upon experience which may vary largely from person to person.
2) The existing classification table is out of date and can no longer be used as a guide, while a great effort has to be made in order to produce a new revision.
3) The drillability is severely affected by the technical specification, like bit type and drilling parameters. The ratio relation of drillability index between rocks will change with the change of technical specification, so an index of one rock cannot be determined by the index of the other known rock.

Due to the above disadvantages, some attempt to work out the effect and the relation of rock physical properties to drillability has been made worldwide. Some new type of classification of rock drillability reflecting the inner link between rock physical properties and its drillability has been established. The following list indicates some of the outcomes of the research catalogued in respect to drilling methods.

1. Rotary Drilling Method

Tsoutrelis (1969) carried out a drillability study with a rotary hard metal bit. He concluded that the penetration rate correlated significantly with the compressive strength of the rock, and that the method could be used to predict accurately the compressive strength of an unknown rock to be drilled. Paone et. al. conducted drillability studies with both surface-set diamond bits (1963) and impregnated diamond bits (1966) in both the laboratory and the field. Fig. 4.4 (Howarth, 1986) shows a comparison of their work. The penetration rates seem to correlate quite well with compressive strengths. Other drillability studies (Duklet etc, 1981 & Warren, 1981) with rotary drilling methods all show a similar tendency that the uniaxial compressive strength is a useful rock strength parameter for prediction of the penetration rates. The other mechanical properties of a rock that may affect the drillability are Shore hardness, Young's modulus, shear modulus, abrasiveness and quartz content.

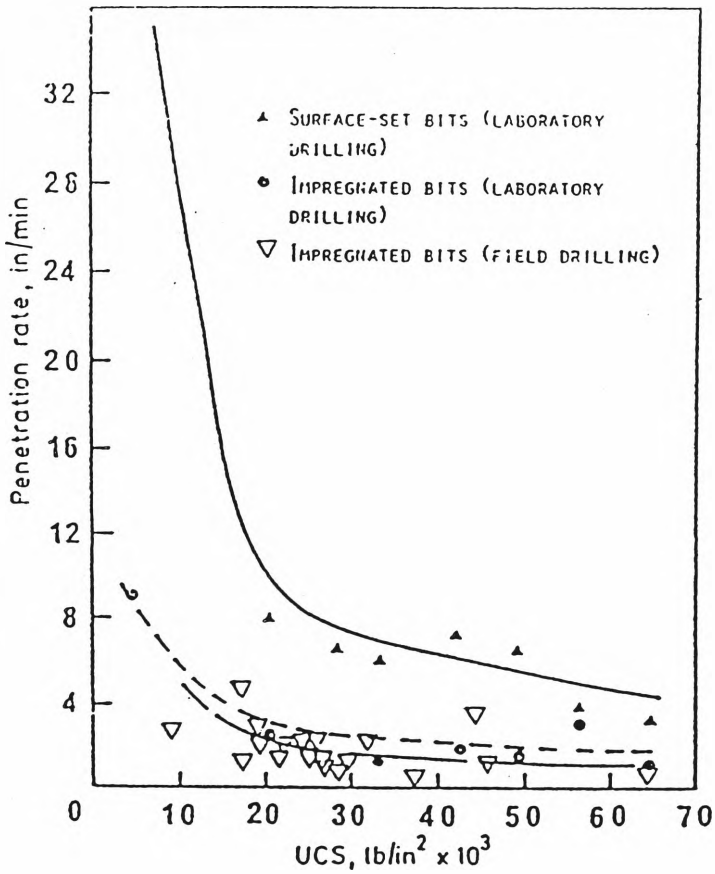

Fig. 4.4 Penetration Rate of Diamond Drill Bits vs. Uniaxial Compressive Strength of Intact Rock

Fowell (1970) commented that uniaxial compressive strength is the most commonly used parameter of drillability, though it is not a reliable one, as it fails to take into account the abrasive properties of the rock and bears no relationship to the cutting process employed by cutting tools. Much care is required in the preparation of the samples and the method of applying the compressive load is also important. Many samples have to be tested to obtain a reliable estimate of the compressive strength (Yamaguchi, 1970).

2. Percussion Drilling Method

The typical drillability study for the percussion drilling method was conducted by Selmer-Olsen et al. (1970). The authors introduced the drilling rate index (DRI), established by correlating drilling results and laboratory-measured properties of rock samples. The drilling rate in cm/min (hammer drill, simple edge and carbide tips) is about 65% of the DRI value.

The DRI is estimated on the basis of two parameters (Selmer-Olsen et al., 1970): the rate of laboratory drilling (Sievers' test) and the result of the Swedish test of brittleness, which is essentially a shatter test. The DRI, expressing the rock properties that are important in drilling, namely hardness, strength, brittleness and abrasivety, is a relative drillability value given to various rocks. The higher the DRI value, the greater is the drillability of the rock. Table 4.4 is the typical values of DRI in various rock types.

Table 4.4 DRI Value in Some Typical Rock Types

Rock type	tanconite	quartzite	slate	marble
DRI value	25 - 45	30 - 50	50 - 70	70 - 90

Later, the field drillability tests conducted by Blindheim (1979) also showed a close correlation between drilling rate and the empirical drilling rate index, DRI (refer to Fig. 4.5).

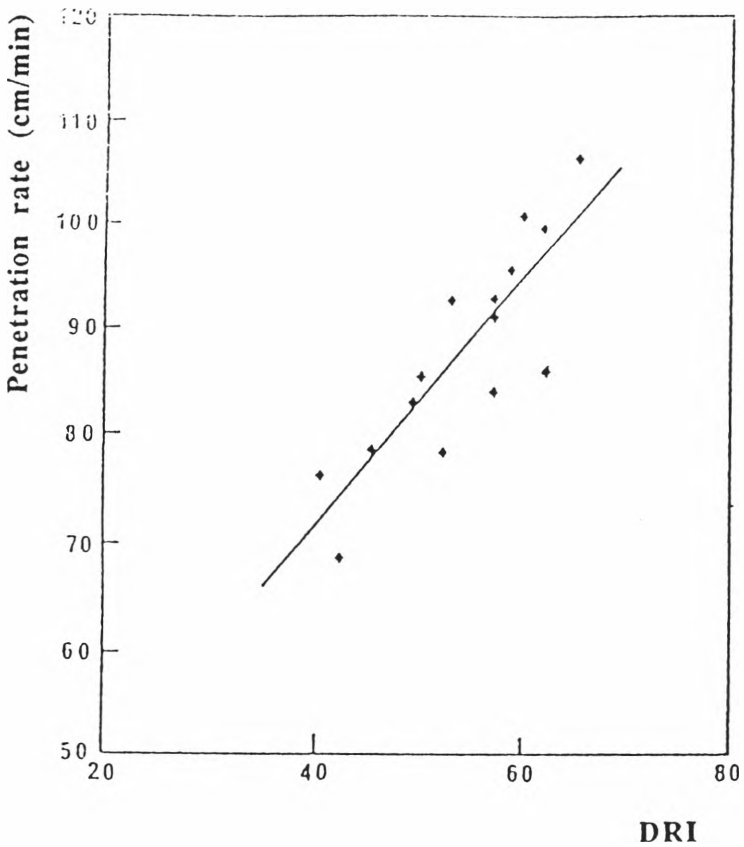

Fig. 4.5 Measured Penetration Rate vs. DRI

One disadvantage of the method is that it requires equipment that is unique to the test procedures.

A drop-test studied by Hartman (1959) showed that a wedge was the most effective shape of indenter for percussion drilling when assessed in terms of specific energy consumption. A drilling-rate model was proposed that incorporated the volume of the bit crater produced in the drop test as the parameter expressing the behaviour of the rock under the action of a drill bit, which is expressed by following formula:

$$PR = \frac{VBW}{A}$$

where	**PR**	penetration rate
	V	volume of crater produced by single blow in drop test
	B	frequency of blows
	W	number of bit wings
	A	cross-sectional area of drill-hole

There are a few other drillability classifications based on the physical properties of rock, for instance, the pendular-ball rock hardness (Yang, 1979), abrasive hardness and shear strength of rock (Yang, 1979) and rock dynamic strength and abrasiveness (Gao, 1979).

In summary, although no single physical property of a rock is completely satisfactory as a predictor of penetration rate, all the physical properties have been found to be highly correlated with each other and some single property demonstrates promising potential in predicting the drillability of a rock. It is almost certain that site investigation data will improve drillability prediction, but until new, low-cost methods are available, cost-benefit consideration will continue to favour elementary prediction methods.

Diamond rotary drilling performance can be predicted through a knowledge of the ultimate compressive strength of the rock, whereas percussion drilling penetration rates can be usefully predicted by means of an empirical indenter drop test, which closely resembles the physical action of a percussion drill.

Chapter Five

Mechanisms of Rock Comminution by Drag-bit and Bit Wear Analysis

5.1 General Remarks

Material cutting and drilling can be traced back to about 4,000 BC when Egyptians drilled holes in stone to make tombs by rotating a bow device or simply by rotating a tool by hand, although the first report of scientific studies of cutting did not appear until 1851 by Cocquilhat (Black, 1961). Since then, a series of research projects regarding metal cutting processes have been reported, and the theory of metal cutting has been gradually developed. The review by Finnie (1956) gives an excellent account of metal-cutting analysis during the preceding 100 years.

It is only over the past 40 years or so that a serious attempt has been made to understand how rock breaks under the action of mechanical devices, though engineers have been inventing and using machines to dig rock for more than 100 years. For a long time drilling tools were, and in some cases still are, being developed without a proper appreciation of the rock breaking processes on which their actions depend (Roxborough, 1986). Mechanical rock fragmentation has been

the subject of important scientific investigations, but the mechanism of rock reaction to the drilling processes involved has not been fully understood because of the influence on the processes by rock properties, the type of rock attack and other factors (Schmidt et al., 1988).

Bit wear in rock drilling is a major factor in determining the cost of drilling and may determine the drilling method for a given rock. Wear decreases penetration rates and increases drilling forces, which in return may cause major fracture of cutting tips. The type and degree of the wear depends on the strength and abrasiveness of the rock and on the properties of the carbide tips. In the four decades of the use of tungsten carbide alloys for cutting rocks, there has been considerable research on the wear of tungsten carbide tips, but very few effects have been made on the quantitative analysis of the stresses on the cutting edge, which may be the main cause of the wear of a cutting tip.

In this chapter, the rock cutting process is analysed. The mechanisms of rock cutting by a drag-bit and the wear of the bit tips are reviewed. Also, a three dimensional finite element program, STRAND5, is introduced to analyse the stress distribution on, and the possible failure region of, a cutting tip of a drag-bit.

5.2 Rock Cutting Process

A drag-bit is used to make boltholes in soft and medium-hard rocks, such as coal, shale, marls, some sandstones, lignite, salt, gypsum potash, and

weaker sediments in general. The evolution of bit design for such applications has largely followed empirical lines, and has resulted in a range of forms. After reviewing the characteristics of available drag-bits, Fish et al. (1956) recommended the bit illustrated in Fig. 5.1 for use in carboniferous sediments. Most of the currently used drag-bits for the bolthole drilling are different versions of the one recommended by Fish et al.

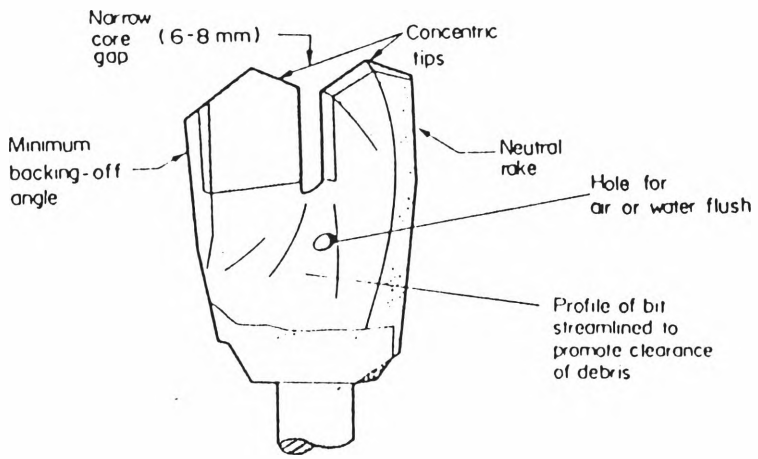

Fig. 5.1 Features of Drag-Bit Proposed by Fish et al. (1956)

The bit presents a continuous cutting edge or edges to the rock on a helical path, and the process is similar to that found by dragging a material on a straight path past the chisel edge of a cutting tool. The cutting tips are comprised of tungsten carbide inserts, mounted on the bit body.

The process of rock drilling with a drag-bit is a process whereby the hard metal tips are subject to load, ie. thrust and torque, and comminute the rock while being worn by the rock being drilled.

Rock cutting with a drag-bit can be seen as two stages, tools cutting into rock under thrust, and ploughing of the rock under rotary torque, which is explained in detail in the following paragraphs.

5.2.1 Process for a tip to cut into rock

The prerequisite for a cutting tip to cut into rock is that the compressive force per unit area imposed on the rock by the tip should be greater than or at least equal to the ultimate compressive stress of the rock (Gao, 1979), that is:

$$P_y / S \geq \sigma \qquad (5.1)$$

where P_y thrust imposed on a cutting tip

S the contact area between a cutting tip and rock drilled

σ ultimate compressive stress of rock.

If this prerequisite cannot be met, the cutting tips of a bit then will not be able to cut the rock, but will be worn out on the rock surface. It is essential that sufficient tip thrust should be guaranteed, so that effective cutting can be created.

Fig. 5.2 shows the load distribution when the cutting tip of a bit cuts into rock.

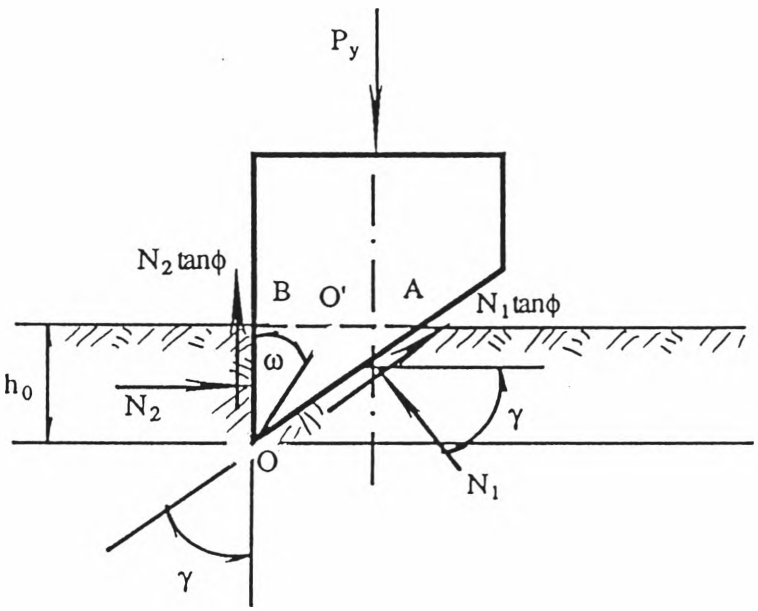

Fig. 5.2 Load Distribution on a Tip when Cutting into Rock

A wedged cutting tip with a tool angle γ under a thrust of P_y cuts rock to a depth of h_0. Because of the back wedged plane of the tool, the edge point of the tool is not vertically cutting into the rock, but along an assumed line $\overline{0'0}$, which forms a angle of ω with the vertical, into the rock. Therefore, the normal compression N_2 and friction resistance $N_2 \tan\phi$, where $\tan\phi$ is equal to the frictional coefficient f between the tool and the rock, will occur on the front plane of the tool. A normal compression N_1 and friction resistance $N_1 \tan\phi$ will occur on the clearance plane of the tool.

The balance of all acting forces is as following:

$$\Sigma F_x = 0$$

$$N_2 = N_1\cos\gamma - N_1\tan\phi\sin\gamma = N_1\cos(\gamma+\phi)/\cos\phi \qquad (5.2)$$

$$\Sigma F_y = 0$$

$$\begin{aligned} P_y &= N_2\tan\phi + N_1\sin\gamma + N_1\tan\phi\cos\gamma \\ &= N_2\tan\phi + N_1\sin(\gamma+\phi)/\cos\phi \end{aligned} \qquad (5.3)$$

Substituting (5.2) into (5.3), then:

$$\begin{aligned} P_y &= N_1\cos(\gamma+\phi)\tan\phi/\cos\phi + N_1\sin(\gamma+\phi)/\cos\phi \\ &= N_1\sin(\gamma+2\phi)/\cos^2\phi \end{aligned} \qquad (5.4)$$

Again, according to the prerequisite of rock cutting (5.1), then approximately:

$$N_1 = \sigma_n b_0 \overline{OA} = \sigma\sin\gamma b_0 h_0/\cos\beta = h_0 b_0 \sigma\tan\gamma \qquad (5.5)$$

where b_0 the width of the cutting tool.

σ_n normal compressive stress on plane $\overline{OA}$.

σ normal compressive stress on horizontal plane $\overline{AB}$, which is equal to the rock compressive ultimate stress.

Substituting (5.5) into (5.4), then:

$$P_y = h_0 b_0 \sigma\tan\gamma\sin(\gamma+2\phi)/\cos^2\phi \qquad (5.6)$$

So the cutting depth h_0 should be:

$$h_0 = \frac{P_y}{b_0 \sigma \tan\gamma} \times \frac{\cos^2\phi}{\sin(\gamma+2\phi)} \qquad (5.7)$$

As stated before, ϕ is the frictional angle between the tool and the rock, and is a constant for a certain situation.

From equation (5.7), it can be concluded that the cutting depth of a cutting tip, h_0, is in a direct proportion to the thrust, P_y, imposed on the tool and in an inverse proportion to the width of the tool, b_0, the angle of the cutting tool, γ, and the rock compressive ultimate stress, σ.

5.2.2 The process of rotary cutting

The tool loaded by the rotary cutting force P_x will shear out the rock after cutting into the rock a depth of h_0.

In the case of rotary cutting, assuming the number of the tips on a bit is **m** (in case of drag-bit, the **m** usually equals to 2) the following conditions must be met so as efficiently to cut rock:

the vertical thrust:

$$F = m P_y \qquad (5.8)$$

the horizontal rotary torque:

$$M = P_x m R_m = P_x m (R-r)/2 \qquad (5.9)$$

Then the penetration rate (m/min) of the drag-bit will be:

$$V_m = h_0 \, m \, n \qquad (5.10)$$

where

m number of cutting tips on the bit

n rotary rate of the bit (rpm)

P_x rotary cutting force on a single cutting tip

P_y vertical thrust on a single cutting tip

R_m average radius of a cutting tip

R outside radius of the cutting tip

r inside radius of the cutting tip.

5.3 Mechanisms of Rock Cutting by a Drag-Bit

Fish et al. (1956) and Goodrich (1956), who carried out the extensive study on the mechanisms of rock cutting by drag-bits, suggest that the cutting action of a rotary drag-bit in rock is not at all a perfect continuous process, but is, to a certain extent, a discontinuous one with three terms (refer to Fig. 5.3):

1) Beginning the cycle immediately after the formation of a large fragment, elastic strain builds up due to angular deflection of the bit and torsional strain in the drilling rod (Fig. 5.3a).

2) Strain energy is released, with consequent impact of the cutting edge against the clean rock surface, and comminution of rock fragments (Fig. 5.3b).

3) Build-up of stress at the bit-rock contact, with further crushing and displacement of rock debris, until the cutting

edge is effectively bearing on a step of unbroken rock which subsequently fails and thereby creates a large fragment or chip (Fig. 5.3c). This action completes the cycle.

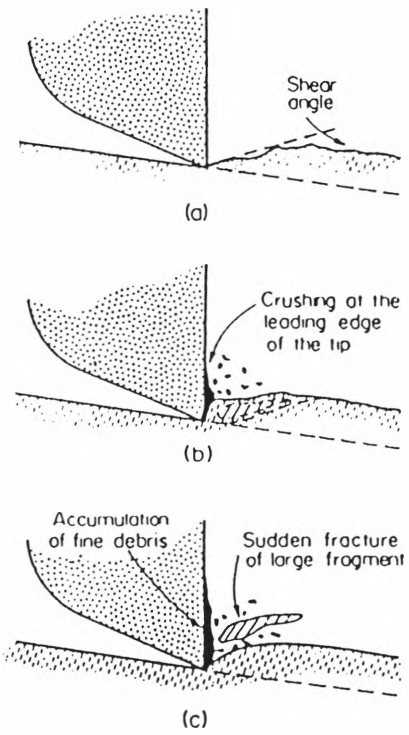

Fig. 5.3 Drag Bit Cutting Sequence

The experiment carried out on a hard sandstone (Darley dale Sandstone) by Fairhurt (1964) confirmed the above assumption. The work shows the rapid oscillations of the thrust and torsional forces on a drag bit corresponding with the discontinuous stages of chip formation as shown by Fig. 5.4. The thrust force goes through two or three oscillations as minor chips are formed and then it builds up to a higher peak just before the formation of a major chip, immediately

after which the thrust falls, almost to zero force. The torsional force goes through similar oscillations, but at a lesser magnitude.

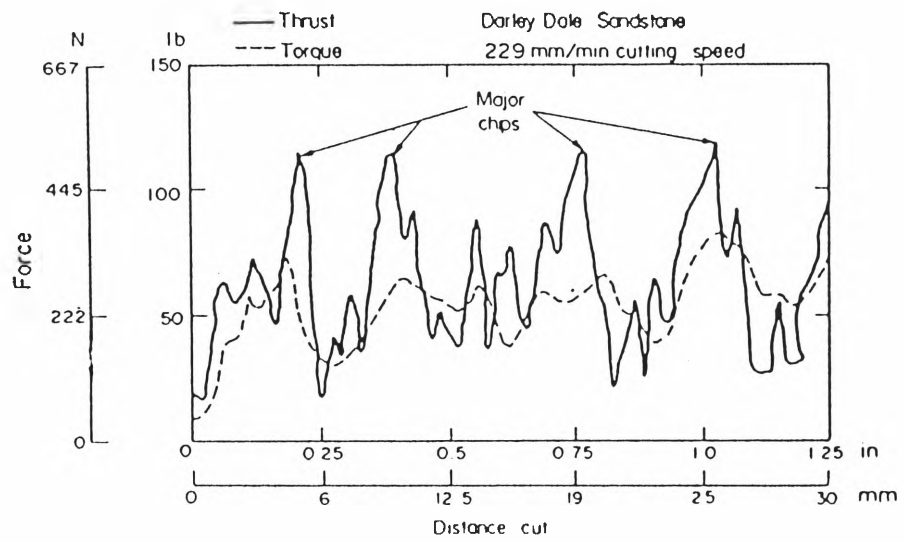

Fig. 5.4 Drag-Bit Force-Displacement Curves

This assumption is also verified by a phenomenon called the waving shape of cutting slots (Fig. 5.5) in rock cutting observed by Gao (1979) in his experiments. He explains the drilling process as follows. With the accumulation of cutting force, the rock in front of the tip will be shear off first, this massive chip sheared is called a large shear. Afterwards, the horizontal torque will reduce to a lower level. With the advance of the cutting tip, some small shearing is continuously occurring. The contact area between the rock and front face of tip will increase while the shearing force increases. Up to the stage when the front face of the tip is fully in contact with the rock, another large sheared chip will be created and the torque will reach its highest level. Consequently, rotary cutting of rocks comprises cycles of several mini-shears followed by a large shear. During the mini-shear process, the width and depth of the slot is the same as the width of the tip b_0 and the initial cutting depth h_0, while in the large shear process, the width b

and depth **h** of the slot are much greater than the tool width and the initial cutting depth. The horizontal cutting force responds to the sequence of the cutting process, it falls to its lowest point after the large shear and then gradually increases to its highest point just before the large shear, as shown in Fig. 5.6

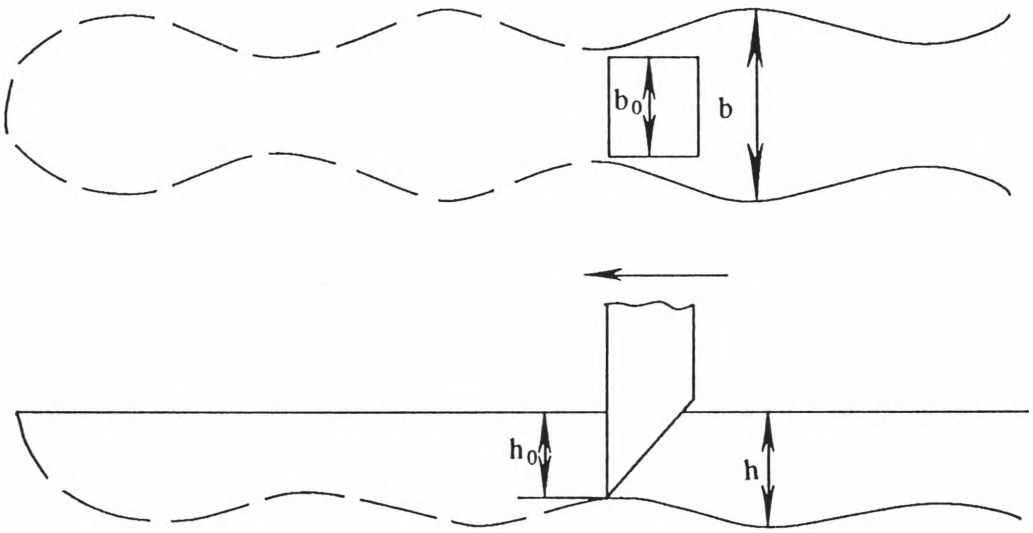

Fig. 5.5 Waving Shape of Cutting Slot

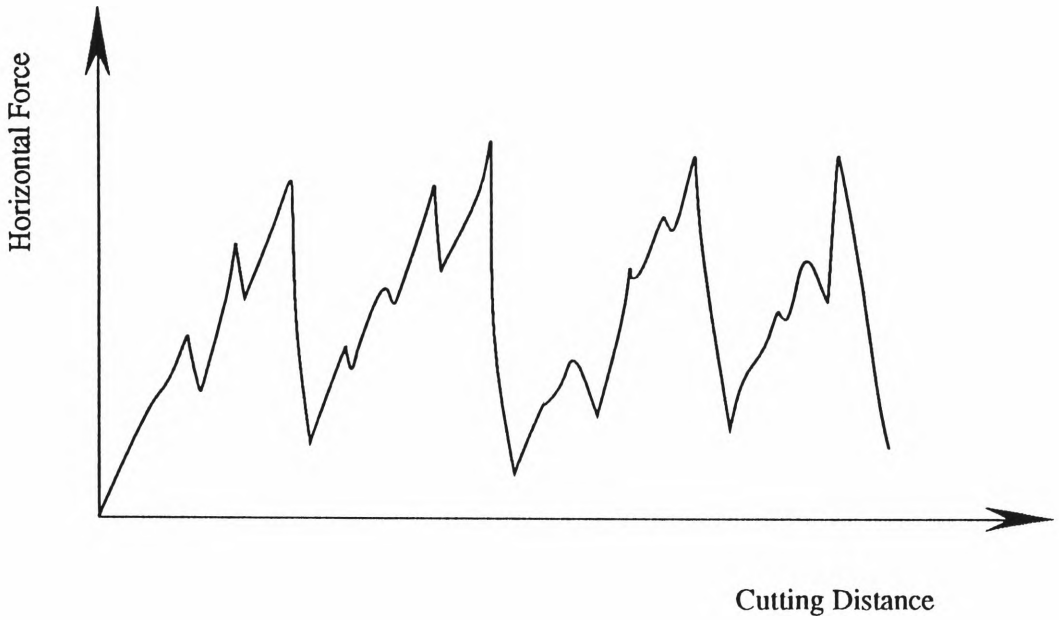

Fig. 5.6 Variation of Horizontal Force with Cutting Distance

The mechanism of rock cutting with drag-bits studied later by Nevill et al. (1962), Jackson et al. (1962), Gray et al. (1962), Maurer (1967) and Larsen-Basse (1973) includes a force build-up from the applied torque creating fracture of the rock initiated at or near the cutting tip. The depth of cut could advance beyond the tip of the cutting tips. The fracture usually would extend beneath the plane of cut, then curve upwards and connect with the free surface. The tool then loses contact with the rock and, again, impacts the rock. The later chipping and crushing of the rock take place at the front and clearance faces of a tip, resulting in some bit material removal. Tool impact with oscillations of frequencies up to 2,000 per minute causes fine ridges on the rock and chip surface. The thrust and torque on the bit increase rapidly with depth of cut and with decreasing rake angle, and the penetration rate increases with increased clearance angle.

There is some difference of opinion as to whether the major failure process in drag-bit drilling is by tension or by shear. Studies by Gray et al. (1962)

on drag-bit drilling show it is most unlikely that tensile failure is important in drag-bit drilling. The fact is the rock fragments are generally uniform in shape, even with widely different rocks. This suggests that the line of fracture may be related to the plane of maximum shear stress. While the angle that this plane makes with the direction of the cutting force will be subject to variation, depending upon the internal friction characteristic of the rock, this variation will be small, even for a wide range of rock types. Also, tensile failure would be evidenced by the propagation of a crack in the direction of the cutting force, and this failure process does not appear to happen. Instead, the fracture was seen to be propagated below the cutting plane after initiation and then curved upwards to the rock surface. The nature of the fracture observed in Gray's experiment was taken to suggest that the initiation of failure was by tension fracture, which propagated into a combined tension-shear failure process.

5.4 Wear of Tungsten Carbide Tips of a Drag-Bit

The study of wear mechanisms of a tungsten carbide cutting tip in rotary drilling of sandstone by Blomberry et al. (1974) shows that the main abrasive wear is due to two factors, selective cobalt removal and microfracture of the carbide skeleton. It was observed during their experiment that fine abrasive particles removed cobalt initially, forming small pits. This removal of cobalt may lower the fracture strength of the surface layers, and cracks propagate from the pits followed by microfracturing of carbide grains and microspalling of the surface layer. Cobalt content and its distribution, the size of abraded particles (from the abrasive material, rock), and other factors control the abrasive wear.

The importance of fundamental abrasive mechanisms, rather than the gross types of wear, became clearer as a result of the microscopic investigations of the effects of rotary drilling of sandstone by Clark (1982). Two apparent distinct types of wear were found:

1) Fracture of surface layers, and
2) the removal of the cobalt binder, which was followed by the pull- out of tungsten carbide grains.

No correlation was found with either cobalt content or wear rate. A possible explanation may be in the simultaneous action of two wear modes in that cobalt removal affected the fracture resistance.

Fish et al. (1959) conducted full scale rotary drilling tests in Darley Date sandstones. The rate of wear increases with rpm but decreases with penetration rate (refer to Fig. 5.7). The experiment study of rotary drilling in a fine-grained sandstone with cemented carbide by Stjernberg et al. (1975) led to the conclusions that the rate of wear was a function of cutting speed and is markedly less for a coarse-grained alloy. It has been stated that high temperatures induced in the carbide may have a marked effect on its hardness and wear resistance. An increase of rotary speed increases the temperature, followed by deformation, reduction of cobalt content, and possible increase of hardness below the surface. Thus, at low temperatures the wear is by abrasive carbide grain removal, and at high temperatures by plastic deformation and grain boundary sliding, which results in greater wear of coarse-grained carbide.

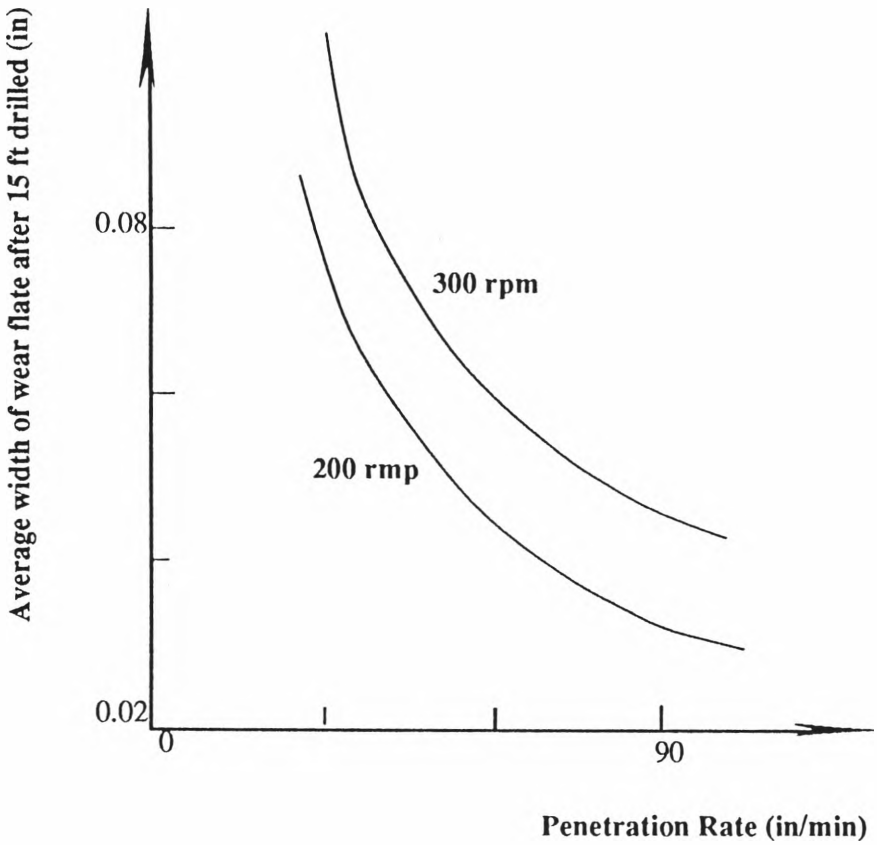

Fig. 5.7 Effect of Rotation Speed & Penetration Rate on Bit Wear in Darley Dale Sandstone

It is suggested (Nevill et al., 1962; and Appl et al., 1973) that the major wear is due to abrasion of the front face of the cutting tip, while some wear loss also occurs on the clearance face. They argued that the contact area between the rock and the front face is smaller than the depth of cut, therefore, wear takes place only in the area of the tip nose. Rock fracture in chipping begins at the tool tip, and hence the rounding of the tip requires that the downward thrust must be increased to maintain the penetration rate. This increased thrust creates an increase in the friction over the clearance face and also in the torque, but the increase of

torque is not as pronounced as the increase in thrust. The wear is proportional to the linear distance traversed by the cutting edge.

After studying the abrasive wear effect in rotary drilling, Fish et al. (1958) suggested that the optimum drill speed be determined by the applied thrust and an economically acceptable bit-life, and pointed out that the rate of bit wear was dependent not solely on the intrinsic abrasiveness of the rock, but also on the strength of the rock. It is argued that in a stronger rock a high level of thrust must be exerted to achieve penetration, consequently the frictional force between the bit and the rock increases. Also, at a higher thrust, the temperature, which is generated at the cutting edge, is so high as to reduce the hardness of the sintered tungsten carbide and thus increase its susceptibility to wear.

The relationship between the machine torque and penetration shows less sensitivity to bit wear than does the thrust-penetration characteristic. The reason is attributed to the fact that the rotational shearing component is less sensitive than is the normal stress component to the increased thrust that wear on the bit makes necessary if penetration is to be maintained. The same effect is also displayed in the speed-thrust-penetration characteristics. An increase in the speed of rotation of the drill reduces the thrust requirement as shown in Fig.5.8 (Fish et al., 1956), but at the same time it increases the rate of frictional wear on the bit. It also reduces the maximum thrust that can be applied without stalling the drill. This observation again confirms the viewpoint that the optimum drill speed should be determined by the applied thrust and an economically acceptable bit life.

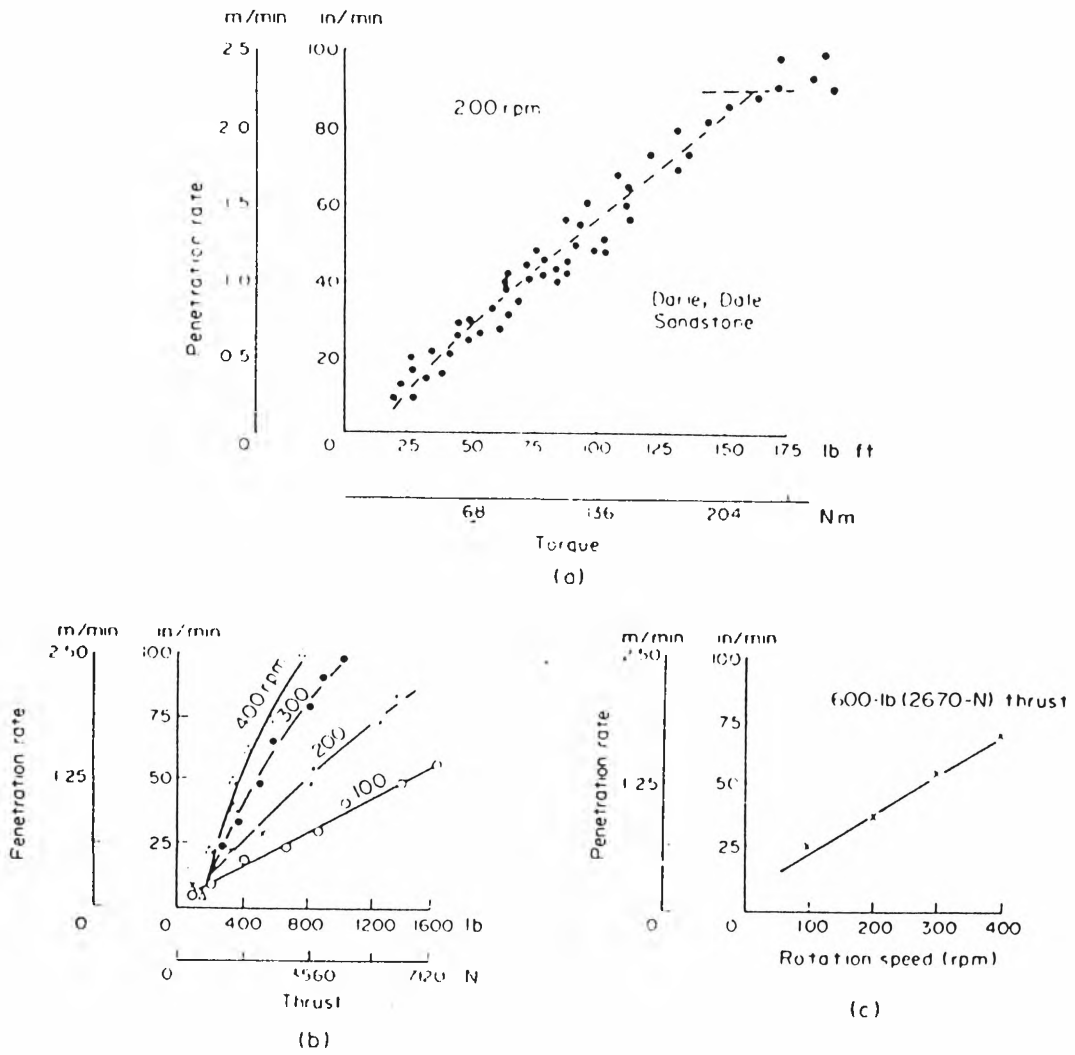

Fig. 5.8 Characteristic Curves for Rotary Drag-Bit Drilling

The stresses in the cutting edge can be severe, as shown by Appl et al. (1973), where a large chip is about to be formed. They concluded that the stress reached a maximum at the top point of the cutting edge where cutting tip fractures tend to initiate. Nevill et al. (1962) noted, when cutting granite, some initial flaking of the insert front face at the start of the test with each bit, partially due to the stress concentration on the sharp edges of the tip. Again, in a qualitative way, Fish et al. (1959) found a general correlation between bit wear in rocks and their abrasiveness

which was measured in sliding with loads proportional to the crushing strength of the rock. All of these facts indicate that the wear of a cutting tip, especially the cutting edge of the tip, is more or less due to the high stress concentration on this area, which is induced by its feature of a sharp edge together the thrust load.

5.5 Finite Element Approach to Analyses of the Stress of a Drag-Bit Tip

Among a number of methods to analyse the wear of a cutting tip, stress analysis seems the only quantitative way to describe the pattern of the tip wear. By the traditional methods, the stress analysis on a cutting tip can be a complicated and time consuming job. However, with the emergence of the finite element method, the stress analysis on a cutting tip becomes convenient and a high accuracy can be obtained. In this section, a three dimensional (3D) finite element package, called STRAND5, is employed to analyse the stress state on a cutting tip.

5.5.1 STRAND5 finite element package (G+D Computing Pty. Ltd., 1988)

STRAND5 is a finite element software for the analysis of sophisticated structures within the reach of most of industry. The package is designed to run on most personal computers with a hard disk and a maths co-processor. The package uses the full capacity of the machine through a database which expands to the full capacity of the hard disk storage available, and can be implemented on a range of computers. STRAND5 is a suite of finite element

programs, including pre-processors (graphics oriented input program), the main assembler and solver, and graphics oriented post-processor for interpreting the results.

The basic philosophy behind the software has been to develop a reliable package of programs incorporating the latest developments in finite element technology with the following features:

1) extensive use of graphics to check input data, and display response of the structure and stress contouring,
2) file handling and archiving that is transparent to the user but almost indestructible and dynamically structured to respond easily to changes in the design,
3) interactive operating mode, and
4) data structure which can be converted to or converted from other CAD or FE programs.

Applications include small displacement, small strain, linear elastic structural analysis in mechanical and structural engineering, including frame, plate, shell and solid structures.

No limitation is imposed on the size of the structural model by the programs except for a maximum semi-bandwidth in the stiffness matrix of 4000. Limits are imposed by the user's hardware, both by the available memory and the real time taken to solve the problem. On modern microcomputers with a 40 megabyte hard disk and a 80287 math co-processor, problems with up to 4000 elements and the order of 6000 degrees of freedom can be solved overnight.

The 3D element in STRAND5 is a 20 node isoparametric brick. Regardless of the global node system, the local node numbers 1 to 20 must always form a right-hand coordinate set in (ξ, η, ζ) space, as shown in Fig. 5.9. The definition of the mid-side nodes may be entered as 12 individual numbers. However, when the global node numbers form a regular sequence, STRAND5 can then take the appropriate mean global node number (refer to Fig. 5.10). The spatial transformations involved in this 20 node isoparametric brick are such that each edge of the brick can only be a quadratic curve in Cartesian (x, y, z) space.

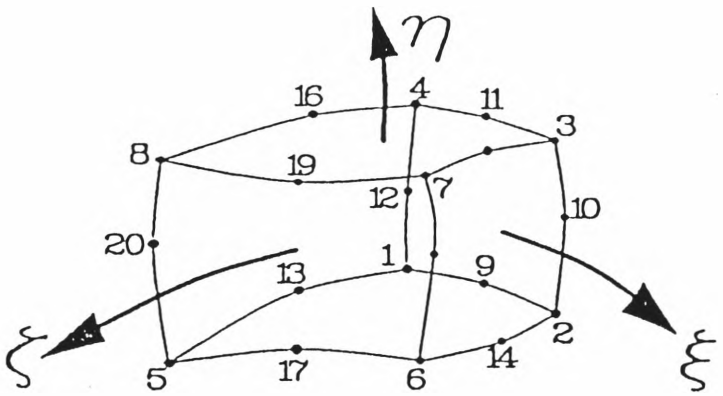

Fig. 5.9 Node Numbering Order for a Brick Element

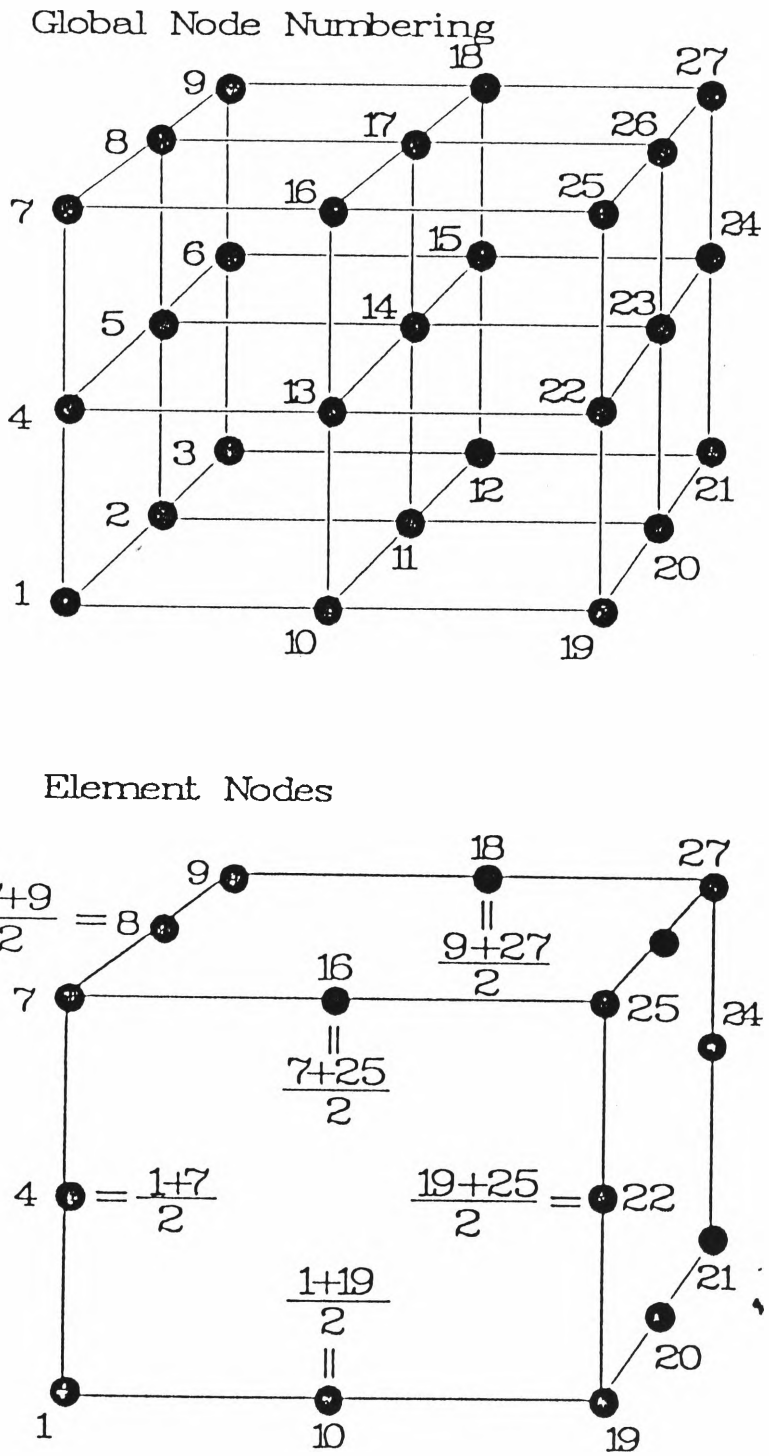

Fig. 5.10 Automatic Midside Node Numbering

The 20 node brick element has three degrees of freedom at each node. Nodal rotations are not required to define the strains in 3D elasticity; rotation of a plane face in the model is accommodated by relative translation at the nodes.

5.5.2 Physical model of cutting tip of drag bit

The general configuration of the currently used drag bit is shown on Fig. 5.11, which has two eccentric cutting tips, defined as a right-hand tip and a left-hand tip, respectively. The right-hand tip is the one mounted on a drag bit which peaks to the right when looking from behind and the left-hand tip is the one peaking to the left.

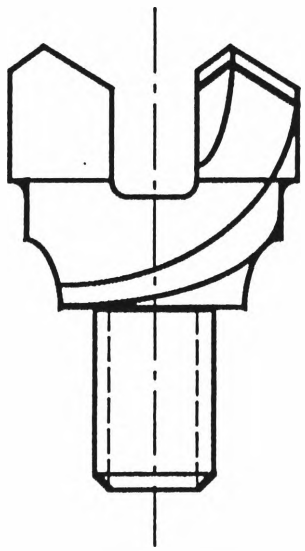

Fig. 5.11 Drag Bit Currently Used

The stress analysis by the finite element method is only conducted here in the right hand tip. The reason for this is that the tangential force, induced by the rotary torque during drilling process, acting on a certain point of a cutting tip is proportional to the distance between the point and the axis of the bit.

Consequently, the peak point of the right-hand tip bears a greater tangential force, and therefore a more severe stress exists than that for the left-hand tip, as the former is farther removed off the axis of the bit than the latter.

The 3D finite element model of the right-hand tip is shown in Fig.5.12. The whole structure contains 2835 nodes, and a mesh of 14×11×3 divides the cutting tip into 260 quadratic brick element with approximately 1 mm on each edge.

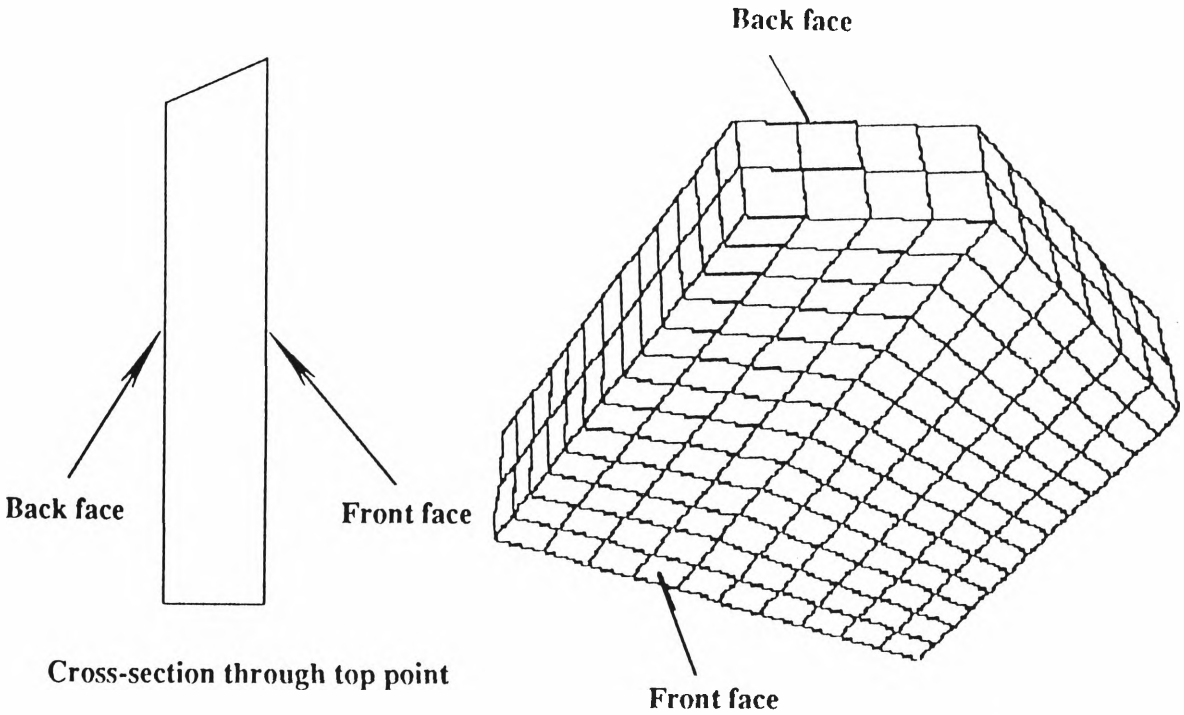

Fig. 5.12 3D Finite Element Model of Bit Tip Analysed

The tip is welded to the bit body on its bottom face and on its back face, except the first row of the top brick elements. Those nodes which are supported on the bit body are supposed to be fully fixed and to have no degrees of freedom, whereas the nodes which are not on these two faces have 3 degrees of freedom at each node, as shown in Fig. 5.13.

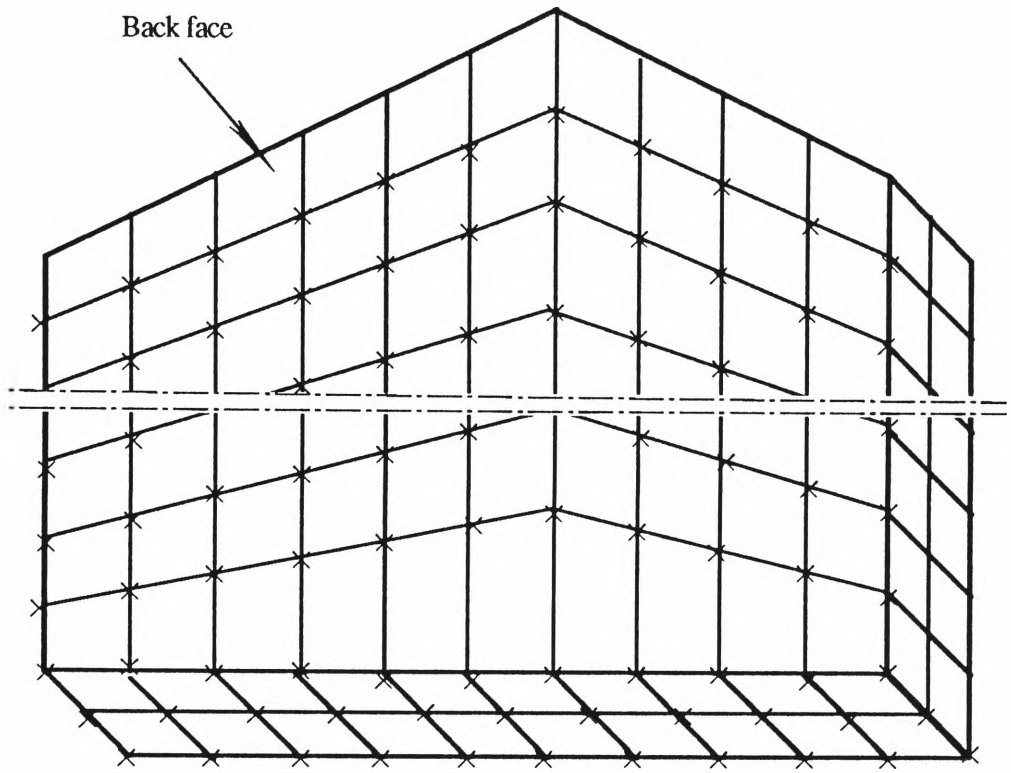

Nodes with ' × ' are all fixed and have no freedom

Fig. 5.13 Freedom Condition of Structure

The material of the cutting tip is tungsten carbide, containing approximately 91% of WC and 9% of cobalt. Its physical properties are listed on Table 5.1.

Table 5.1 Physical Properties of Cutting Tip Material

Young's Modulus	Poisson Ratio	Ultimate Tensile Strength	Specifical Gravity
520,000 MPa	0.22	1,800 MPa	14.5

5.5.3 Model of load distribution

The load imposed on the tip is divided into two type of forces, ie. an axial force is induced by the thrust of the drill machine, and is distributed on the nodes of the top face which cuts into the rock, and a tangential force is induced by the rotary torque of the drill machine, and is vertical to the front face of the tip and is distributed on the nodes of the top line of the front face.

The probable torque and thrust values are obtained from physical observation of the drilling performance of this style of bit in the Strata Mechanics Testing machine.

The capacity of the thrust of the machine from 100 lb/in^2 on a 6" diameter ram is:

$$100\ lb/in^2 \times \pi \times (3\ \text{in})^2 = 2800\ lbs = 12600\ \text{N}$$

So the maximum thrust on each tip is 6300 N.

The torque on the machine varies, depending mainly upon the rock drilled, in a range of 60 to 110 Nm during a drilling operation, which imposes a possible maximum torque of 50 Nm on each tip.

The axial force acting the nodes of the top face depends on the cutting depth of the tip. It is assumed that only those nodes which cut into rock will bear the axial force, and that the axial force acting on a node is proportional to the depth of the node cutting into the rock.

The tangential force is assumed to act on the nodes of the top line of the front face. The force acting on a node increases with both the cutting depth and the radius from the axis of the bit to the node the force acts on.

Three load cases are considered. The original load case, defined as load case 1, is about 60% of the capacity of the drill rig, with a total axial load of 3500 N and a total tangential load of 3200 N which equals a torque of 30 Nm to the axis of the bit. The pattern of the load distribution on the cutting tip in this case is shown in Fig. 5.14. Those load which is smaller than 50 N is not shown in the diagram. The other 2 load cases, namely load case 2 and load case 3, are 1.4 and 1.8 times of the original load case respectively. At 1.8 times the original load case, the load imposed on the tip is at the capacity of the drill machine.

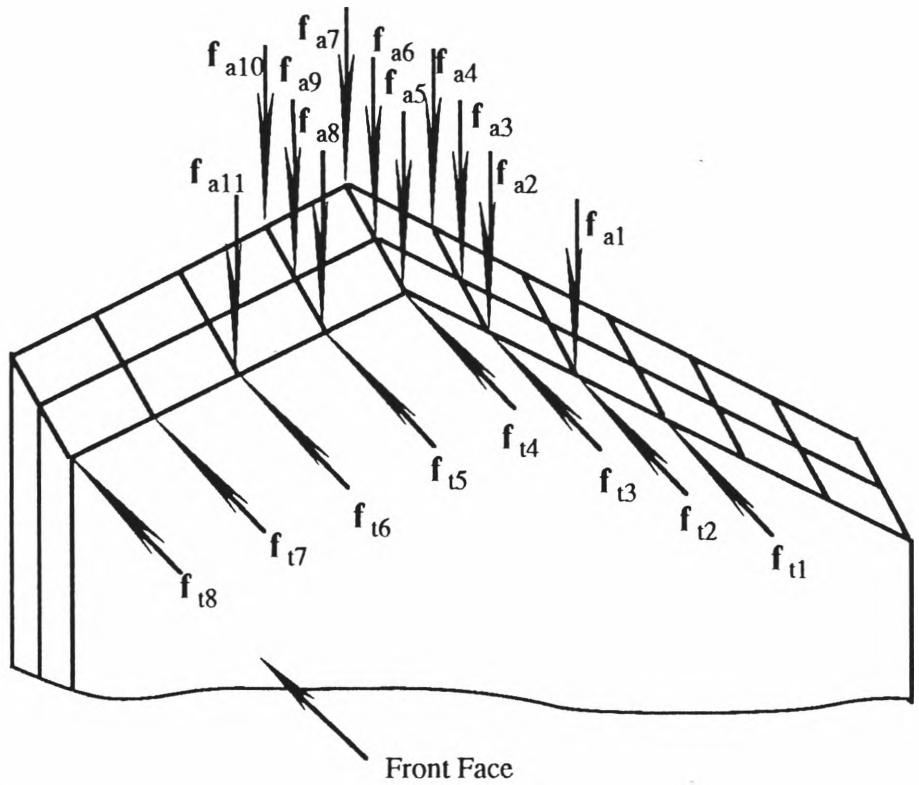

Newton

f_{t1}	f_{t2}	f_{t3}	f_{t4}	f_{t5}	f_{t6}	f_{t7}	f_{t8}
75	150	200	900	400	300	300	400

f_{a1}	f_{a2}	f_{a3}	f_{a4}	f_{a5}	f_{a6}	f_{a7}	f_{a8}	f_{a9}	f_{a10}	f_{a11}
100	300	200	125	1000	500	350	300	200	125	100

Fig. 5.14 Load Distribution in Normal Drilling Condition

The load case 1 refers to a normal drilling condition when an adequate cutting depth and appropriate drilling parameters are implemented, and the rock condition remains consistent. During this period, the penetration of the drill bit is smooth and constant.

The load case 2 refers to an inapproriate drilling operation. In this case, a much higher drilling parameter than usual is applied to a certain rock condition due to the improper operation of the drilling crew. A situation like this happens very often, especially when a different rock formation occurs in the drilling process, or an inexperienced operator joins the crew.

The load case 3 refers to a severe drilling condition, when very high loads have to be imposed in order to remove the extremely hard granules in the rock drilled. An instance occurs when a sandstone with a high quartz content appears.

5.5.4 Result of finite element analysis and discussion

In order to interpret and analyse the results of the computation and to determine the failure of the material, a failure theory, called the maximum shearing stress theory or Tresca-Guest theory (Collins, 1981), concerning combined stress states is reviewed first.

The maximum shearing stress theory, proposed by Tresca and later experimentally supported by Guest, may be mathematically formulated in terms of principal normal stresses as follows:

Failure is predicted by the maximum shearing stress theory to occur if

$$|\sigma_1 - \sigma_2| \geq |\sigma_0|,$$

$$|\sigma_2 - \sigma_3| \geq |\sigma_0|, \quad \text{or}$$
$$|\sigma_3 - \sigma_1| \geq |\sigma_0| \qquad \textbf{(5-10)}$$

where $\sigma_1, \sigma_2, \sigma_3$ are the principal normal stresses and σ_0 is the uniaxial failure strength in tension.

It is important to note that failure is predicted to occur if any one expression of (5-10) is satisfied. If σ_{max} and σ_{min} are defined as the maximum and the minimum principal normal stresses respectively, the formulae (5-10) then can be simplified as:

$$\sigma_{max} - \sigma_{min} \geq \sigma_0 \qquad \textbf{(5-11)}$$

In words, the maximum shearing stress theory predicts that failure occurs in a multiaxial state of stress when the maximum shearing stress magnitude becomes equal to or exceeds the maximum shearing stress magnitude at the time of failure in a simple uniaxial stress test using a specimen of the same material.

Based on the physical model of the structure, the STRAND5 program was run on a President IBM/PC-AT computer system with a hard disk of 30 mega bytes and a RAM of 640 K.

Under the load conditions on the structure, described previously, the linear elastic static solver is executed in each case. The element stresses associated with each load case can be listed at 8 corner points, or at 27 corner and centroid points, of each brick element. Each listing gives the following information:

1) The global **x**, **y** and **z** co-ordinates of the point at which the stress is evaluated.
2) Normal stresses on each of 3 directions in a global coordinates system, ie. σ_x, σ_y and σ_z.
3) Shear stresses in a global coordinate system, ie. τ_{xy}, τ_{yz} and τ_{zx}.

According to the maximum shearing stress failure theory stated before, the maximum shearing stress, ie. the Tresca stress (σ_{max}-σ_{min}) is used to determine if the material of the structure is failed or not.

The stress results of brick elements can be shown by stress contours in the modules for the post-processing of the STRAND5 package. By setting up a contour file, the stress contour of a brick element can be graphically plotted. There are eleven stresses available for display, which include the Tresca stress (σ_{max}-σ_{min}).

From experience and observation, it is known that a stress concentration is centred on the cutting edge of a cutting tip, which is also the focus of the F.E. analysis. Therefore, the stress contour display is limited in the 40 brick elements of the top part of the structure.

Focused on these points, each of the contour files of the maximum principal normal stress and the Tresca stress on the 40 brick elements under each load case has been established, respectively.

Table 5.2 shows the range of the Tresca stress on these elements under each load case.

Table 5.2 Range of Tresca Stress

Load case no.	1	2	3
Range of σ_{max}-σ_{min} (MPa)	300 - 3000	600 - 4100	700 - 5800

The Tresca stress seems to increase with the increase of applied load as shown in Table 5.2. Its distribution pattern under each load case is such that the maximum occurs at the point of the tip and gradually reduces from that point.

By applying the Tresca-Guest failure theory, the top point of the structure would fail under any load case, as the Tresca stresses at this point all exceed the critical stress, ie. the ultimate shearing stress, set by the Tresca-Guest failure theory (refer to Fig. 5.15).

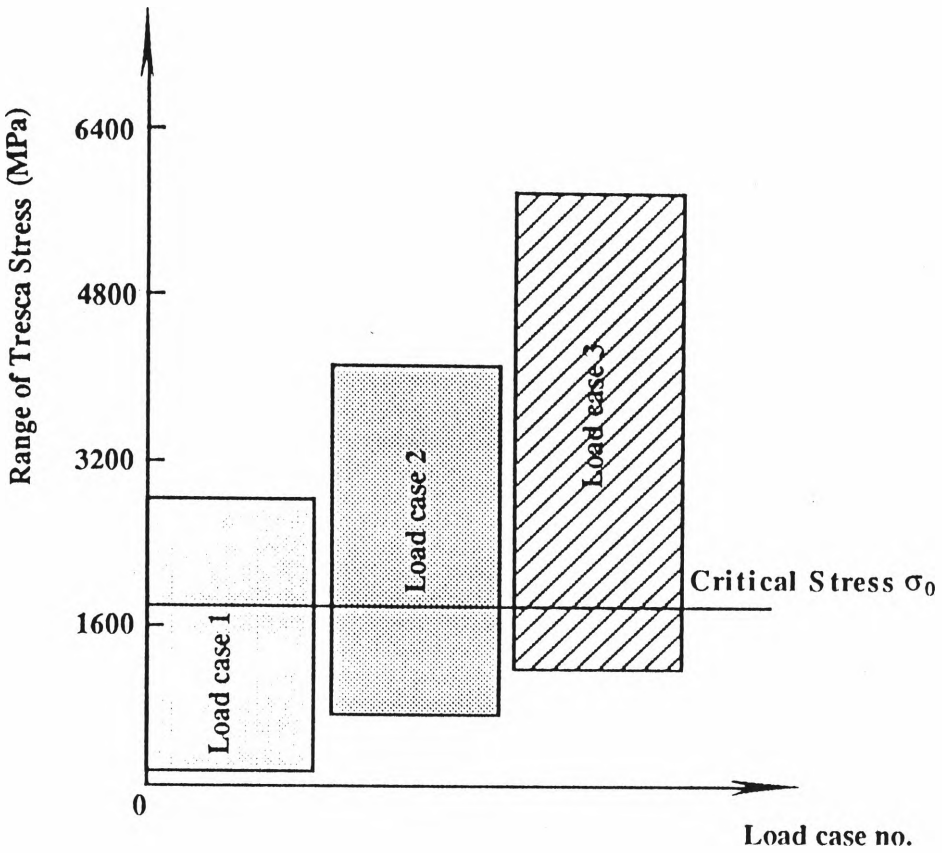

Fig. 5.15 Range of Tresca Stress Under each Load Case

With the increase of the loads applied on the cutting tip, the region of the Tresca stress exceeding the critical stress will extend, as shown by the Tresca stress contours in load cases 1 and 3 in Figs. 5.16 and 5.17, respectively.

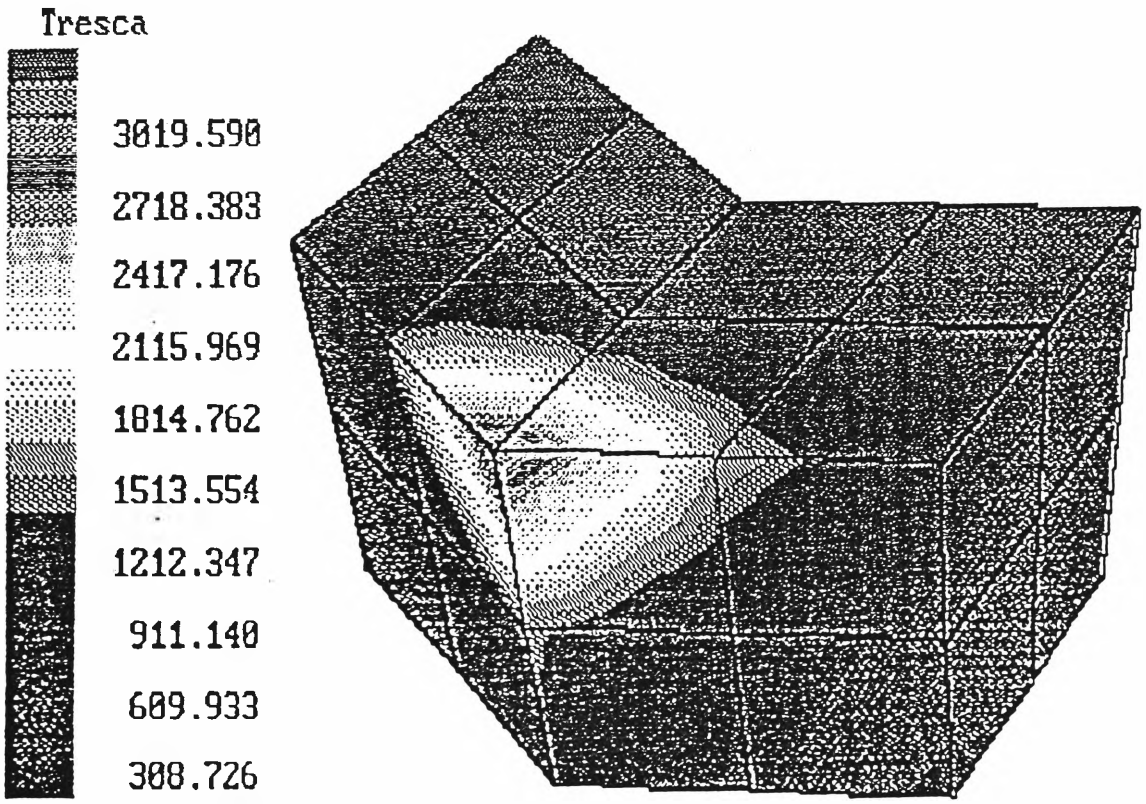

Fig. 5.16 Tresca Stress Contour in Load Case 1

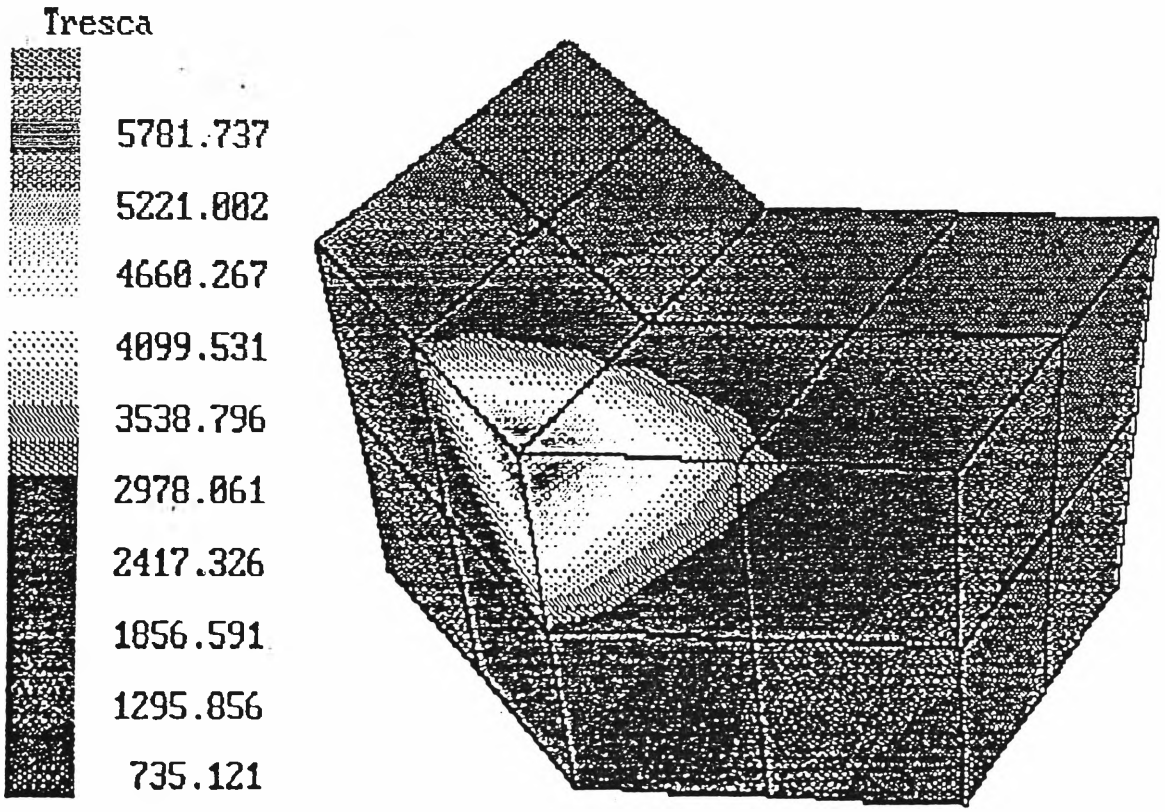

Fig. 5.17 Tresca Stress Contour in Load Case 3

In load case 1, the Tresca stresses exceed the critical stress only in 2 brick elements, while the stresses exceeding the critical stress have extended to 8 brick elements in load case 3.

Expansion of the critical stress region suggests that the possible failure area is extended with the load increase. It can be assumed that the failure of a cutting tip starts at the top point of the tip under normal drilling conditions, and gradually extends to the rest of the cutting edge of the tip as the drilling conditions become severe.

In summary, the stresses in a cutting tip were calculated by using a 3D finite element model under specified loads. The complex geometry of a cutting tip and load condition can be properly modelled for the computation. The distribution of the Tresca stress on the cutting tip in all load cases shows that the top point of the tip has the greatest value, and the stress diminishes gradually from there. In normal drilling conditions, only the top point of a drill bit will fail. Under severe drilling conditions, a high load case has to be applied, and consequently, the failure region of a cutting tip would be extended, as in the load cases 2 and 3.

Chapter Six

Experimental Study

6.1 Scope of Work

The previous theoretical study shows that the tip of the conventional obtuse cutting tool of a drag bit will suffer a much greater stress than any other part of the cutting tool. Consequently, the failure of bits by chipping of the tips will dominate other effects. But the result of the theoretical study has to be verified by experiment. Moreover, the failure pattern should also be revealed through experiment, so that a better tip configuration of drag bit tips may be proposed.

Based on the above idea, a series of experiments, which model the process of underground roof drilling, has been conducted at the laboratory of the Department of Civil and Mining Engineering, the University of Wollongong. By the adoption of a Keithley Data Acquisition System to the drilling testing operation unit, the operation parameters and the specific energy have been generated as the outcome of the test. In addition, a specially-designed cutting sample collector and a sieving shaker have provided information on the size distribution of the cuttings.

6.2 Parameters of the Bits Tested

Two groups of bits were tested, with positive and negative rake angles, with six in each group. The bits all have eccentric tips, and are most widely used as roof bits around the Illawarra collieries. The bits were provided by Seco-Titan from stock without special selection. Fig. 6.1 is the sketch of the test bits. The details of the tested bits, shown in Table 6.1, were measured respectively before testing, and the weighted average values were based on the independently measured values.

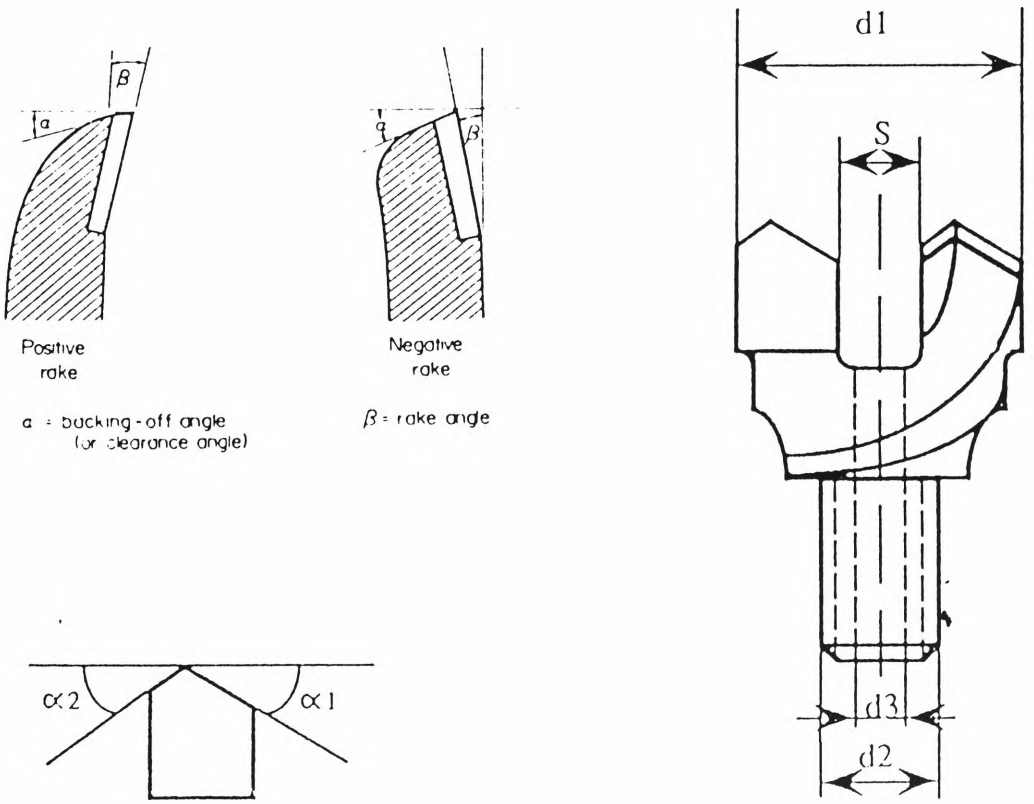

Fig. 6.1 Sketch Tested Bit

Table 6.1 Parameters of Test Bits*

Bit Type	d1 (mm)	d2 (mm)	d3 (mm)	S (mm)	β (°)	α (°)	α1=α2 (°)
Positive	27.21	12.32	4.96	6.42	4.25	15.75	30.1
Negative	27.33	12.27	5.02	6.01	-2.5	18.5	24.8

Bit Code	P1	P2	P3	P4	P5	P6
Rake (α°)	4.07	3.97	4.68	4.33	3.84	4.59

Bit Code	N1	N2	N3	N4	N5	N6
Rake (α°)	-3.01	-2.41	-2.88	-2.09	-2.21	-2.28

* **Refer to Fig. 6.1 for definitions.**

The positive and negative rake angle bits are used in different situations. Basically, they have different features.

The special features of positive rake roof bits:

1) give faster penetration rate than bits with a negative rake for a given feed thrust and torque,
2) have a more acute angle than bits with a negative rake, and this feature may lead to severe edge chipping in heavily banded or broken roofs, and
3) are usually the fastest and most economic configuration when used in homogeneous roofs.

The special features of negative rake roof bits:

1) give greater durability in non-homogeneous roofs than positive rake angle bits,
2) require more feed thrust and torque than bits with a positive rake for a given penetration rate,
3) are usually the most economic configuration for medium hard or banded sandstone roofs when used with hand-held drill rigs.

A bit code number is named with a capital letter P (for positive rake bits) or N (for negative rake bits) followed by a number from 1 to 6 representing bit number. Therefore, the code numbers of P1 to P6 represent the positive rake bits tested from number 1 to number 6, and similarly for the code numbers of the negative rake bits N1 to N6. A hole code number is named with a bit code number followed by a dash line and a number, for example a hole with a hole code number of P5-17 is the seventeenth hole drilled by the tested bit P5.

6.3 Unit Used in the Test Operation

The unit used in the test operation consisted of a drilling medium, a Wombat roof drill rig, a Keithley Data Acquisition system, as well as the test framework, and has the following advantages:

1) follows closely the practice of drilling roof bolt holes in mines,
2) provides a standard homogeneous drilling medium which reflects the physical mechanical properties of in situ strata,

3) uses high speed data logging of the dynamic characteristics of rotary drilling, and

4) allows control and monitor of all operation parameters.

Fig. 6.2 shows a photograph of the operation unit.

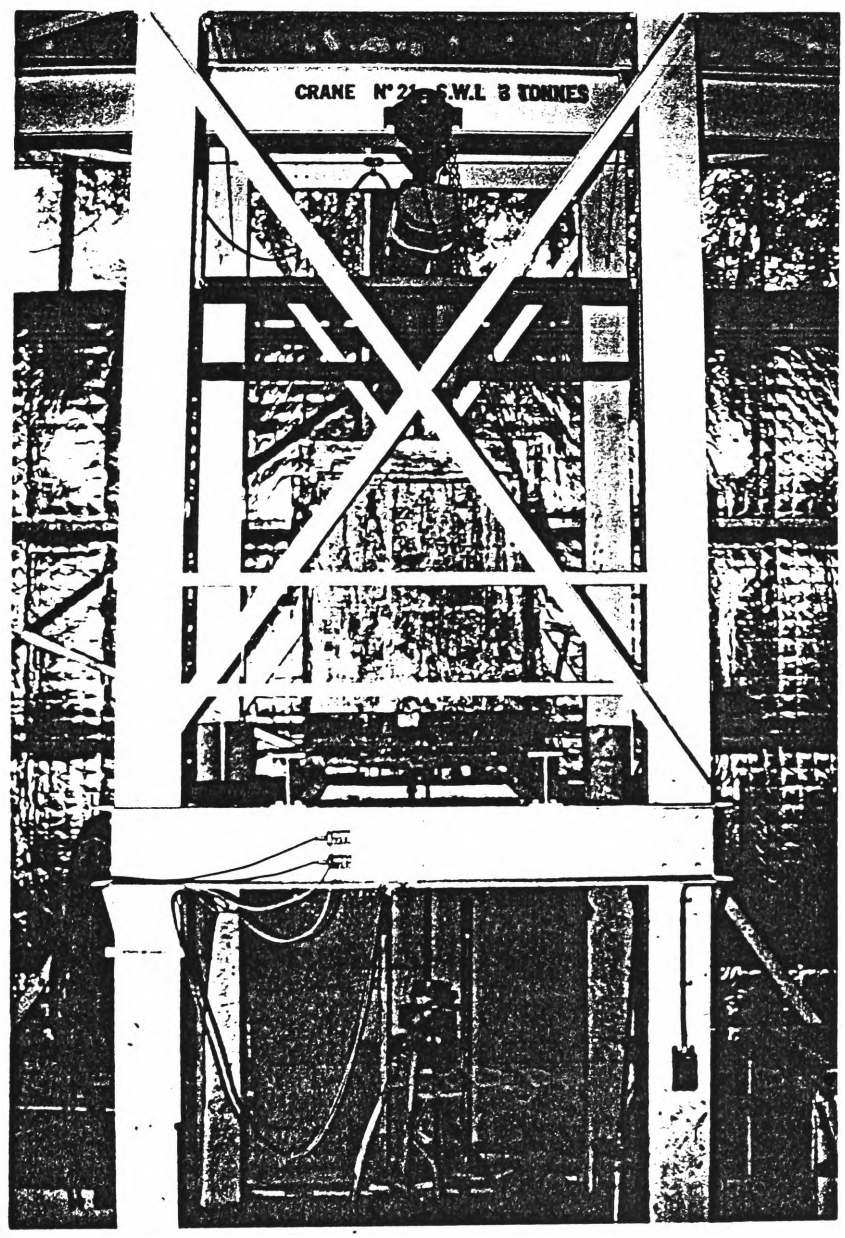

Fig. 6.2 Test Operation Unit

6.3.1 Drilling medium

Field strata vary from place to place, even in the same drilling site, and so the drilling medium can be largely different from one hole to the other.

The experimental work is different from field work in light of the treatment of the data obtained. On one hand, the drilling medium for an experiment should simulate the field condition as closely as possible so that the result from the experiment will readily apply to field practice. But on the other hand, the experimental conditions have to be constant enough to make the data collected from the experiment consistent and comparable, and not subject to errors due to randomness of the drilling medium.

The drilling medium made for this particular experiment is a homogeneous concrete block shown on the upper half of Fig. 6.2. The concrete block is cast in the laboratory with a metal form of one cubic metre volume, and the basic constitution of the block is sand, cement and water. The change of the ratio of the constituents yield different specifications for the block. The mechanical properties of the concrete block for the tests reported here are:

Ultimate Compressive Strength:	50 MPa
Young Modulus:	35.5 GPa

6.3.2 Drill rig

A "Wombat" roof bolting drill rig is employed for the testing. The machine is powered by compressed air, and the cooling medium for the drill bit is water. Its technical specifications are shown on Table 6.2.

Table 6.2: Technical Specifications of Wombat Roof Rig (RG Cram & Sons, 1985)

Operating Air Pressure	551 - 758 kPa
Air Consumptions at Free Speed	3.4 - 4.3 m^3/min
Operating Water Pressure	760 - 1240 kPa
Output Torque at Stall	216.93 Nm
Chuck Free Speed	960 RPM +
Air Inlet Size	13 mm Snap Coupling
Water Inlet Size	13 mm Snap Coupling

The drill rod used during the test is a Seco-Titan 19 mm hexagonal drive shown in Fig. 6.3.

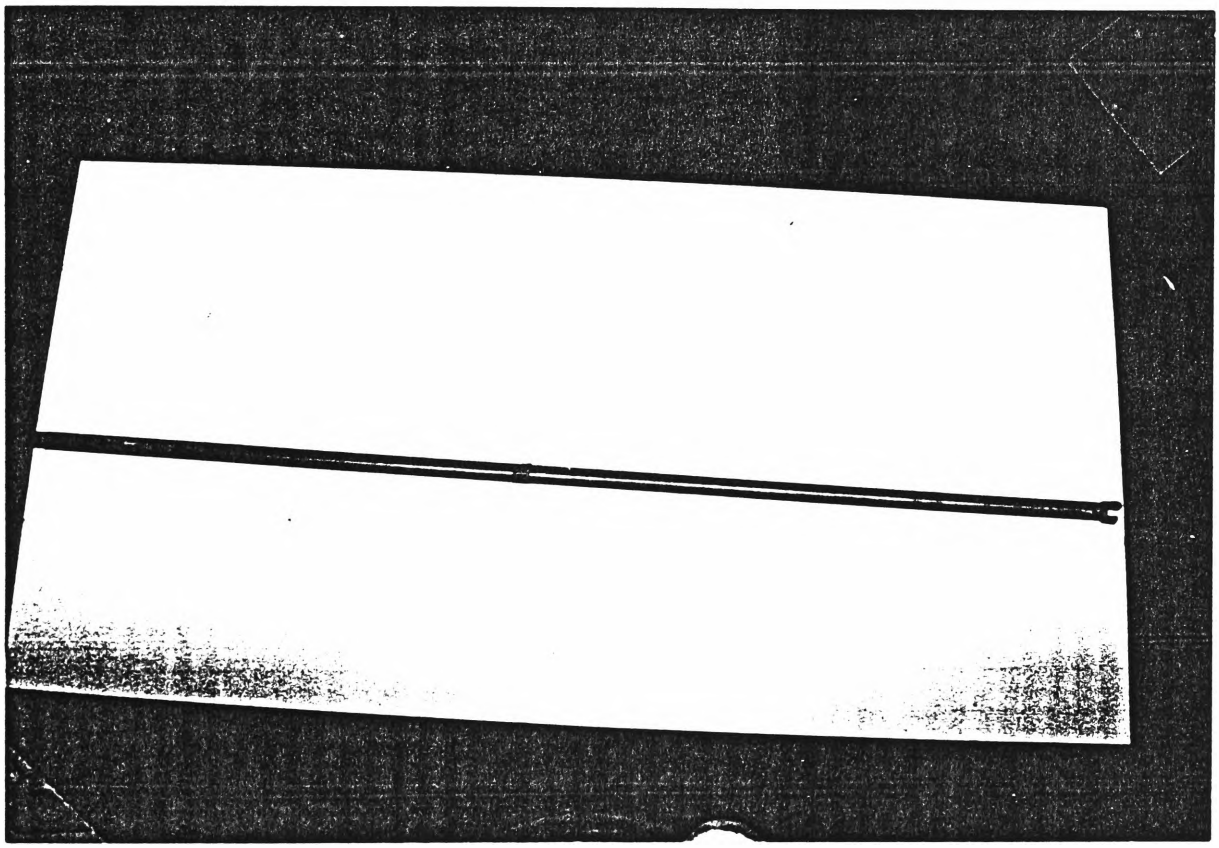

Fig. 6.3 Hexagonal Drill Rod

6.3.3 Keithley data acquisition system

The drilling test system has been developed to model the practice of drilling roof bolt holes in underground coal mines, while monitoring with a highly efficient data logging unit, a Keithley Data Acquisition System. The drill rig is connected to peripheral data acquisition equipment to determine the performance characteristics of the bits and drill. Fig. 6.4 shows the schedule of the monitoring and data acquisition system.

Fig. 6.4 Schedule of Data Acquisition System

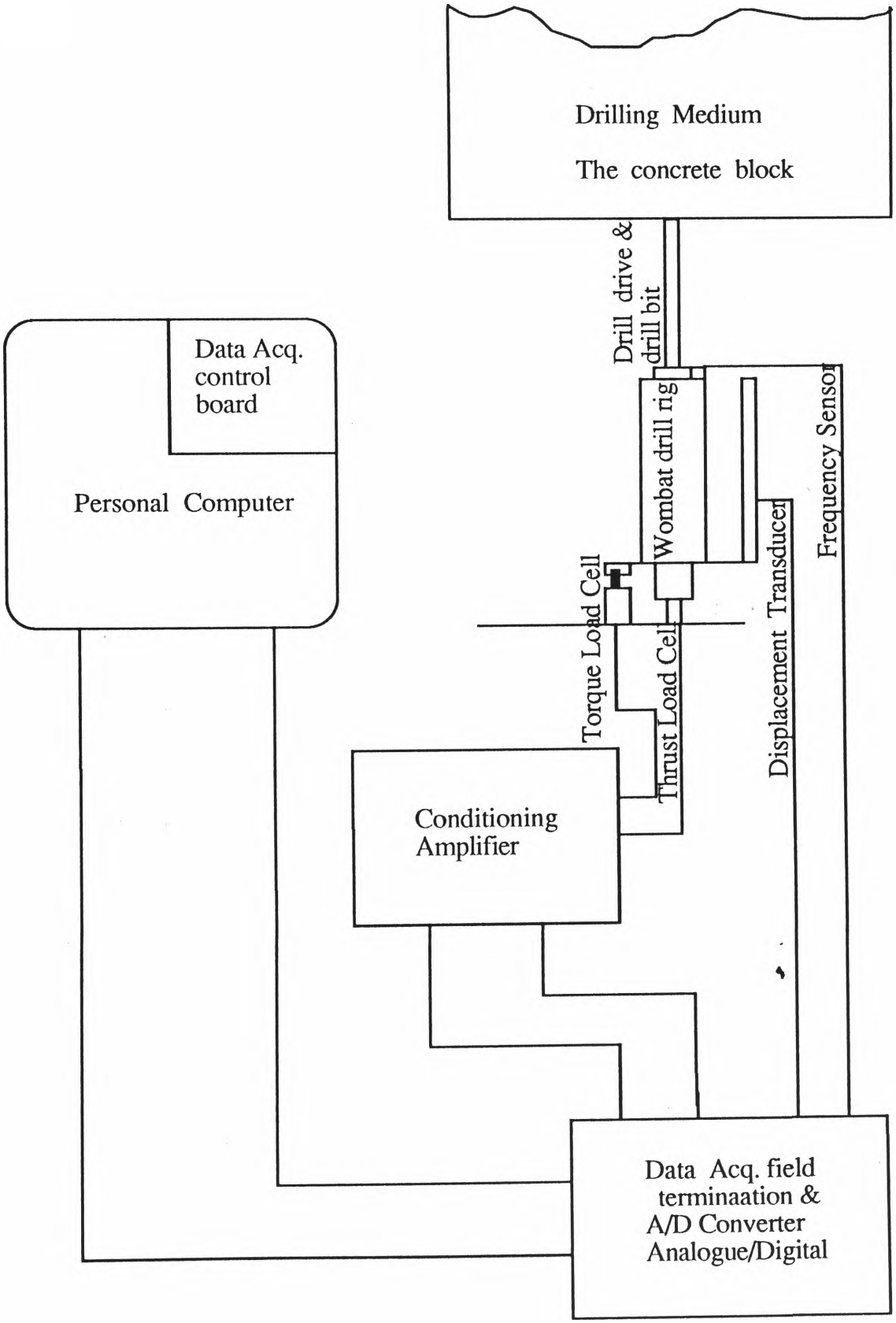

This data acquisition system, which integrates hardware, the System 570 data acquisition workstation and Soft 500 software, has been employed to obtain, store and analyse the operating parameters of the drill rig. The System 570 is a work station data acquisition and control device -- an interface between a personal computer and the operator. With this system, an IBM or an IBM compatible personal computer can be used for direct data acquisition and intelligent process control. Soft 500 is a powerful software package for data acquisition and process control written for the Keithley series 500 Measurement and Control System and the IBM personal computer and Personal Computer - XT. Fig. 6.5 shows the Keithley data acquisition system in operation next to the drill rig.

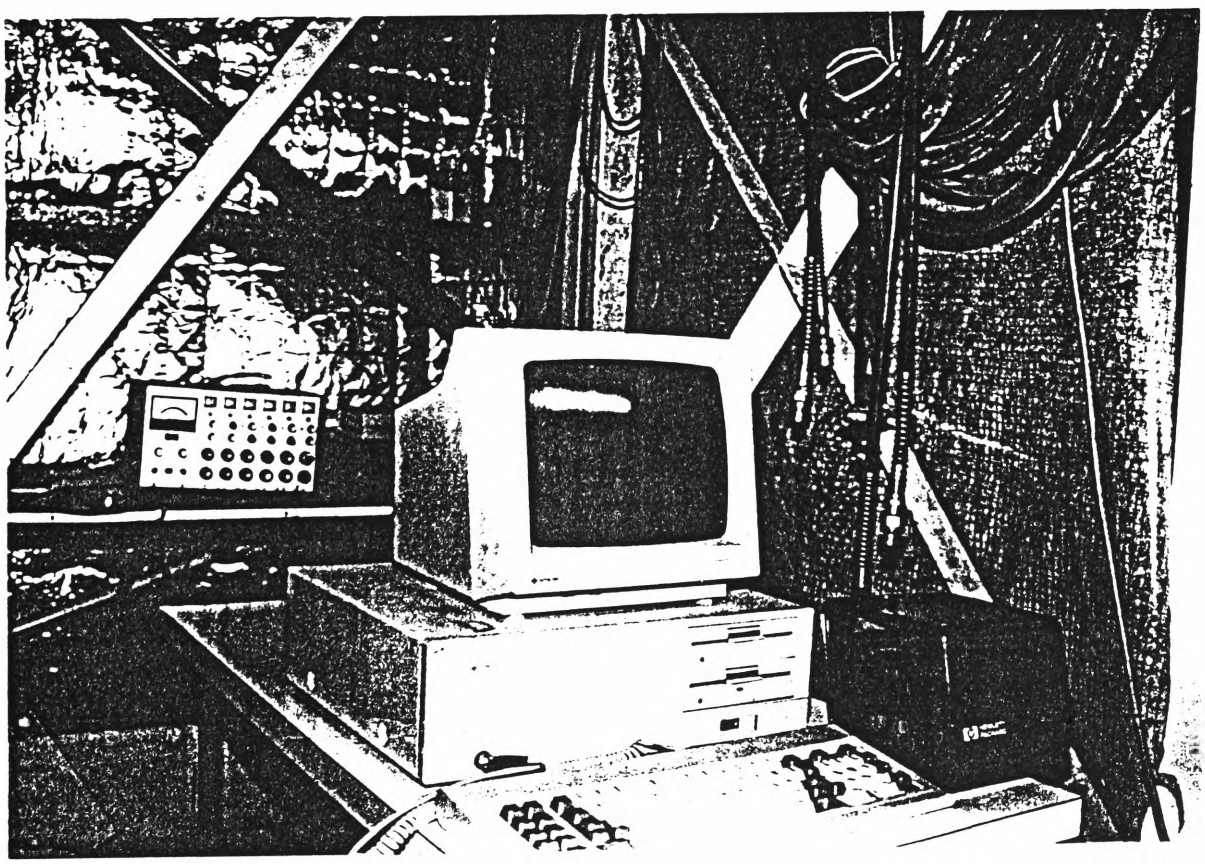

Fig. 6.5 Data Acquisition System in Operation

The operation of the rig is controlled by the machine operator and the operation parameters are stored by the Keithley system. The real time of the roof drilling operation is precisely recorded. The load cell, strain gauge, turn potentiometer and inductive sensor are installed on the rig to monitor and measure the operation parameters, i.e. the thrust, torque, revolution rate and displacement, respectively. These gauges and sensors are connected to the System 570 data acquisition unit. Programmes have been developed to acquire data from the System 570 unit, and direct them to a Sperry computer (640 k RAM, and IBM compatible).

6.3.4 Cutting sample analyzing system

A special sample collector and seal ring has been designed to collect cuttings while the drilling operation is underway. Figs. 6.6 and 6.7 show the sample collector, seal ring and their use in the drilling process.

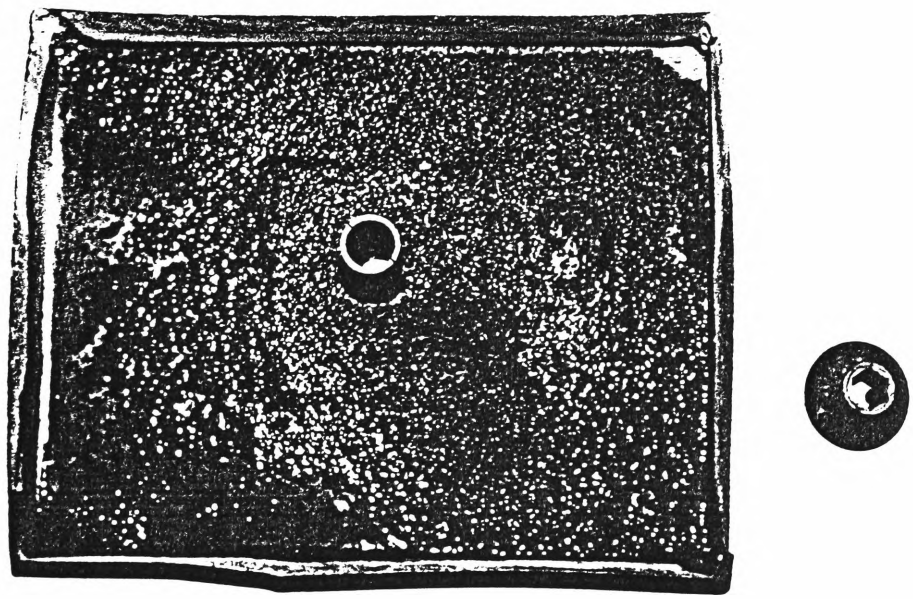

Fig. 6.6 Cutting Sample Collecting Accessaries

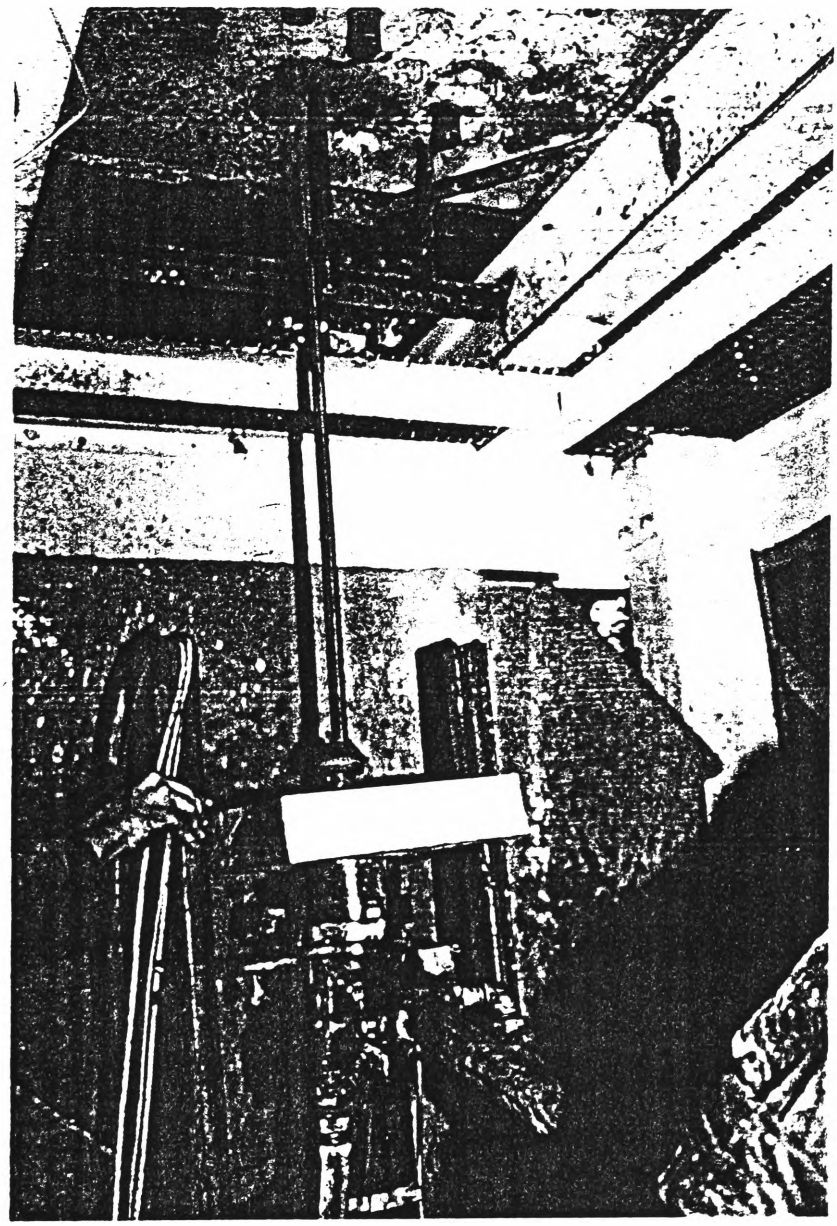

Fig. 6.7 Sample Collector in the Drilling Process

The cutting size distribution is determined by a series of sieves, A, B, C, D, E &F with mesh square aperture sizes of 6.70 mm, 2.36 mm, 1.18 mm, 0.60 mm, 0.30 mm and 0.15 mm respectively, and by a sieving shaker, which are shown in Figs. 6.8 and 6.9.

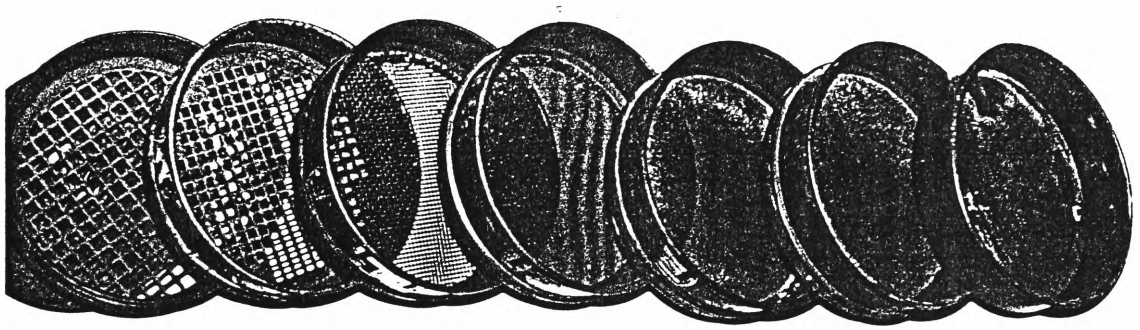

Fig. 6.8 A Series of Sieves for Analysis of Cutting Sample

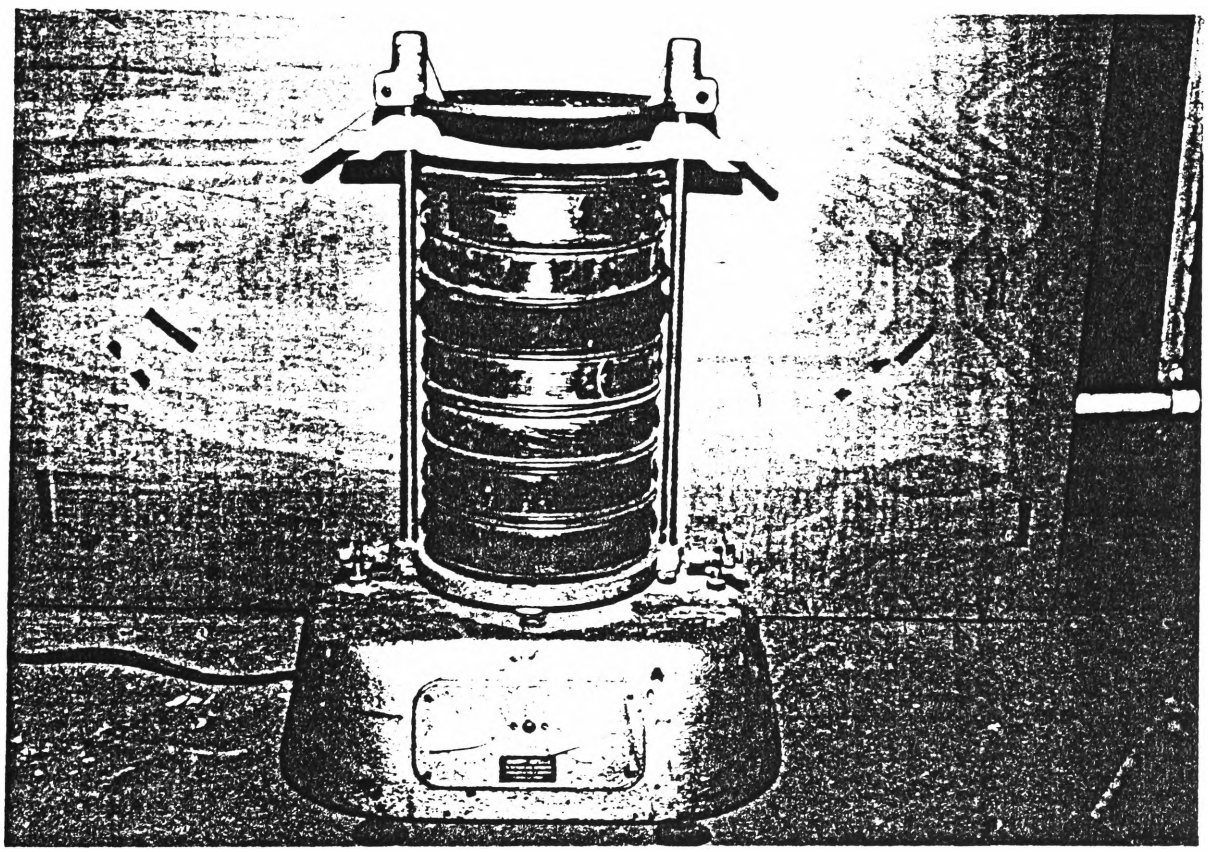

Fig. 6.9 Electric Sieving Shaker

6.4 Experimental Procedure and Results

The experimental work was carried out under the previously described conditions and the experimental procedure was designed to obtain detail data for each test as follows:

1) Connection of all monitoring and data acquisition instrumentation facilities to the drill rig.
2) Measurement of all required parameters of the new drill bits to be tested.
3) Attachment of the cutting catcher to the drill rig.
4) Commencement of drilling while data logging system in action.
5) Cease drilling when the maximum displacement was reached, which is dependent on the space available to the hole drilled on the concrete block.
6) Qualitative observation and recording of the bit condition, especially the chipping of the cutting tips.
7) Start drilling next hole with the same bit.

6.4.1 Number of holes drilled by the tested bits

The length of a hole in this experiment varies approximately from 0.7 m to 0.9 m. So the number of holes drilled by a tested bit is in proportion to

the total length drilled. For convenience of description in the following context, the number of holes drilled is used instead of the length drilled.

The number of holes drilled by a tested bits is an important index determining the bit life. Usually, the more holes a bit can drill, the longer life the bit will be considered to have. In this experiment, the tested bits, at first thought, were allowed to be used repeatedly until they completely failed or were worn out to demonstrate their performance, but soon it was noted that some bits were still in a very good condition after drilling more than 20 holes. It was then decided that a maximum of 20 holes per bit were to be drilled due to the limitation of space in the drilling medium. Definite trends of a bit performance could be established after drilling 20 holes. So for some bits, the number of holes drilled by the tested bits does not necessarily represent the real life of the bits.

Fig. 6.10 shows the number of holes drilled by each tested bit.

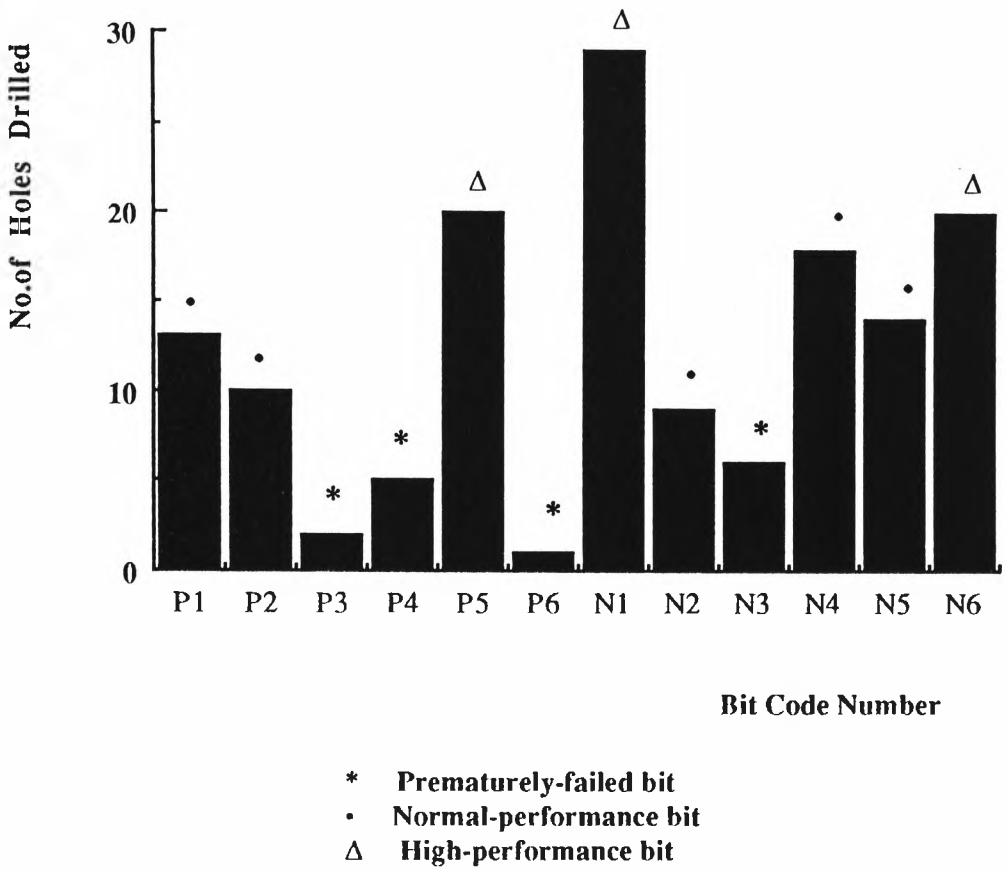

Fig. 6.10 Number of Holes Drilled by Tested Bits

6.4.2 Penetration rate

Penetration rate is an indicator of the performance of a bit and therefore the quality of a bit. Usually, the penetration rate of a bit will decrease with the increase of the total length of holes drilled by the bit, provided that the other drilling conditions remain the same. The fact is the cutting tips of a bit will be chipped off and worn out gradually with the advance of the drill, simply because the drilling operation is a process during which the tools cut rock while being chipped off and worn out by rock. The chipping and wearing will degrade the

sharpness of the cutting tool, and consequently will slow down the penetration rate. When the penetration rate decreases to a certain level, the bit will be considered to have reached the end of its life.

The penetration rate is usually measured by the length drilled against the time spent during the drilling process. The length drilled can be the length of a hole or the total length drilled by a bit. So a penetration rate here can be a mean value based on a hole length or the total length drilled by a bit.

Fig. 6.11 is the diagram of the average penetration rates versus the number of holes drilled respectively by the tested bits. Here the average penetration rate is calculated by dividing the total drilling length of a bit by the time spent in drilling.

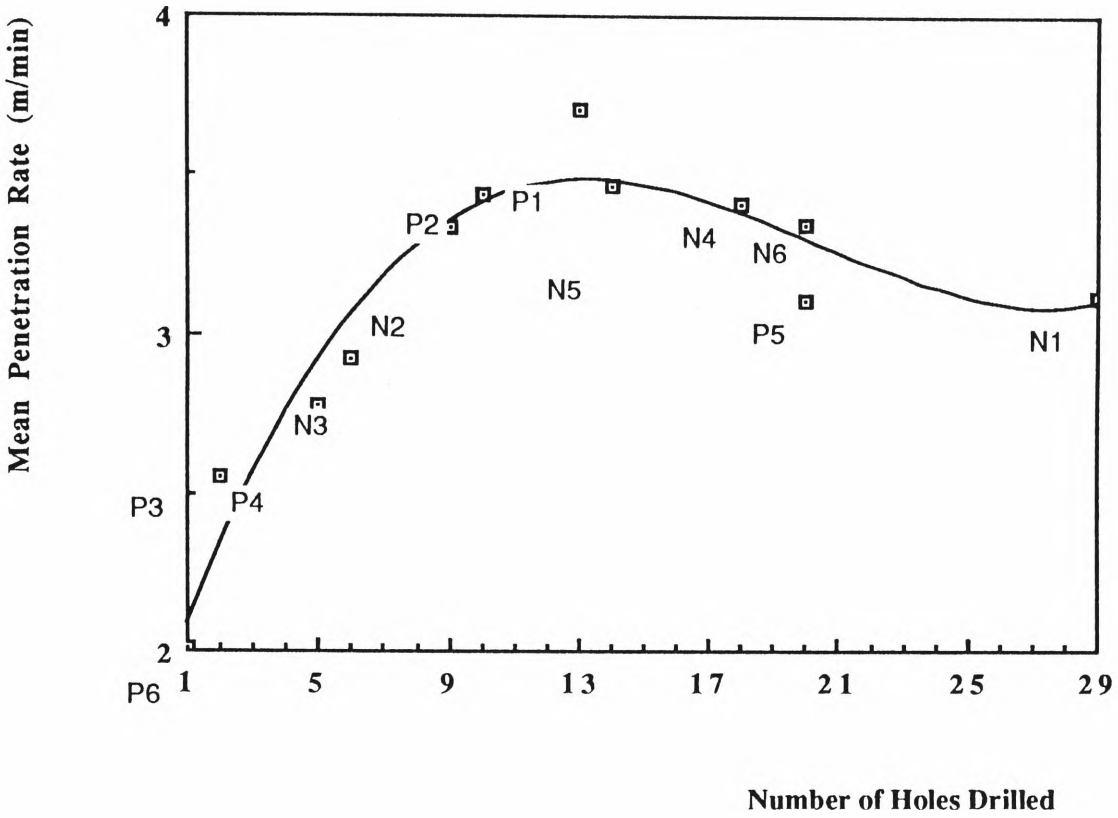

Fig. 6.11 Mean Penetration Rate vs. Number of Holes Drilled by Each Tested Bit

Figs. 6.12, 6.13, 6.14 and 6.15 are the diagrams of the penetration rate versus holes drilled by bits P4, P1, N6 and N1 respectively, which are picked up from different performance groups, or for its special feature of performance.

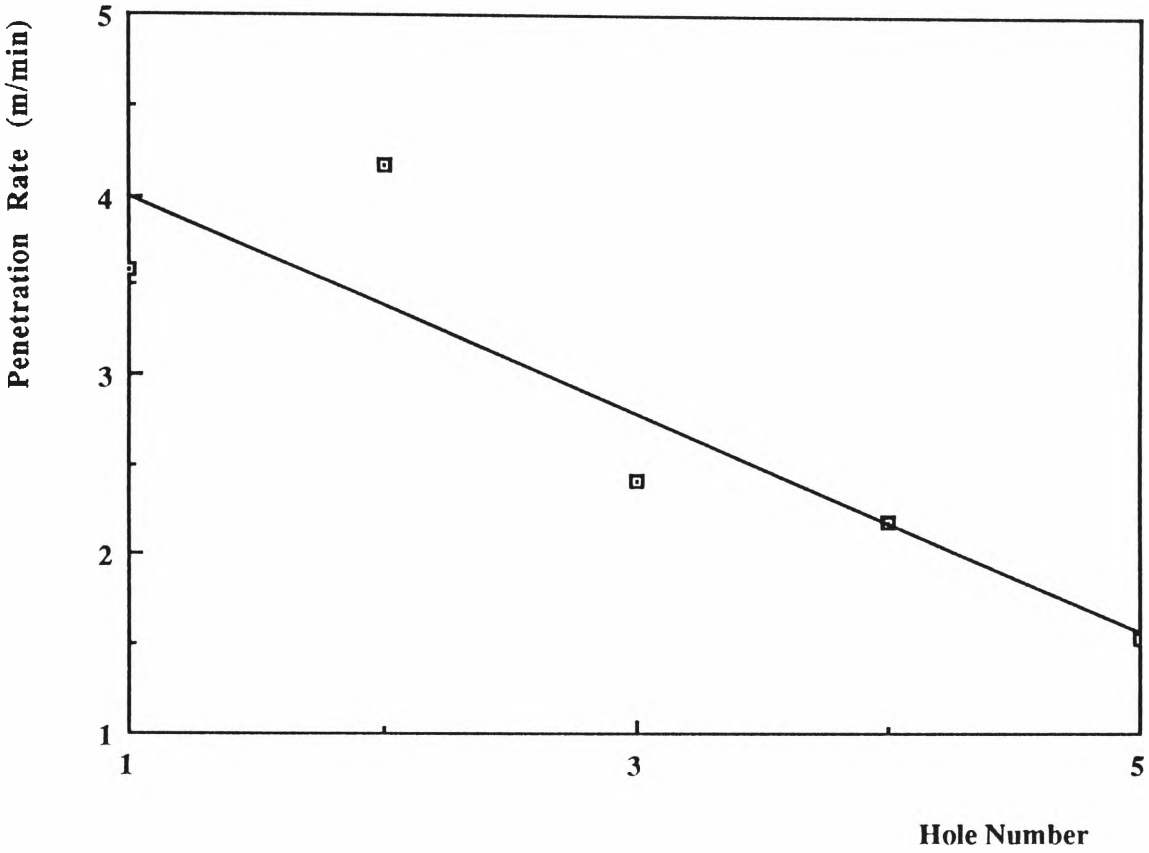

Fig. 6.12 Penetration Rate vs. Holes Drilled by Bit P4

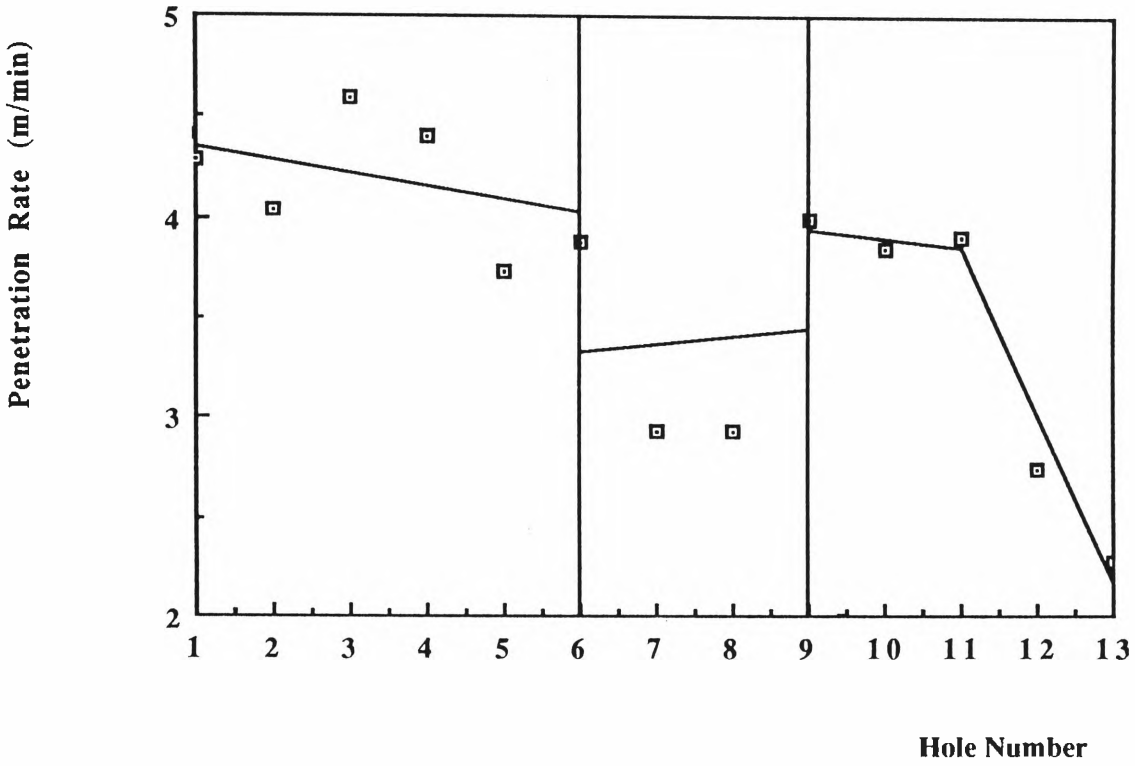

Fig. 6.13 Penetration Rate vs. Holes Drilled by Bit P1

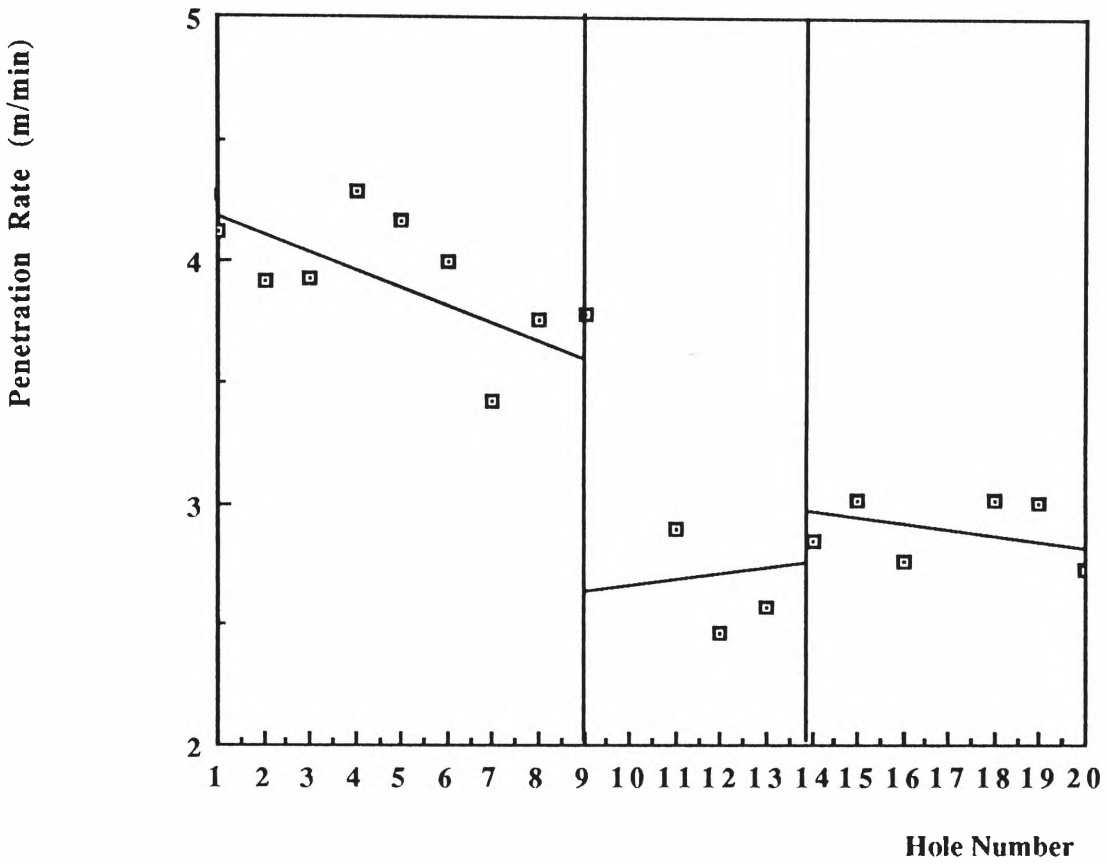

Fig. 6.14 Penetration Rate vs. Holes Drilled by Bit N6

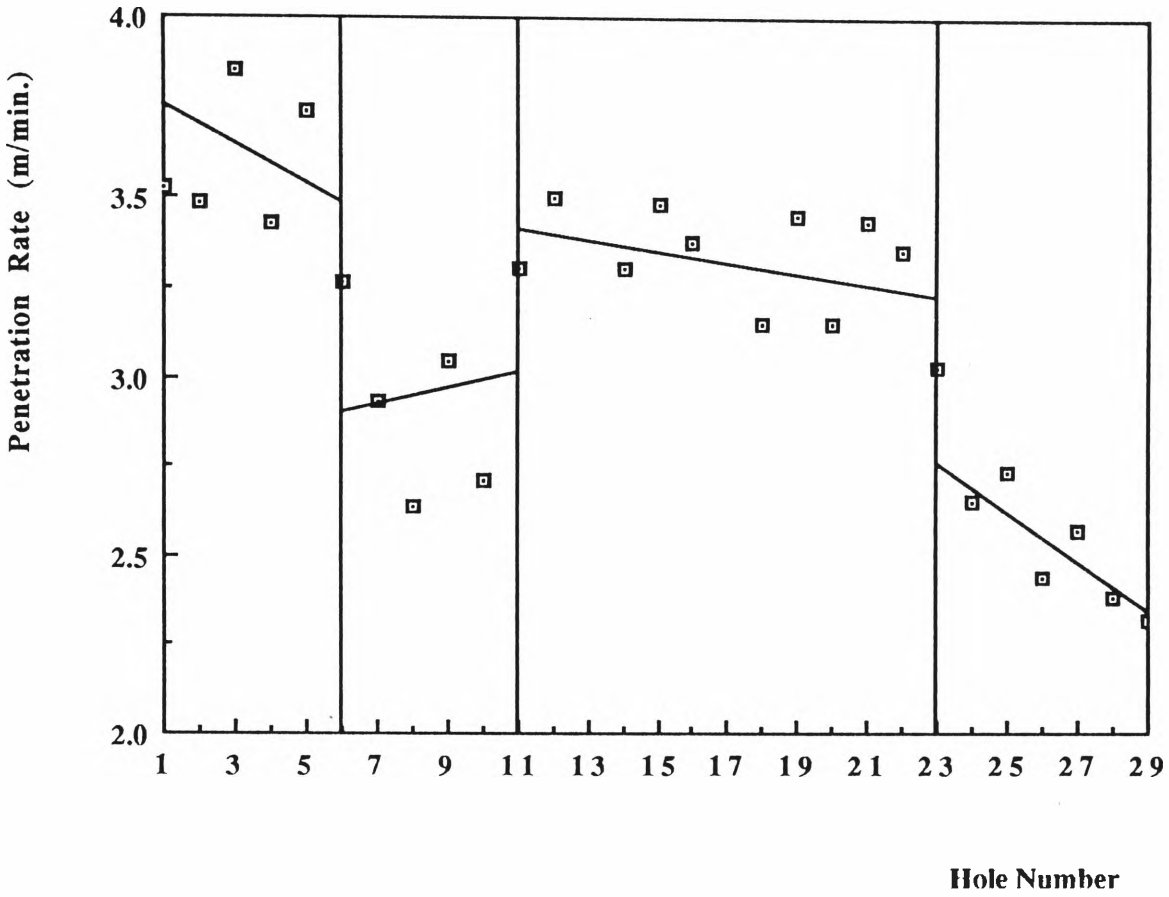

Fig. 6.15 Penetration Rates vs Holes Drilled By Bit N1

6.4.3 Specific energy

Specific energy, in terms of rock drilling, is defined as the amount of energy required to remove a unit volume of rock. It is a useful parameter to help predict performance and power requirements when a certain drilling pattern is set, and may be taken as an index of mechanical efficiency of a rock drilling process.

Maurer (1981) expressed specific energy for general drilling activity as:

$$E_S = \frac{P_{in}}{dv/dt} = \frac{P_{in}}{A\,R_P} \qquad (6.1)$$

where

E_S	specific energy
P_{in}	power input
dv/dt	volume time derivative
A	drill hole cross-sectional area
R_P	penetration rate

This expression is a general formula to calculate specific energy for any kind of drilling activity. For rotary non-percussive drilling, Teale (1965) proposed a formula to calculate specific energy.

$$E_S = e_t + e_r = \frac{F}{A} + \left(\frac{2\pi}{A}\right)\left(\frac{N\,T}{R_P}\right) \qquad (6.2)$$

where

e_t	thrust component of specific energy (J)
e_r	rotary component of specific energy (J)
F	applied thrust force on drill bit (N)
A	drill hole cross-sectional area
π	pi, a constant
N	rotary speed of drill bit (rpm)
T	applied torque (Nm)
R_p	penetration rate (m/min).

The formula here divides specific energy of rotary non-percussive drilling into the components of the thrust and rotary actions, which are directly related with the power input in this sort of drilling. It is interesting to note that the thrust component (F/A) is equivalent to the mean 'pressure' exerted by the thrust over the cross-sectional area of the hole. Specific energy is, in fact, dimensionally identical with pressure or stress, since (m N/m^3) is equivalent to (N/m^2). Physically, this arises from the fact that if a force F acting on and normal to a surface of area A moves it through a distance ds, the increment of work done, dw, is equal to Fds. The volume change effected by the movement, dv, is Ads. If e is the specific energy at any point, then

$$e = dw/dv = F/A = p \qquad (6.3)$$

where p the pressure at that point.

Fig. 6.16 shows the specific energy for the first holes drilled by all tested bits. Figures 6.17, 6.18 and 6.19 plot the specific energy versus the hole number drilled by the tested bits P4, P1 and N6.

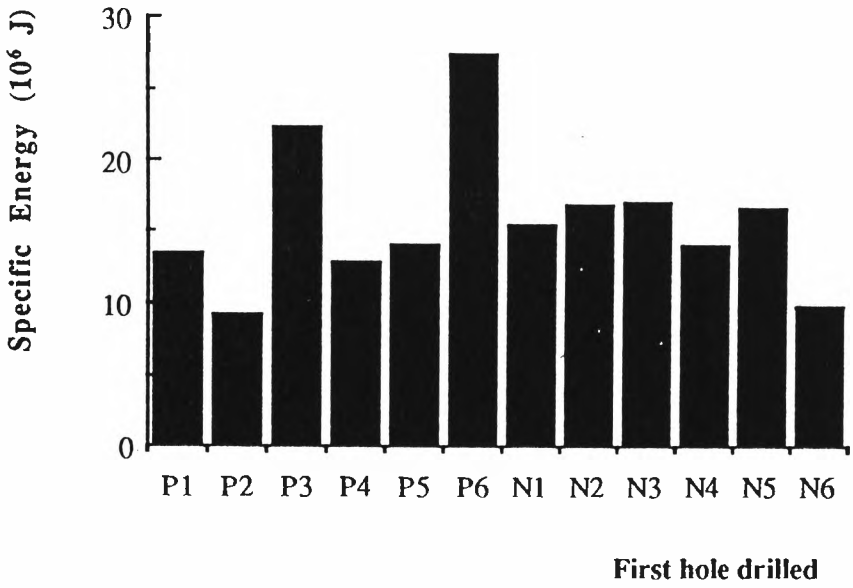

Fig. 6.16 Specific Energy vs the First Holes Drilled by Tested Bits

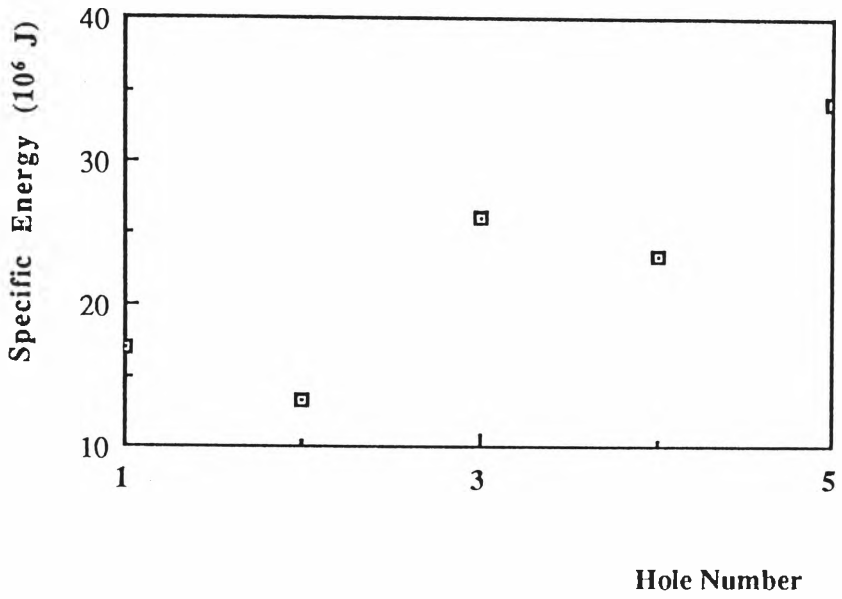

Fig. 6.17 Specific Energy vs. Holes Drilled by Bit P4

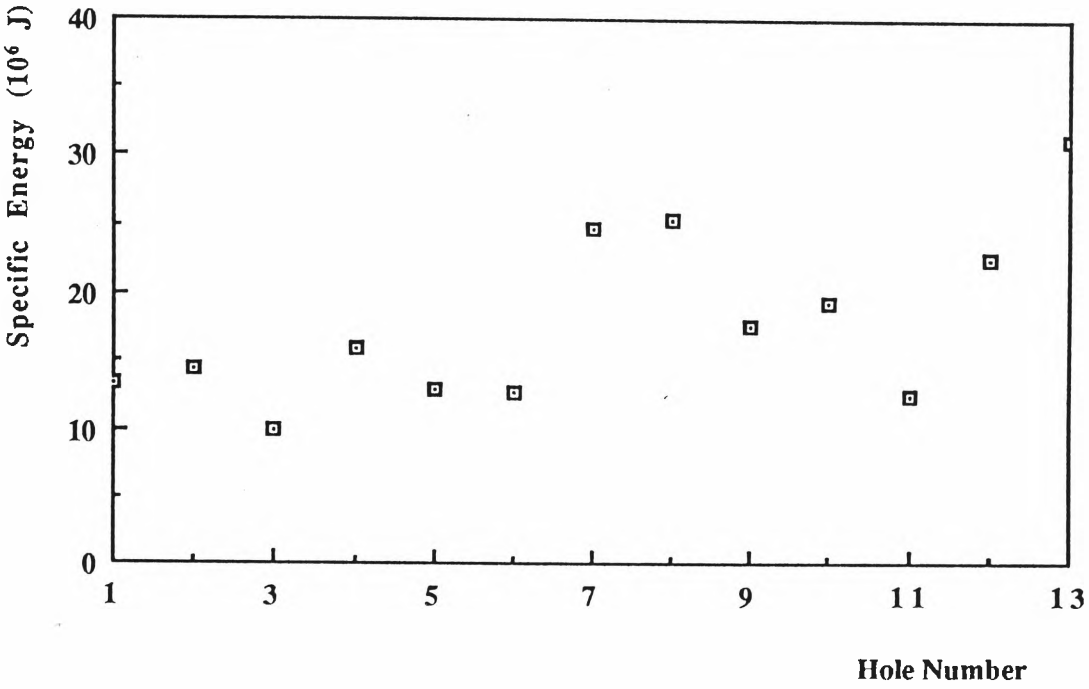

Fig. 6.18 Specific Energy vs. Holes Drilled by Bit P1

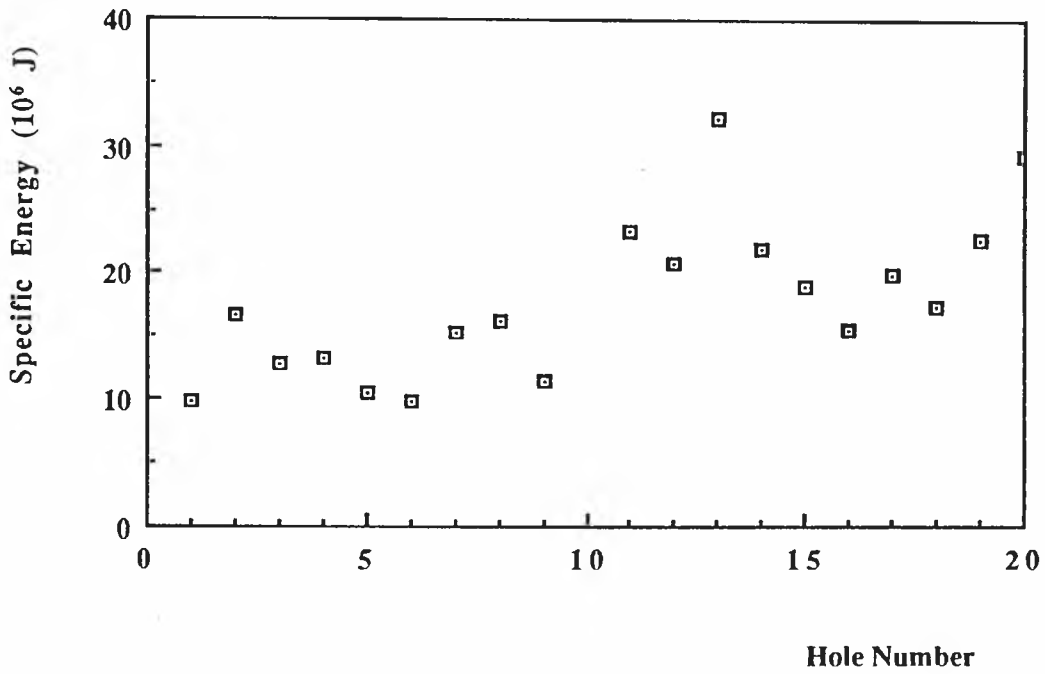

Fig. 6.19 Specific Energy vs. Holes Drilled by Bit N6

6.4.4 Cutting size analysis by sieving

Sieving analysis is one of the simplest and most widely used methods for particle size analysis, that covers the approximate size range 0.02 mm to 125 mm using standard woven wire sieves.

The purpose of sieving the cutting samples in this experiment is to find out the cutting size distribution, so as to understand the cutting characteristics of different bits, and of the same bit as it is wearing out.

Collected cutting sample from a drill hole was put into a tray and then dried in a oven. Determination of cutting size distribution was obtained by sieving each sample of cuttings and then weighing the amount of cuttings caught on each of the sieves used. The weight percentage of cuttings retained on each sieve were calculated. Based on those data, the mean weighed size was worked out to interpret the data, after Allen (1981):

$$\overline{S} = \frac{\sum_{i=1}^{n} S_i \, dw_i}{\sum_{i=1}^{n} dw_i} = \sum_{i=1}^{n} S_i \times P_i \qquad (6.4)$$

where $\overline{S}$ the mean size of the cutting sample obtained from a drill holes

S_i the average size of the cuttings retained on the *i*th sieve

dw_i the weight of cuttings retained on the *i*th sieve

P_i the weight percent of the cuttings retained on *i*th sieve in the total weight of the cutting sample

Cuttings retained on sieves A, B, C, D, E & F are named respectively as cuttings A, B, C, D, E & F, and cutting with a size of smaller than mesh size of sieve F (0.15 mm) is named as cutting G. The size range of cuttings A, B, C, D, E, F & G is shown by Table 6.3

Table 6.3 Size Range of Cuttings

Cutting Code	A	B	C	D	E	F	G
Size Range	≥6.70	6.70-2.36	2.36-1.18	1.18-0.60	0.60-0.30	0.30-0.15	<0.15

The data concerning the cutting distribution of bits P4, P1, N6 and N1 are given in the Appendix of the thesis.

6.5 Analyses of the Experimental Results

6.5.1 Number of holes drilled by, and failure patterns of, the tested bits

From Fig. 6.10, the test bits can be divided into three groups according to their performance. The first group refers to the bits with a bit life of not more than 6 holes (approximately 4 metres), and can be called the prematurely-failed group. The bits in this group, including bits P6, P3, P4 and N3, completely failed up to the number of holes drilled. The second group are the bits with a bit life of 9 to 18 holes (approximately 7 to 14 metres). The bits in this group are called the normal-performance bits, including bits N2, P2, N5, P1 and N4. The third group includes bits N1, N6 and P5 which did not fail up to the number of holes drilled, and is called the high-performance group.

Qualitative observation and records show that the bits in the prematurely-failed group all had early severe chipping on the cutting tips, and failed by sudden fatal chipping developing on the cutting tips of the bits or a full tear-off of the cutting tips. Fig. 6.20 is a photo of these prematurely-failed bits.

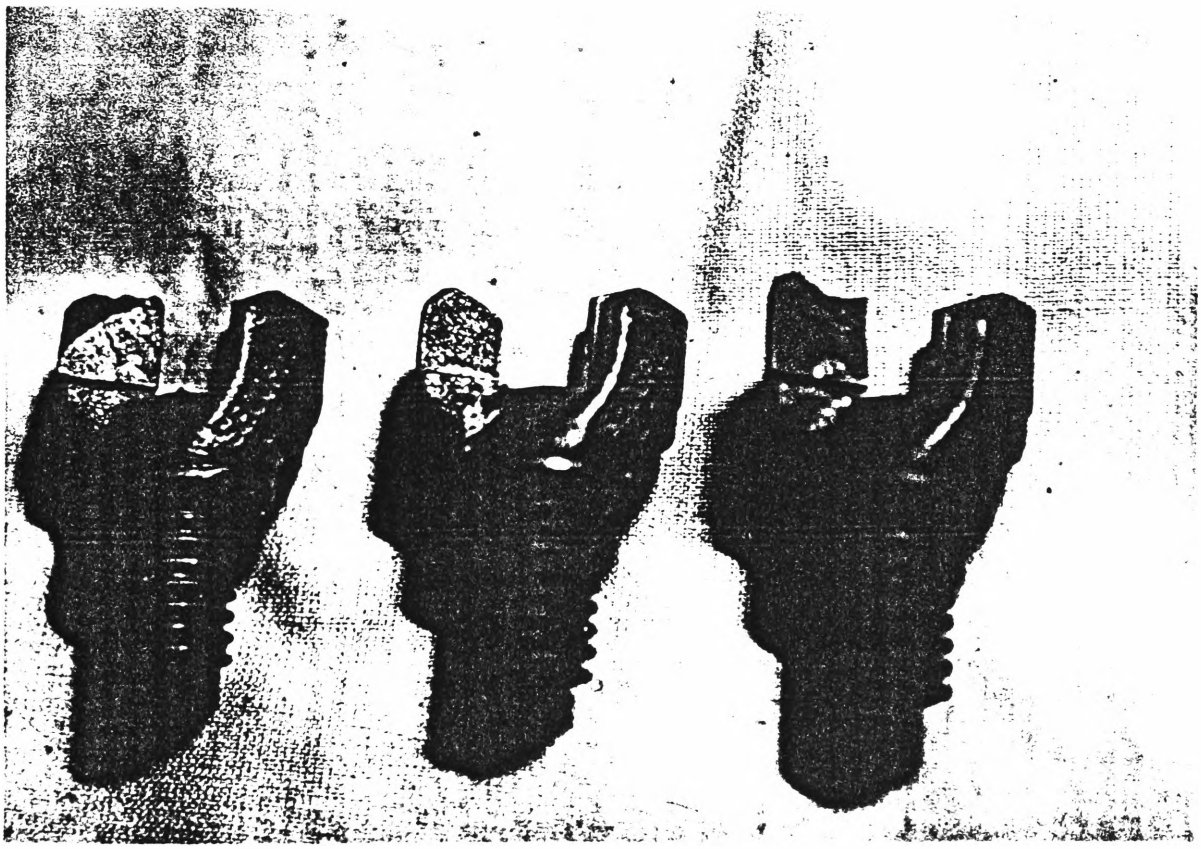

Fig. 6.20 Photo of Prematurely-Failed Tested Bits

So the failure pattern of the prematurely-failed bits can be summarised into three stages: early severe chipping, sudden fatal chipping and failure, as demonstrated by the diagram of Fig. 6.21.

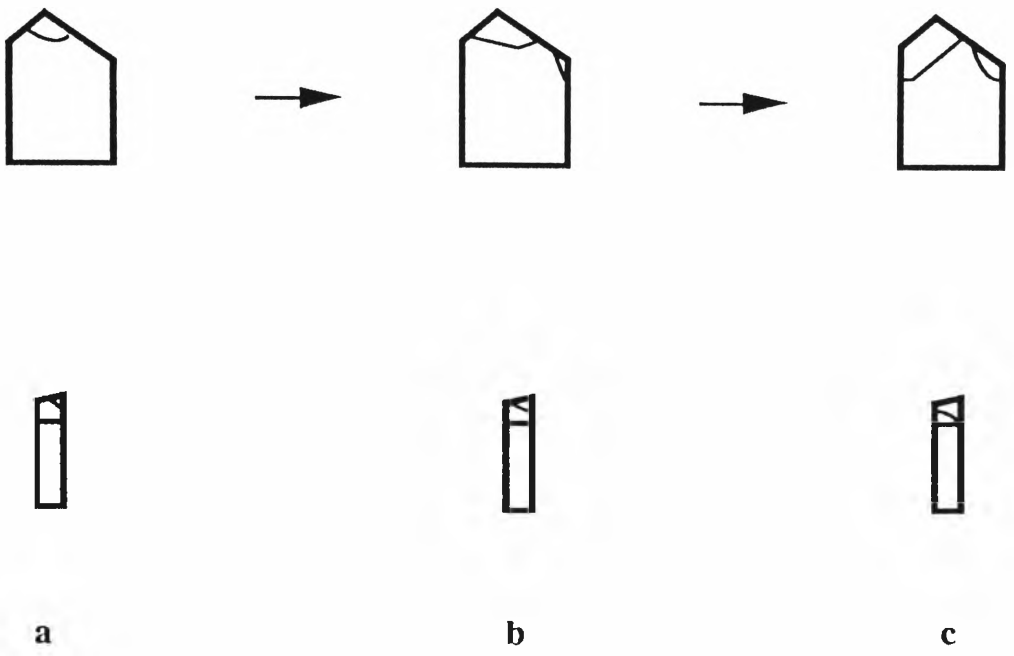

Fig. 6.21 Failure Pattern of the Bits in Prematurely-failed Group

Those bits in the high-performance group always showed a record of a gentle development of a smooth chipping pattern. Fig. 6.22 is a photo of bits N1 and N6 taken after drilling 29 and 20 holes respectively. The cutting tips, especially the top point of these bits, were gradually chipped off after drilling a few holes, and major chips were formed on the top points of the tips after completing about 7 holes. Afterwards, the cutting tips seemed to be self-resharpening, and their front and side faces of the top points smoothly developed into a round shape after completing approximately 9 holes. The rounded shape of the front face of the

top point is very much similar to the shape of the tips on the bits shown on Fig. 6.22. The cutting tips with the rounded shape then only developed a little more minor chipping in the further drilling until the termination of the testing.

Fig. 6.22 Photo of High-Performance Tested Bits

The chipping development process on the the bits of the normal-performance group, i.e. bits N2, P2, P1,N5 and N4, was similar to the chipping pattern developed on the bits of the high-performance group. The only difference was that the round shape of the cutting tips formed by the action of self-resharpening on the bits of the normal-performance group lasted a shorter period than that on the bits of the high-performance group. The normal-performance bits

then developed some fatal chipping, and failed, instead of developing a little further chipping as in the case of the bits of the high-performance group.

So the chipping pattern of the bits in the normal performance or high-performance group can be described as: chipping off the top points of the tips; self-resharpening of the tips and development of a round shape on the front and side faces of the tips, which was normally maintained for a good period; smoothly further minor chipping, or developing fatal chipping and failed, as explained by the diagram of Fig. 6.23.

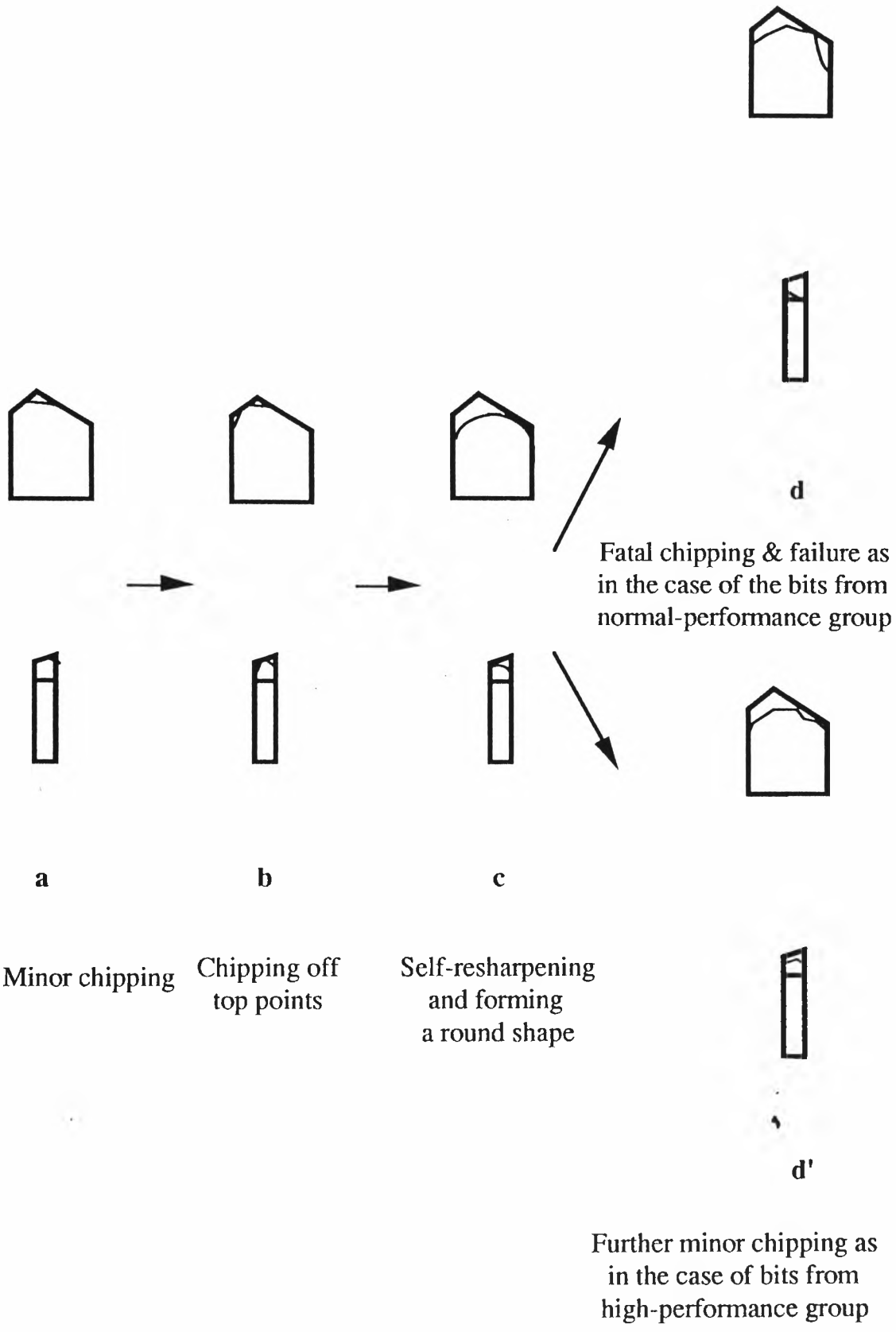

Fig. 6.23 Failure Pattern of the Bits

in Normal- & High-Performance Group

In terms of the number of holes drilled by the test bits under the circumstances of this particular testing program, the positive rake bits obviously showed a poorer performance than the negative rake bits. Half of the positive rake bits tested fell into the prematurely-failed group, and only one bit from the 6 positive bits tested drilled more than 15 holes.

The reason for the fatal chipping or the full tear-off of the tips of the bits in the prematurely-failed group was probably attributable to the too aggressive cutting tools of the bits, which cut into the drilling medium to a depth greater than what the material of the cutting tools could withstand under the imposed forces. Actually, a much greater specific energy almost always accompanied these premature failures, as shown by the values of the specific energy of first hole drilled by bit P6 on Fig. 6.16 and the fifth hole drilled by bit P4 on Fig. 6.17. This observation may be able to explain why more than half of the failures of the positive rake bits tested was due to premature failures, while only one case occurred in the negative bits. It is an accepted fact that a positive rake bit is more aggressive than a bit with a negative rake for a given feed thrust and torque.

6.5.2 Analysis of penetration rate

Fig. 6.11, the diagram of penetration rate versus the number of holes drilled by the tested bits, shows a trend that the average penetration rates of the tested bits increase with the number of holes drilled up to about 10 holes, and

afterwards, the penetration rates seems to be maintained at the same level. The incremental rate of the penetration rates with the number of holes drilled is extremely high for those prematurely failed bits, for each of which the number of holes fulfilled was not great than 6. These prematurely-failed bits usually showed an extremely low penetration rate as they went into the fatal chipping or failure period. The fact that the penetration rates of the bits in normal or high performance group remain consistent, means that these test drill bits demonstrated a similar performance.

Fig. 6.12 shown the diagram of the average penetration rates in each of 5 holes drilled by the bit P4 from the premature-failed group. In holes No.1 and No.2, the penetration rates are as high as the penetration rates of bits from the other groups, afterwards the penetration rates decrease sharply. This phenomenon corresponds to the qualitative observation of the cutting tool. There was only a little minor chipping on the cutting tips of bit P4 after drilling the first two holes. The major chipping started when the third hole was drilled, and it developed very quickly. The bit totally failed at the completion of hole No.5.

Although the penetration rates versus the holes drilled by bits P1, N6 and N1, as shown in Figs 6.13, 6.14 and 6.15, appear rather random, the trend is still clear if the hole number is divided into several intervals according to the value of the penetration rate, and appropriate lines are fitted to the points of each interval. The penetration rates of a bit is obviously at three or four levels. All bits had a high initial penetration rate, as can be seen by the penetration rates of the first few holes drilled by each of these bits. This interval may be called the first high penetration rate period. After holes No.6 - No.9, the penetration rates reduced

suddenly, and remained at a low level for a few holes. After further drilling, the penetration rates seemed to rise up to a certain high degree, which was retained for a while, or reduced gently. This interval may be called the second high penetration rate period. Following the second high performance period, some bits failed and the others reduced to a low performance level.

The trends of the penetration rates here again correspond well with the observation of chipping development on the cutting tips of these bits. As stated before, the bits in the normal or high performance group developed some major chipping after drilling the first a few holes, mainly on the top points of the cutting tips. These chipped cutting tips then gradually self-resharpen. Consequently, a round-shape of the cutting edges were developed on the front and side faces of the tips. Most likely, it was this re-sharpening process that brought the penetration rates again to a second high period of performance. Afterwards, some bits developed fatal chipping on the cutting tips and failed, while the other bits were worn out with the progress of drilling.

The other tendency which is noticed from the diagrams of the penetration rates of the bits P1, N6 and N1 is that a bit life is dependent on the length of the second high rate period; that is, the longer this period was maintained, the longer a bit life would be.

6.5.3 Specific energy

Fig. 6.16 shows that the values of the specific energy of the first holes drilled by the tested bits are all fell within the range of $9 \times 10^6 - 19 \times 10^6$ J, except the bits P3 and P6 have much higher values. This phenomenon is quite understandable, for the bits P6 and P3 both required a longer time to drill their first holes because of the major chipping developed on the cutting tips.

In the drilling system used to conduct the experiments, the bit condition i.e. the sharpness of the cutting tools, is the only one of the parameters which may dramatically vary from one hole to another.

In the diagrams of specific energy versus the holes drilled by the tested bits P4, P1, and N6, shown in Figs. 6.17, 6.18 and 6.19, the values of specific energy seem to vary considerably. But if the comparison is made between the specific energy and the relevant bit chipping patterns, the trend is not difficult to be seen. The specific energy values remain at a relatively low level before major chipping starts, while they rise up after severe major chipping occurs. The specific energy also tends to reduce during the process of the bit self-resharpening.

The fact that the specific energy responds to the cutting tool sharpness over a wide range indicates that specific energy is a useful parameter to predict the bit performance in an established drilling system. In fact, comparing the diagrams of penetration rate versus the holes drilled by bits P4, P1 and N6 on Figs 6.12, 6.13 and 6.14, a higher specific energy period generally responds a lower penetration rate period, vice verse.

6.5.4 Bit performance and its rake angle

The analyses on the bit failure pattern, drilling efficiency and energy consuming have made it clear that every bit demonstrates a different performance.

Under the established experimental procedure, the only factor which may severely affect a bit performance can be the parameters of the bit itself. Through Table 6.1, it is apparent that the test bits are featured and grouped by their rake angles, and hence it is of significance to study the relation between the rake angle of a bit and its performance.

A negative rake bit has a longer life and a smoother wearing pattern than a positive bit under the established test conditions. But it still remains unknown how the rake angle has quantitatively affected the performance of a bit from different bit groups. To answer this question, the relations between a rake angle and the penetration rate of, and/or the number of holes drilled by, a test bit of different bit groups have to examined in detail.

The negative rake bit tested has shown its special feature; it usually furnishes a greater durability than a positive rake bit. Then, the interesting thing would be to reveal the relation between the rake value of a negative bit and its average penetration rate, so as to design a durable bit with a feature of comparatively high penetration rate.

Fig. 6.24 shows the average penetration rate versus the rake angle of the test negative bit. There is a trend that the penetration rate is improved with

the increase of the rake angle of a negative rake bit. The average penetration rate of the bit with a rake angle of around -2.3° is much greater than that of the bit with a rake angle of about -3°. Therefore, it may be recommended that the rake angle of a negative rake bit should not be smaller than around -2.3° in order to obtain a possibly high level of penetration rate.

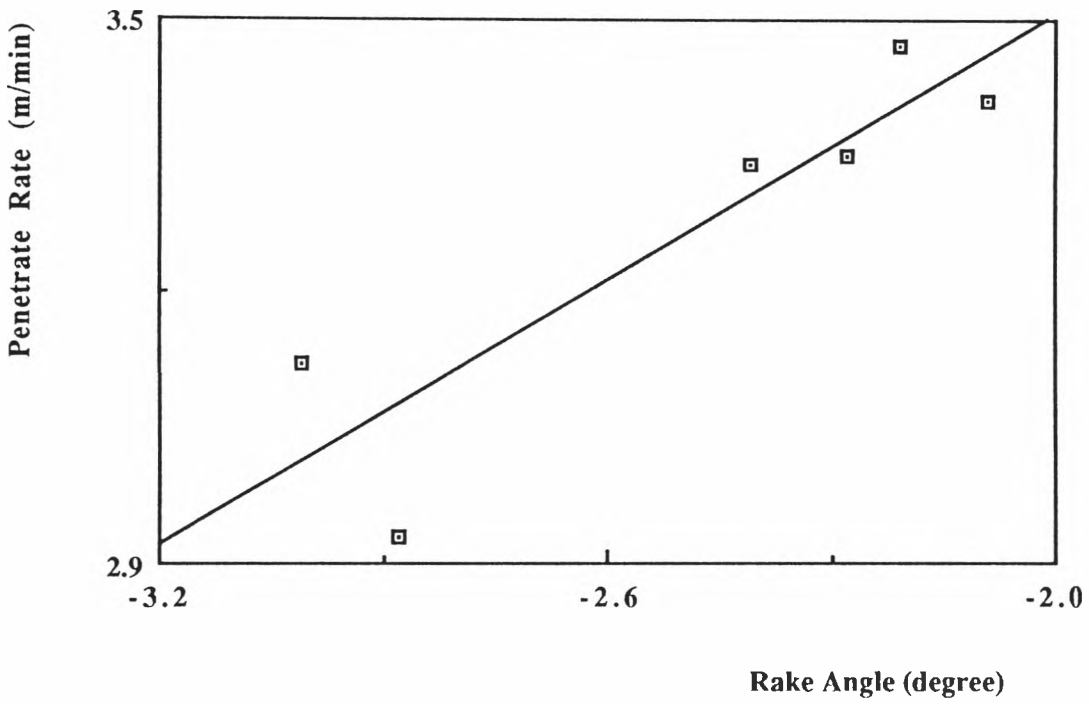

Fig. 6.24 Average Penetrate Rate vs. Rake Angle of Negative Bit Tested

The positive rake bits tested in the experiments showed a shorter average bit life than that of the negative rake bits tested, especially bits P6 and P3, with a bit life of 1 and 2 holes respectively. On the other hand, the best performance bit in terms of average penetration rate, out of all the tested bits, is a positive bit, bit P1, which has the much higher average penetration rate of 3.71 m/min than the mean of the average penetration rates of all the test bits, 2.91 m/min. Moreover, the test positive bits showed a sound initial-performance with a high penetration rate and a low specific energy before the sudden major chipping occurred on their cutting tips. Table 6.4 lists the average penetration rate and specific energy of the first three holes drilled by positive bits P1, P2, P4 and P5, and the means of the penetration rate and the specific energy of the first three holes drilled by all the six negative rake bit.

Table 6.4 Comparison of Penetration Rate & Specific Energy of the First 3 Holes Drilled by Some Positive Bits & Negative Bits

Bit Code	P1	P2	P4	P5	Mean of N Bits
Penet.Rate (m/min)	4.3	4.5	3.5	4.2	3.82
Spe. Energy ($\times 10^6$ J)	13.9	14.6	19.4	14.9	16.6

Apart from bit P4, which had a major chipping when drilling the third hole, the positive bits demonstrated a much higher penetration rate and a lower energy consumption in drilling their first three holes than the negative bits.

It seems that bit life is a major issue to be looked at for positive bits. Fig. 6.25 plots a diagram of the number of holes drilled versus the rake angles of the test positive rake bits. It is clear that the bit life is shortened with the enlargement of the rake angle of a positive rake bit under the established test conditions. The bit life is extremely low when the rake angle is greater than 4.6°, whereas the bit possesses a reasonable life when the rake angle drops to around 4°.

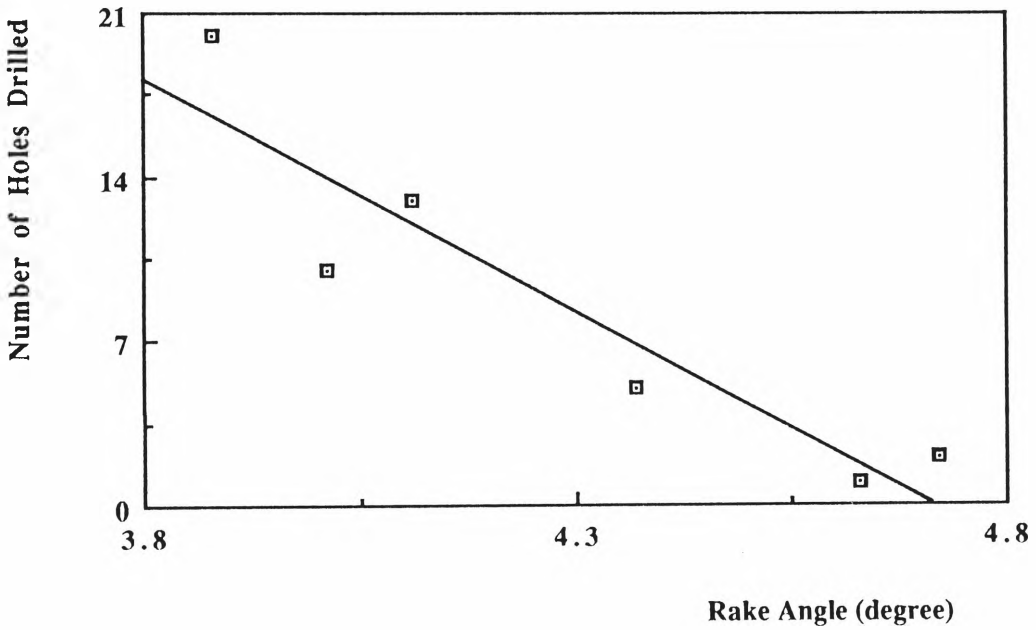

Fig. 6.25 Number of Holes Drilled by Positive Bit Tested vs its Rake Angles

6.5.5 Cutting size distribution of cutting samples

By analysing the data derived from the cutting samples obtained from the boreholes drilled by bits P4, P1, N6 and N1, a tendency is shown clearly. Cuttings of size B (<6.70, ≥2.36 mm) in most of cases take up the highest weight percentage of a sample (between 21-41%), while cuttings A (≥6.70 mm) or cuttings G (<0.15 mm) usually occupy the smallest faction of the weight in a sample (between 1-11% and 3-13% respectively).

A diagram of mean cutting size of each of the 43 cutting samples versus its value order in ascending sequence from 1 to 43 is plotted on Fig. 6.26. Although values of mean sizes all fall into the range of 1.5-2.9 mm, they are mainly concentrated on the intervals of 1.65-2.30 mm.

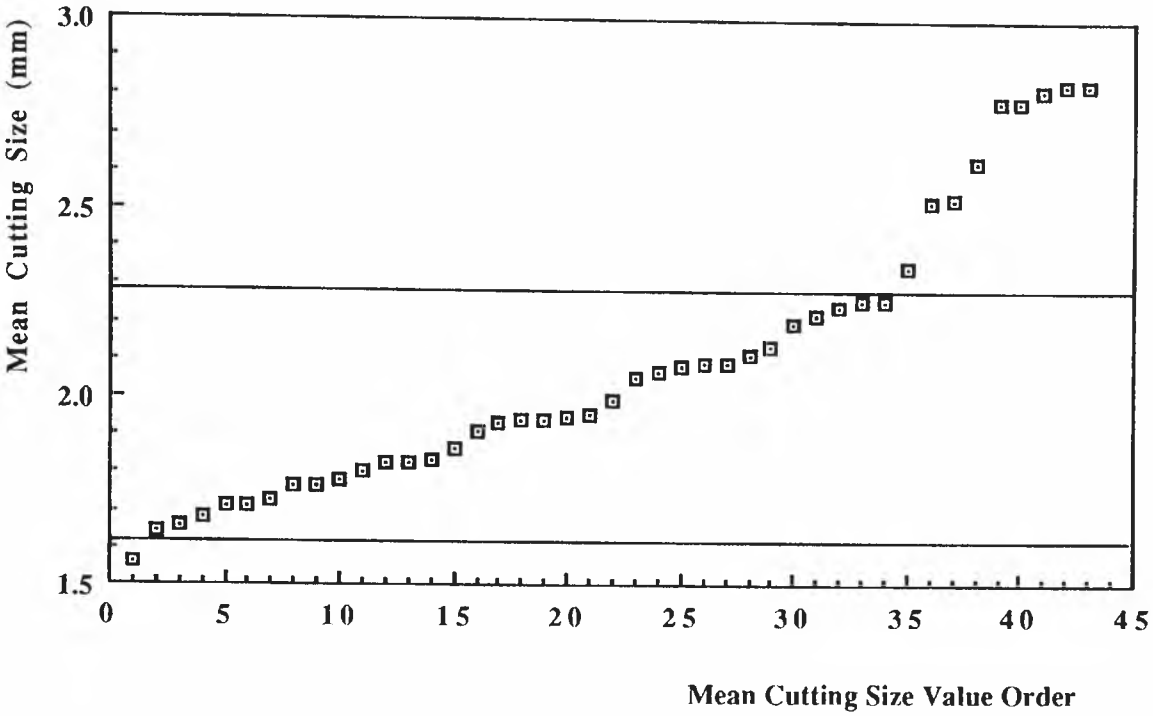

Fig. 6.26 Mean Cutting Size vs. Its Value Order

The arithmetic mean of the mean size is calculated out with a value of 2.085 mm. The interesting thing about the arithmetic mean of the mean cutting sizes is that its value is close to the square aperture size of the second largest sieve, sieve B (2.36 mm), on which the greatest portion of every sample was retained. It is logical to think that the weight percentage of cuttings caught upon sieves A and B, i.e. the cuttings no smaller than 2.36 mm, has basically determined the mean size value order of a cutting sample. In brief, the faction of cuttings A & B in a cutting sample dominates its mean size. Actually, the mean size of a cutting sample is defined as the sum of the average cutting sizes on each sieve times their respective weight percentages. Therefore, the cuttings with a large size and a great portion in a cutting sample should dominate its mean size.

Figs. 6.27, 6.28, 6.29 and 6.30 show the weight distribution of cuttings of three typical cutting samples, the samples with the greatest and smallest mean cutting sizes (2.837 mm and 1.562 mm), and with the mean cutting sizes (2.081 mm and 2.090 mm) closest to the arithmetic mean of mean cutting sizes (2.085 mm). Apparently, the percentage of cuttings A takes up a small portion in a sample and varies randomly, whereas the percentage of cuttings B claims the largest portion and varies with the increase of the mean cutting size.

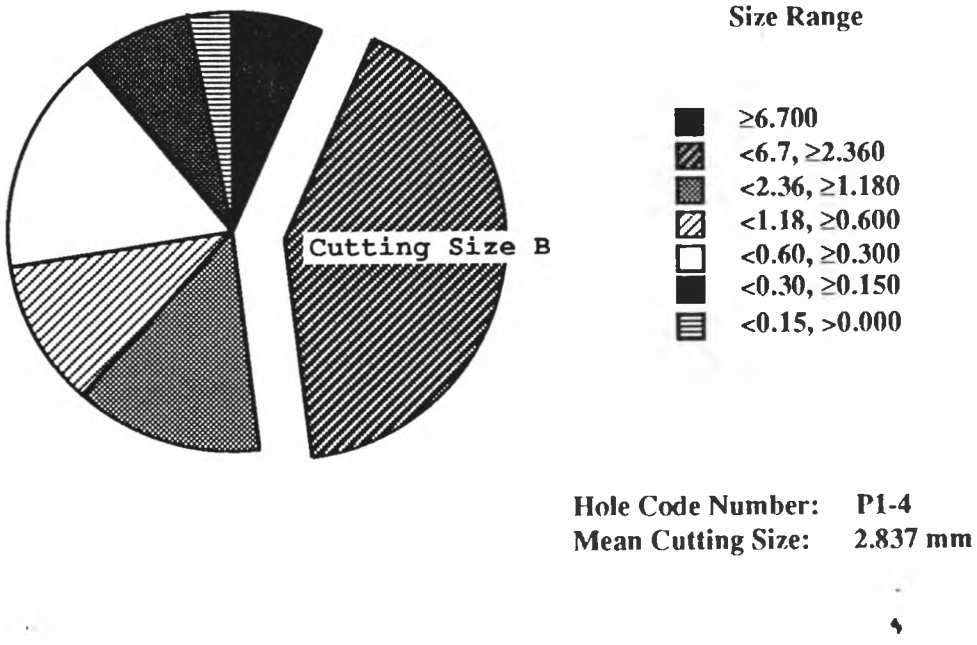

Fig. 6.27 Cutting Size Distribution of the Sample with the Largest Mean Cutting Size

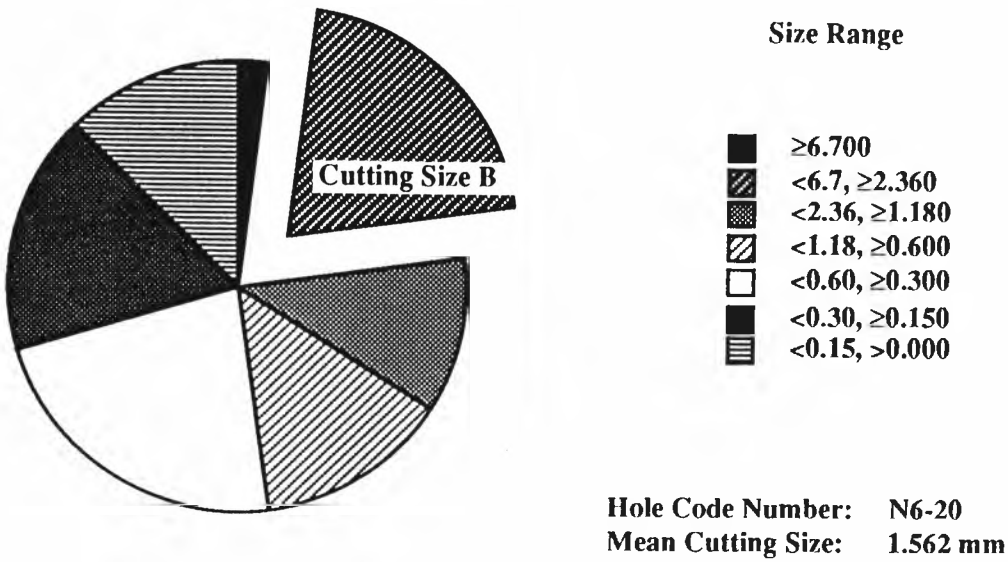

Fig. 6.28 Cutting Size Distribution of the Sample with the Smallest Mean Cutting Size

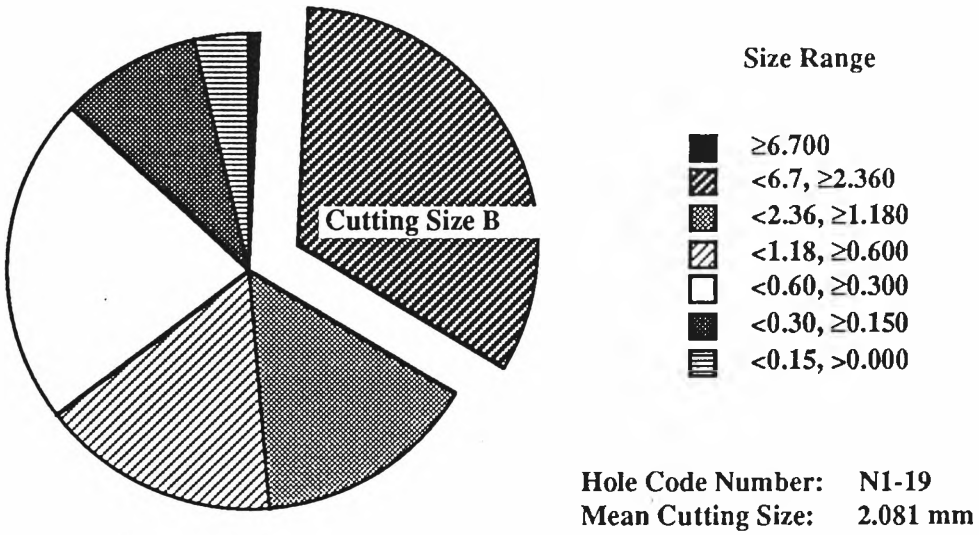

Fig. 6.29 Cutting Size Distribution of the Sample with the Mean Cutting Size Closest to the Arithmetic Mean of Mean Cutting Size

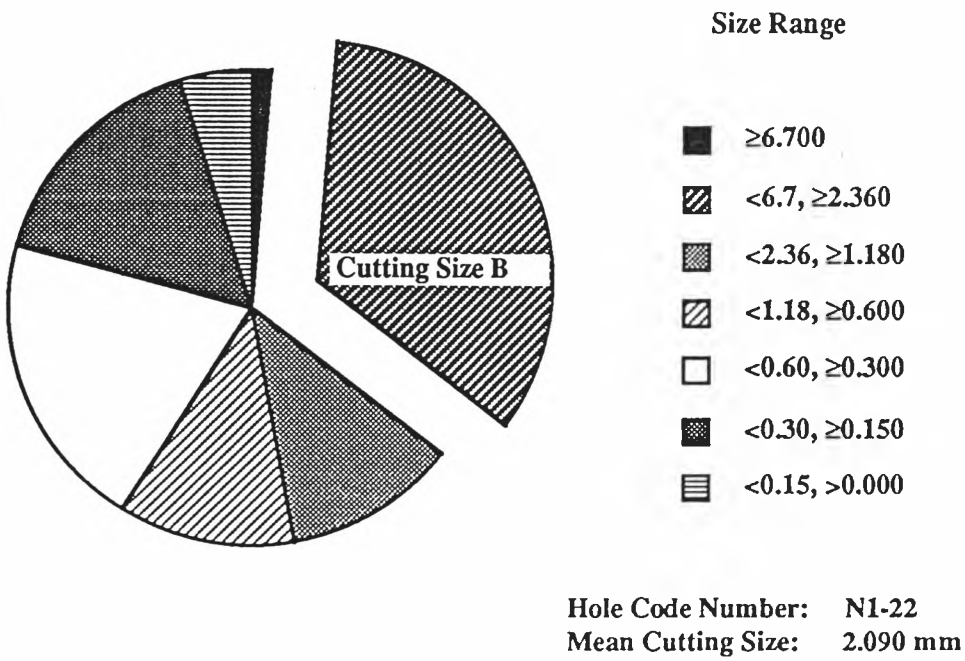

Fig. 6.30 Cutting Size Distribution of the Sample with the Mean Cutting Size Closest to the Arithmetic Mean of Mean Cutting Size

The diagrams of mean cutting size versus the holes drilled by bits P4, P1, N6 and N1 are plotted on Figs. 6.31, 6.32, 6.33 and 6.34. These diagrams show that the mean cutting size corresponds well with the cutting tip sharpness or the chipping patterns of the cutting tips, i.e. under the same drilling condition, the sharper the cutting tips of a bit, the greater the mean cutting size will be produced.

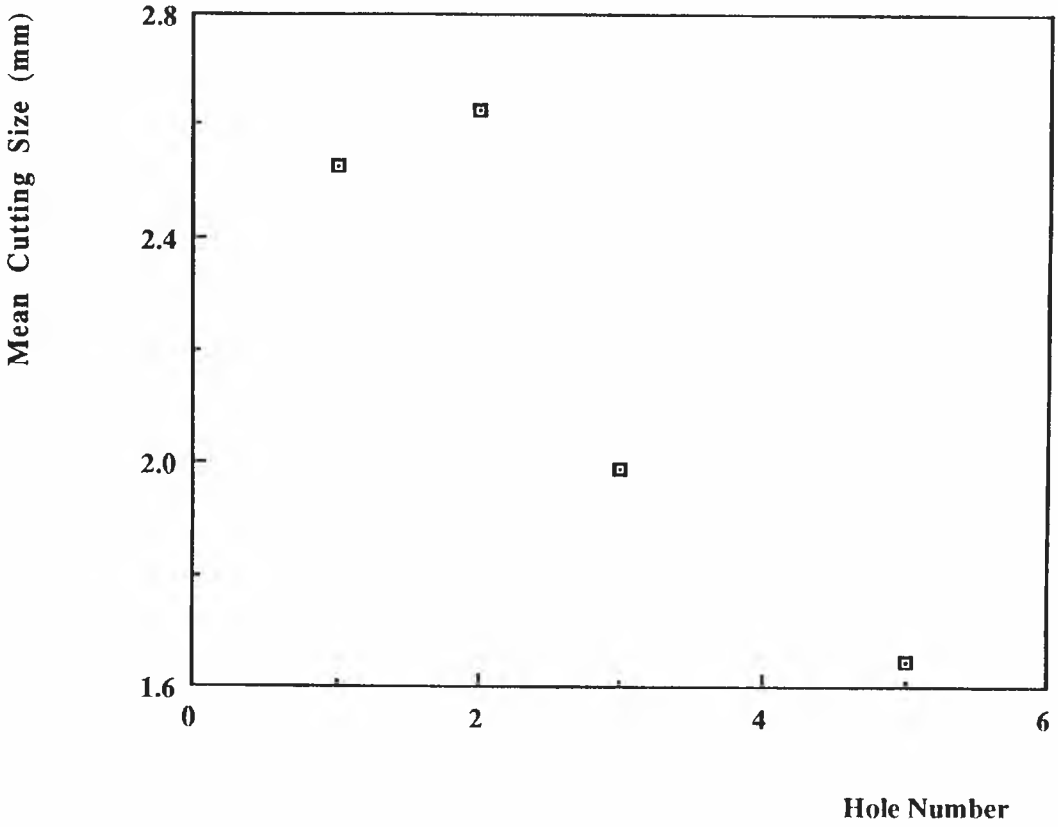

Fig. 6.31 Mean Cutting Size vs. Hole Drilled by Bit P4

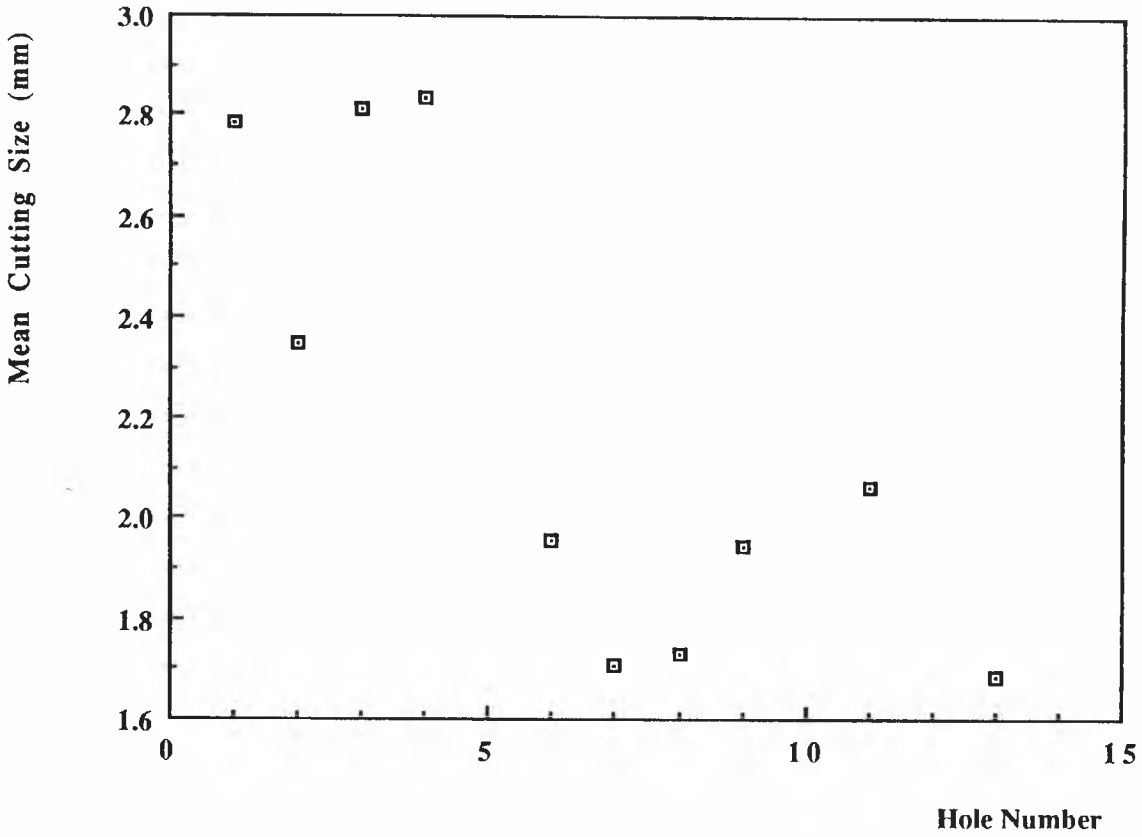

Fig. 6.32 Mean Cutting Size vs. Hole Drilled by Bit P1

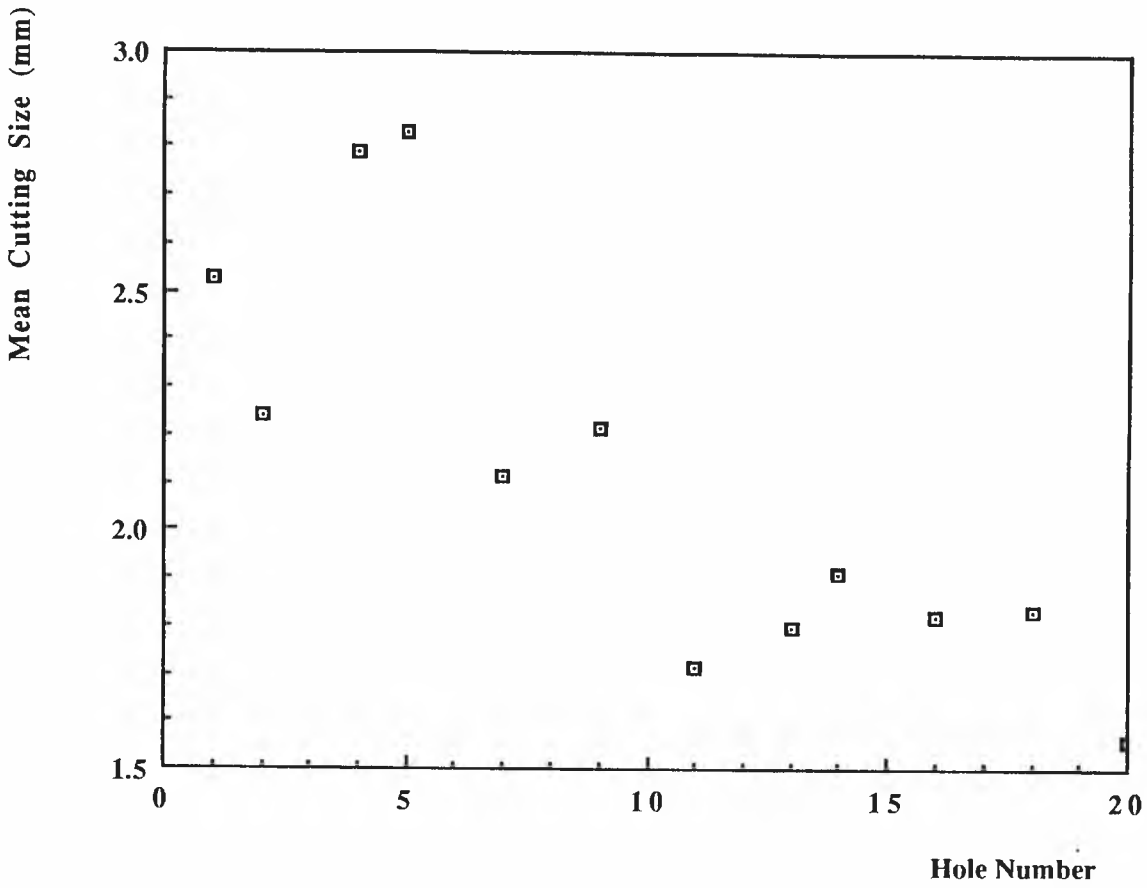

Fig. 6.33 Mean Cutting Size vs. Hole Drilled by Bit N6

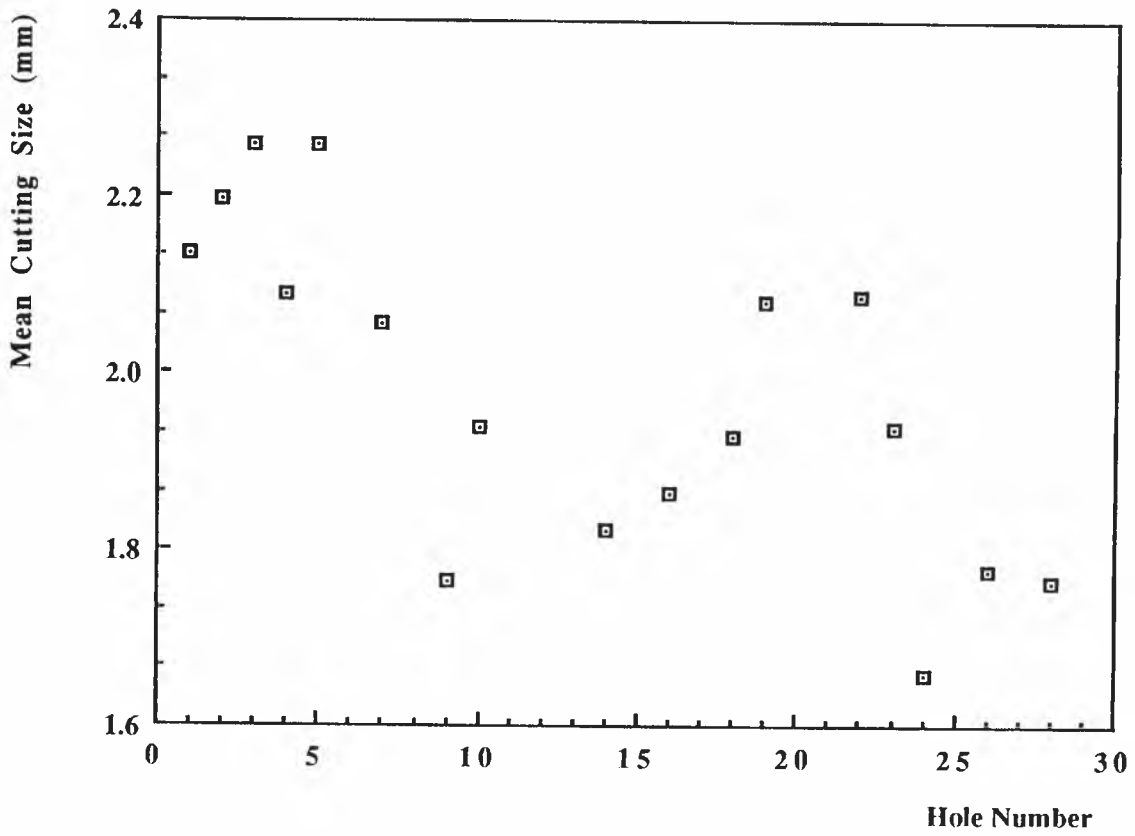

Fig. 6.34 Mean Cutting Size vs. Hole Drilled by Bit N1

But the questions are: what is the real relation between the mean cutting size and the weight percentage of different cutting sizes, how does the percentage of cuttings A and B predict the relevant mean cutting size, and how accurate is this prediction ?

In Figs. 6.35 - 6.42 are plotted the scatter diagrams of the percentages of cuttings of sizes A & B, A, B, C, D, E, F and G versus the mean cutting sizes respectively.

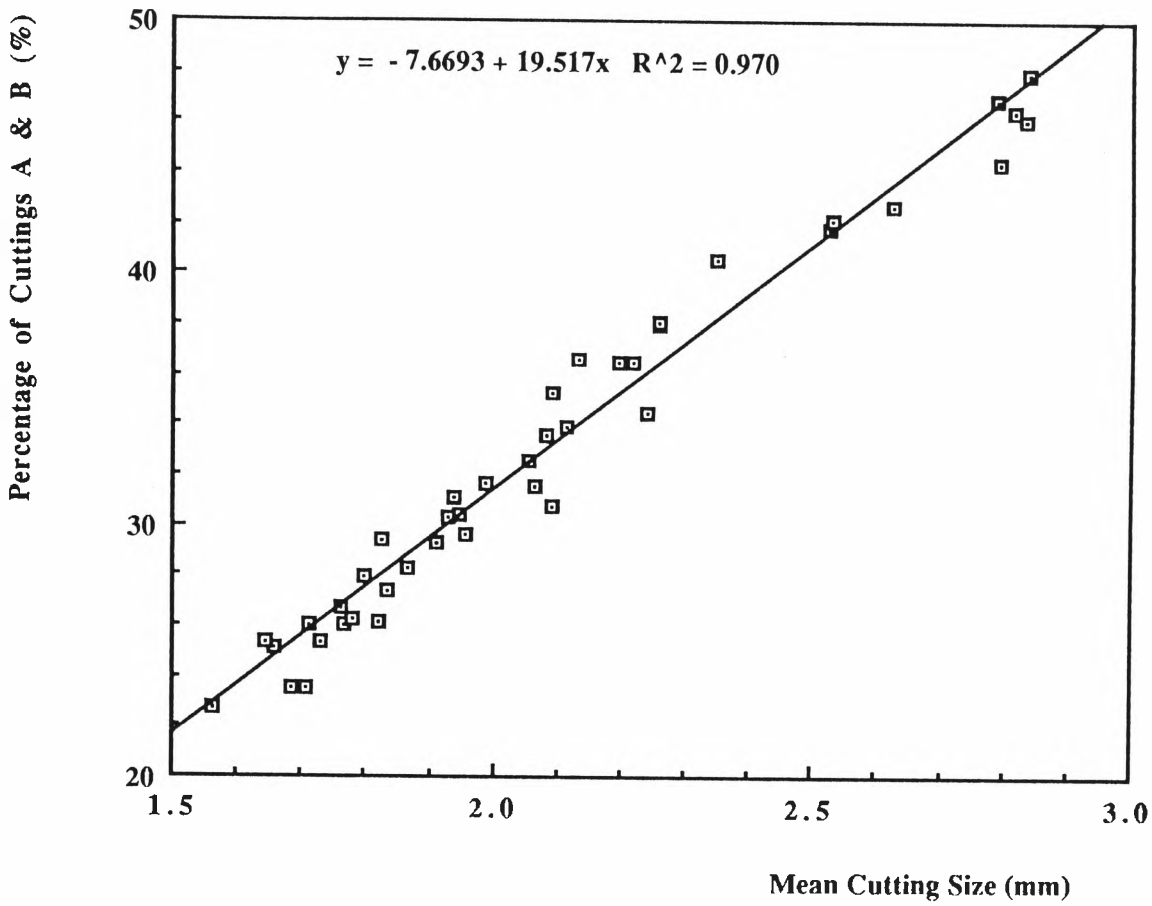

Fig. 6.35 Weight Percentage of Cuttings A & B vs. Mean Cutting Size

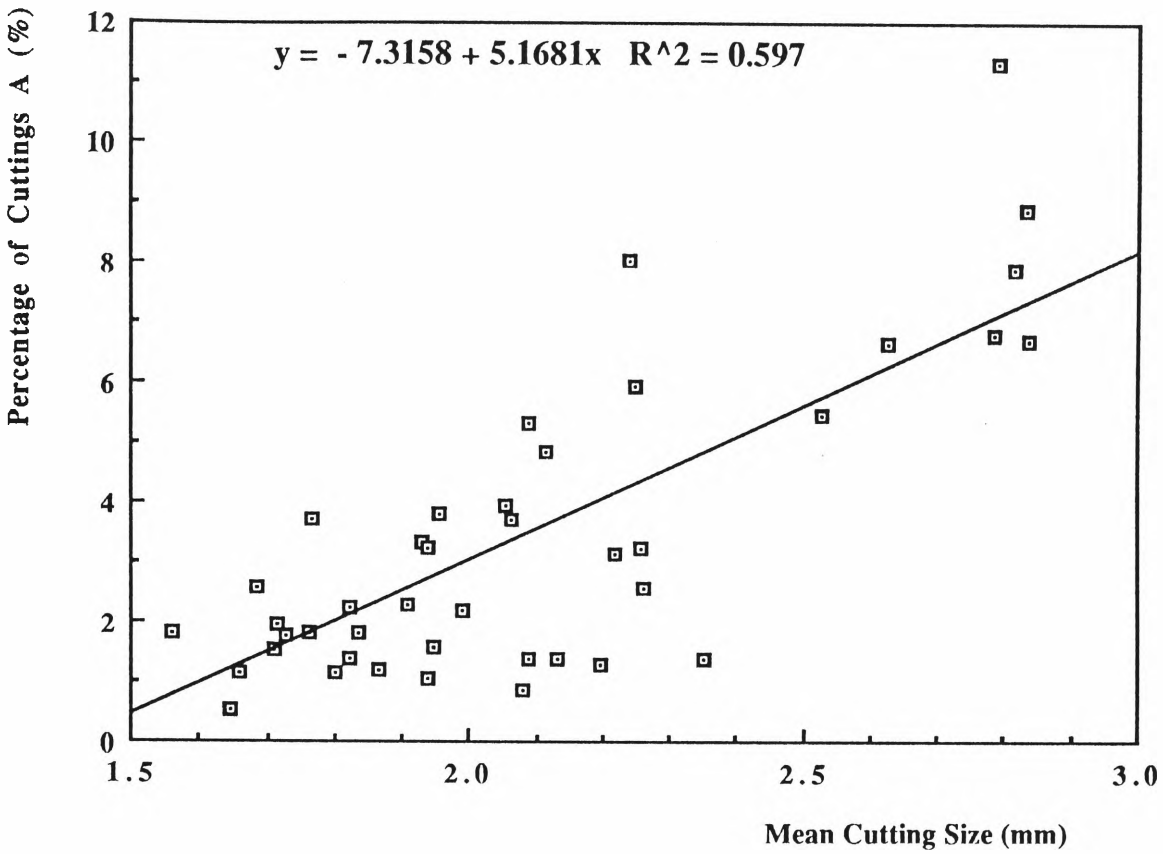

Fig. 6.36 Weight Percentage of Cuttings A vs. Mean Cutting Size

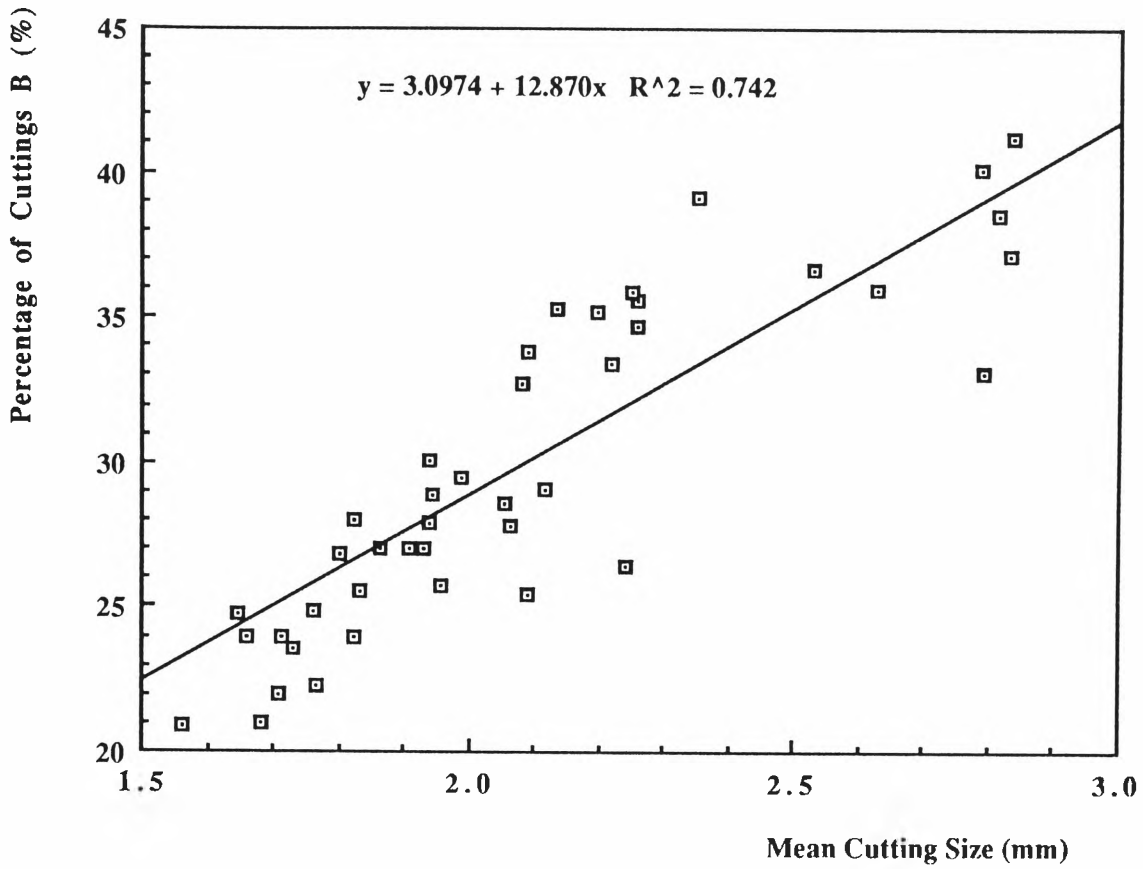

Fig. 6.37 Weight Percentage of Cuttings B vs. Mean Cutting Size

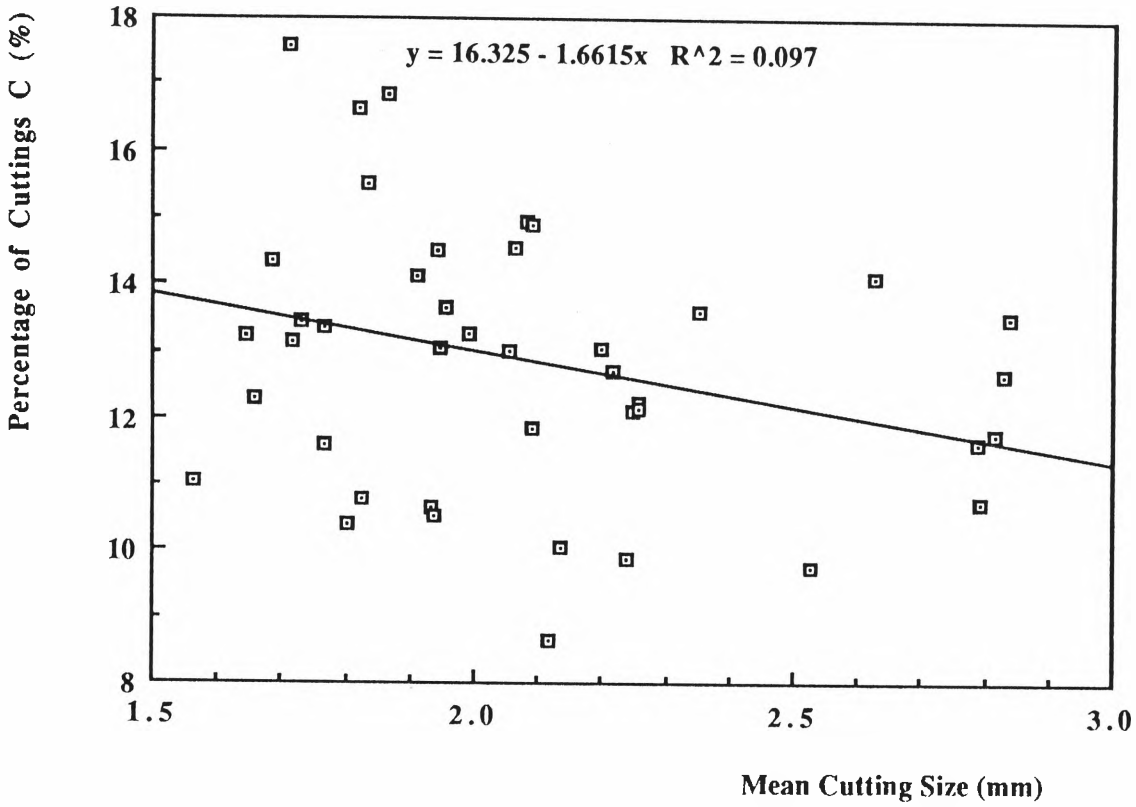

Fig. 6.38 Weight Percentage of Cuttings C vs. Mean Cutting Size

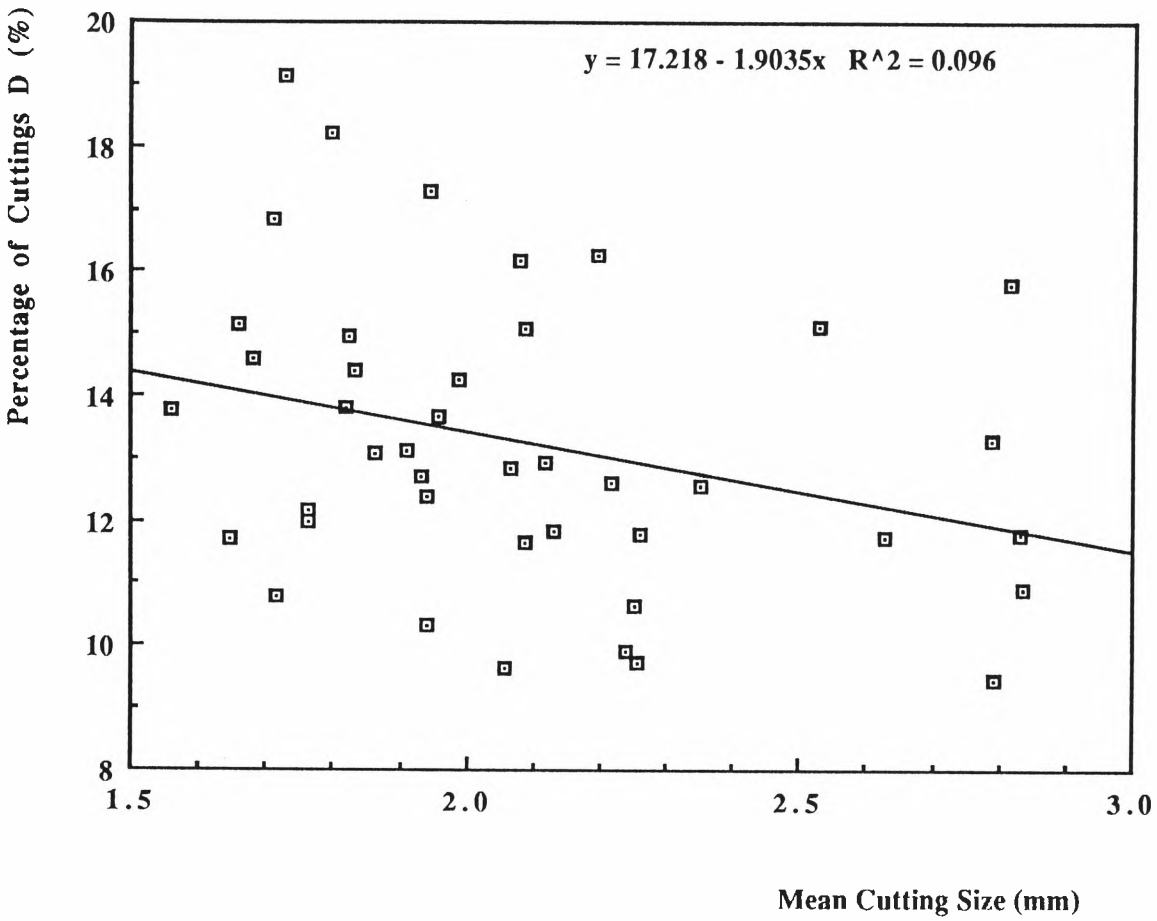

Fig. 6.39 Weight Percentage of Cuttings D vs. Mean Cutting Size

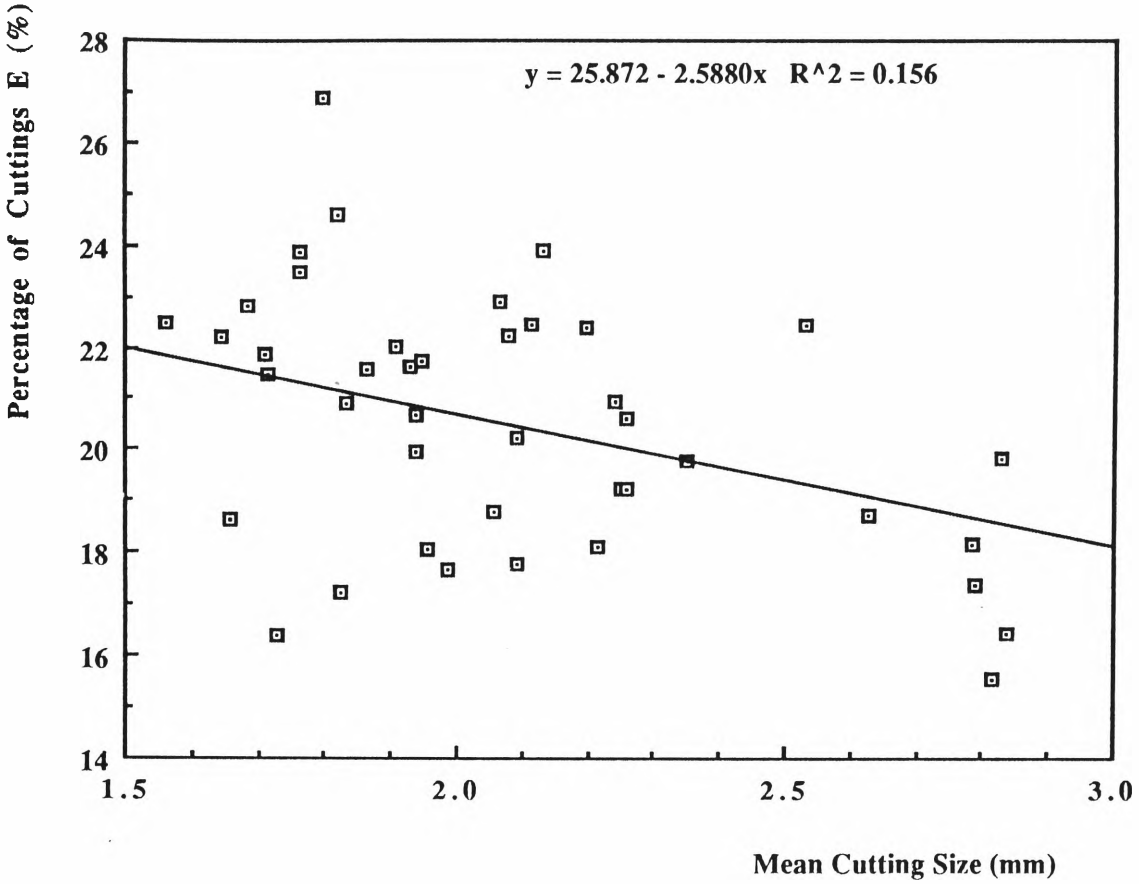

Fig. 6.40 Weight Percentage of Cuttings E vs. Mean Cutting Size

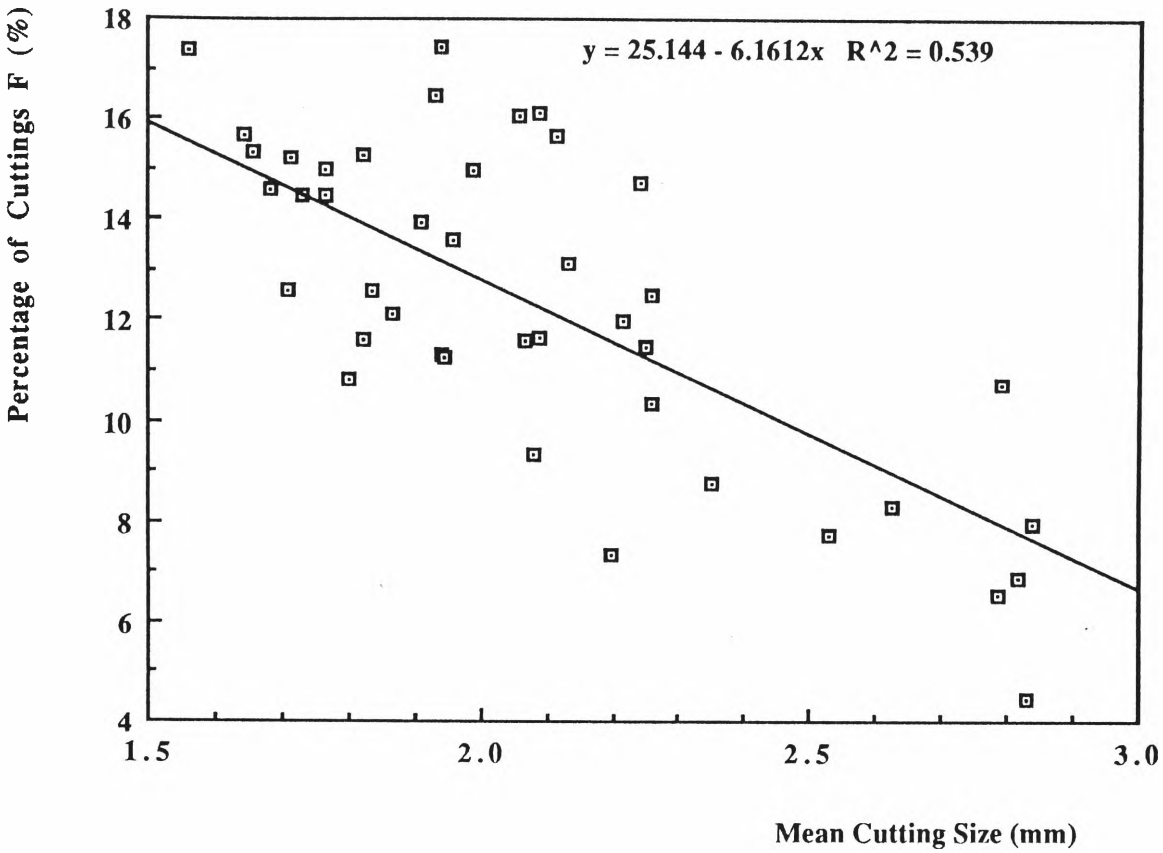

Fig. 6.41 Weight Percentage of Cuttings F vs. Mean Cutting Size

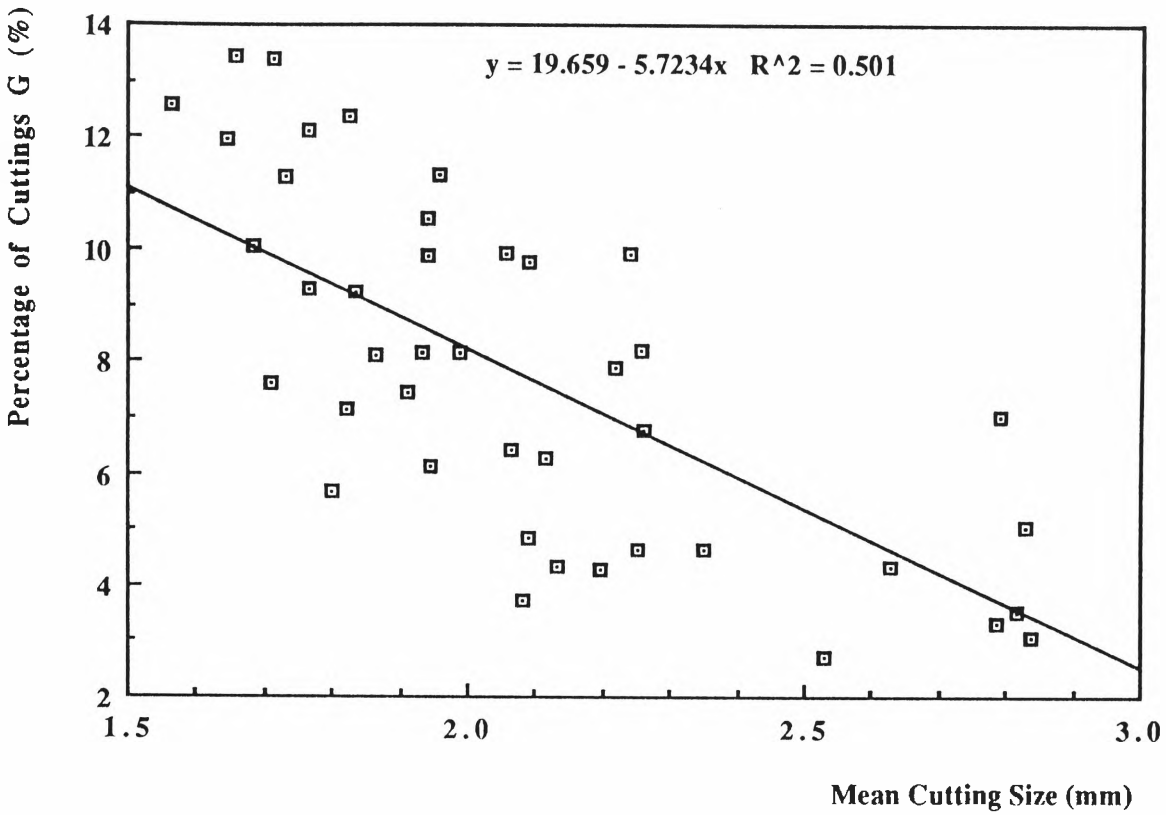

Fig. 6.42 Weight Percentage of Cuttings G vs. Mean Cutting Size

From these diagrams, the following conclusions can be drawn from the scatter of points on these diagrams:

1) Only the weight percentages of cuttings A and cuttings B show an incremental trend with the increase of mean cutting sizes (refer to Figs 6.36 and 6.37). Cuttings A and cuttings B both have an average size (8 mm and 4.53 mm respectively) greater than the arithmetic mean of the mean cutting size (2.081 mm).

2) The cuttings with an average size smaller than the arithmetic mean of mean cutting sizes, i.e. the cuttings of sizes C. D.

E. F and G, seem to decrease with the increase of mean cutting size (refer to Figs. 6.38- 6.42).

3) According to the convergency of the data, the diagrams can be divided into three types, i.e.:

   a) diagrams with data of very low convergency as in the case of Figs. 6.38 - 6.40,

   b) diagrams with data of low convergency as in the case of Figs. 6.36, 6.41 and 6.42 and

   c) diagrams with data of high convergency as in the cases of Figs. 6.35 and 6.37.

No relevant conclusions can be drawn if some data are too divergent. Consequently, there is no point to analyse mathematically the data shown on diagrams of very low convergency.

It is noted that the points on those scatter diagrams of the low convergent group and the high convergent group are more or less distributed nearly on an imagined line. In the other words, there exists a nearly linear relation between the percentage of cuttings and the mean cutting size in these groups.

It should be found out, to what degree the scatter diagrams of the low and high convergent groups indicate a linear relation, whether there is a 'best fit' line to a scatter diagram, and how the line is expressed mathematically if there is a one.

If the 43 sample measurements of mean cutting size are denoted by the symbols x_i (where **i** is equal to 1, 2, 3, ····· 43), and the relevant 43 sample measurements of the percentage of cutting size are denoted by the symbols y_i (where **i** is equal to 1, 2, 3, ····· 43), then the sample mean for the mean cutting size, X_m, and the percentage of cutting size, Y_m, will be

$$X_m = \frac{\sum_{i=1}^{43} x_i}{43} \qquad (6.5)$$

$$Y_m = \frac{\sum_{i=1}^{43} y_i}{43} \qquad (6.6)$$

Suppose the 'best fit' line has a linear deterministic mathematical model, the statistical procedure for finding the line for a set of points would seem, in many respects, a formalization of the procedure employed when a line is fitted by eye. If a predicted value of **y** obtained from the fitted line is denoted as **Y**, the predicted equation for the line will be:

$$Y = A + Bx \qquad (6.7)$$

where **A** intercept on **y** axis, i.e. value of **Y** when **x** equals 0

B slope of the line, i.e. the change in **Y** for one unit increase in **x**.

The least squares method is used to determine the line of best fit (Mendenhall, 1983). Its basic concept is to choose a line that minimizes the sum of squares of the deviations (**SSE**) of the observed value of **y** from those predicted **Y**. Expressed mathematically, the values of **A** and **B** chosen for the 'best fit' line should minimize **SSE:**

$$\mathbf{SSE} = \sum_{i=1}^{n} (y_i - Y_i)^2 \qquad \mathbf{(6.8)}$$

Substituting (6.7) into (6.8), then

$$\mathbf{SSE} = \sum_{i=1}^{n} [y_i - (A + B x_i)]^2 \qquad \mathbf{(6.9)}$$

The method of differential calculus is utilized to determine the numerical values of **A** and **B**, that minimises **SSE**. In brief, the least-squares solutions for **A** and **B** are given by the following formulas:

$$B = \frac{SS_{xy}}{SS_x} \qquad \mathbf{(6.10)}$$

$$A = Y_m + BX_m \qquad \mathbf{(6.11)}$$

where SS_x sum of squares for deviation of x_i from mean X_m

SS_{xy} sum of products of deviations of x_i and y_i from means X_m and Y_m respectively

$$SS_x = \sum_{i=1}^{n} (x_i - X_m)^2 = \sum_{i=1}^{n} x_i^2 - \frac{(\sum_{i=1}^{n} x_i)^2}{n} \qquad (6.12)$$

$$SS_{xy} = \sum_{i=1}^{n} (x_i - X_m)(y_i - Y_m) = \sum_{i=1}^{n} x_i y_i - \frac{\sum_{i=1}^{n} x_i \sum_{i=1}^{n} y_i}{n} \qquad (6.13)$$

Table 6.5 lists the values of **A** and **B** of the line of 'best fit' for the points on diagrams of the low and high convergent groups shown on Figs. 6.36, 6.41, 6.42, 6.35 and 6.37.

Table 6.5 Values of A and B of the Line of 'Best Fit'

Data source	Fig. 6.36	Fig.6.41	Fig.6.42	Fig.6.35	Fig.6.37
Cutting Size	A	F	G	A & B	B
A	-7.3158	25.144	19.659	-7.6693	3.0974
B	5.1681	-6.1612	-5.7234	19.517	12.870

Although the equation of the regression line is established, the strength of the linear relation between the two variables, **x** and **y** still remains unknown. The correlation coefficient, **r**, is defined to measure the strength of the linear correlation between the two variables as follows (Alder, 1977):

$$r = \frac{SS_{xy}}{\sqrt{SS_x \times SS_y}} \qquad (6.14)$$

where SS_y sum of squares for deviation of y_i from mean Y_m.

$$SS_y = \sum_{i=1}^{n} (y_i - Y_m)^2 = \sum_{i=1}^{n} y_i^2 - \frac{(\sum_{i=1}^{n} y_i)^2}{n} \qquad (6.15)$$

The correlation coefficient **r** satisfies the following properties:

1) In any case, **r** is always between -1 and 1.
2) If the absolute value of **r** equals 1, all points of the scatter diagram lie on a straight line.
3) If **r** is 0, then the regression line becomes the horizontal line $Y = Y_m$. This means no linear relationship exists between the **x**- and **y**-values, and for any value of **x**, the same value of **y**, namely Y_m, is the estimated **y**-value, **Y**.
4) The closer the absolute value of **r** to 1, the better the correlation between **x** and **y**.
5) The symbol of **r** is follows the symbol of the slop of the regression line, **B**.

By using formula 6.14, the values of correlation coefficient for regression lines on Figs. 6.36, 6.41. 6.42, 6.35 and 6.37 are calculated and listed on Table 6.6.

Table 6.6 Values of 'r' of the Line of 'Best Fit'

Data source	Fig. 6.36	Fig.6.41	Fig.6.42	Fig.6.35	Fig.6.37
Cutting Size	A	F	G	A & B	B
r	0.773	-0.734	-0.708	0.985	0.861

According to the properties of the correlation coefficient, the closer the absolute value of r is to 1, the stronger the linear relationship exists between the two test variables. Qualitatively, the strength order of the linear relationship between the percentage of cutting size and the mean cutting size descends as shown in Table 6.7.

Table 6.7 Strength Order of Linear Relation Between Percentage of Cutting Size and Mean Cutting Size

|r|	0.985	0.861	0.773	0.734	0.708
Cutting Size	A & B	B	A	F	G
Fig. No.	6.35	6.37	6.36	6.41	6.42

The percentage of cuttings A & B furnishes the best linear relation with the mean cutting size, followed by percentages of cuttings B and cuttings A. Comparatively, the linear relation between the percentage of cuttings G and mean cutting size is the weakest one.

There still remains a question of how to interpret quantitatively the precise strength of the lineality of data from its correlation coefficient. The solution

to this question is a theorem that if from a normal bivariate population which has a population correlation coefficient (denoted by ρ) of 0, all samples of **n** pairs are taken and their correlation coefficients are denoted by **r**, then

$$t = \frac{r}{\sqrt{1 - r^2}} \times \sqrt{n - 2} \qquad \textbf{(6.16)}$$

satisfied a Student's **t**-distribution with **n** - 2 degree of freedom (Alder, 1977).

To a certain level of significance, **a**, the rejection region of the hypothesis, that the sample is taken from a population in which there is no linear relationship, i.e. **B = 0** or **ρ = 0**, should be:

$$|t| \geq t_{a/2} \qquad \textbf{(6.17)}$$

where $t_{a/2}$ value of the **t**-Student's distribution with **n**-2 degrees of freedom and significance level of **a** (Mansfield, 1983).

If the formula 6.17 is satisfied, the value of a correlation coefficient, **r**, can be considered significant with a significance level of **a**, indicating that the **x**- and **y**-values can be assumed to be linearly related.

By using formula 6.16, the absolute values of **t** for the regression lines on Figs 6.36, 6.41, 6.42, 6.35 and 6.37 are calculated and listed on Table 6.8.

Table 6.8 Absolute Value of t for the Line of 'Best Fit'

Data source	Fig. 6.36	Fig.6.41	Fig.6.42	Fig.6.35	Fig.6.37
Cutting Size	A	F	G	A & B	B
$\|t\|$	7.80	6.92	6.42	36.41	12.42

If a significance level of 0.01 is given, the **t**-Student's distribution $t_{\alpha/2}$ gives a value of 2.704 for a sample of 43 pairs with 41 (= 43 - 2) degrees of freedom. Obviously, the absolute values of **t** shown on Table 6.8 are all greater than $t_{0.01}$. The fact of $|t| > t_{0.01}$ implies that all correlation coefficients of the regression lines on the above-described figures are considered significant on the basis of 1% significance level.

After a regression equation is established for a sample of **n** pairs of **x**- and **y**-values and confirmed with a certain degree of correlation between **x**- and **y**-values, the main object is to put the equation into application. One of the principal uses of a regression equation has always been regarded as a predictor, i.e. estimating the mean value of **Y** for a given value of **x**, denoted by $E(y|x)$, that can be very important in a practical problem.

In practice, interval estimates are generally preferred over point estimates because the latter provide no information concerning how much error they are likely to contain. Interval estimates, on the other hand, do provide such information (Mansfield, 1983).

To explain the interval estimates, two definitions have to be presented, confidence interval and confidence coefficient. An interval, which has a certain probability of including the population mean, is called a confidence interval, and this probability is defined as the confidence coefficient. As a rule of thumb, the confidence interval would be appropriate when a sample size is not smaller than 30 (called a large sample). This sample size will be sufficiently large to ensure (for most populations) that the normal distribution will be a very good approximation to the sampling distribution of Y_m, and that the sample standard deviation, **s** is a good approximation to the population standard deviation **s**.

Mendenhall (1983) stated the prediction interval for **y** when $x = x_0$, with a confidence coefficient for prediction (1 - **a**), as:

$$Y \pm t_{a/2} s \sqrt{1 + \frac{1}{n} + \frac{(x_0 - X_m)^2}{SS_x}} \qquad (6.18)$$

where s^2 is estimator of s^2

$$s^2 = \frac{SSE}{df} = \frac{\sum_{i=1}^{n} (y_i - Y_i)^2}{n - 2} \qquad (6.19)$$

where **df** is the degrees of freedom.

SSR sum of squares for regression

$$SSR = \sum_{i=1}^{n} (Y_i - Y_m)^2 \qquad (6.20)$$

The prediction interval in this case is a region between two curvelinears expressed by the formula 6.18. But in practice, a simple and easily-calculating expression is expected.

Zhang (1986) suggests that when the sample size is large enough ($n \geq 30$), the prediction interval can be simplified as:

$$Y \pm 2s \qquad \text{when } (1 - a) = 95\% \qquad \textbf{(6.21)}$$

$$Y \pm 3s \qquad \text{when } (1 - a) = 99\% \qquad \textbf{(6.22)}$$

where $(1 - a)$ is the the confidence coefficient

The formulas 6.21 and 6.22 is simple enough to put into practical use, and calculation is mainly involved with **SSE**. The other feature of the simplified formulas is that the prediction interval described by them is an area between two lines, both of which are parallel to and have an interval of 2s or 3s along the y-axis with the regression line. Fig.6.43 shows the two regression lines of prediction interval with a value of 3s.

According to the previous analysis, the linear relationship between the weight percentage of cutting sizes A & B together (i.e. cuttings not smaller than 2.36 mm) and the mean cutting size is much superior to that between the percentage of any other single cutting size and the mean cutting size. Moreover, the high weight percentage of cutting sizes A & B, and their large average cutting sizes make them the dominating factor in the determination of the mean cutting size of a

sample. As a result, the weight percentage of cutting sizes A & B can be a very good predictor for the mean cutting size of a cutting sample, hence a good predictor for the performance of a drill bit due to the fact that the mean cutting size corresponds well with the cutting tip sharpness as been concluded in the earlier part of this section.

Consequently, it is of particular importance further to analyse the linear relationship between the mean cutting sizes and the weight percentage of cuttings A & B, and to establish the regression equation for predicting the mean cutting size by the percentage of cuttings A & B of a sample.

Fig. 6.43 is a scatter diagram of weight percentage of cuttings A & B versus mean cutting size of 43 samples. It is noted that the 43 points of the scatter diagram lie close to a straight line.

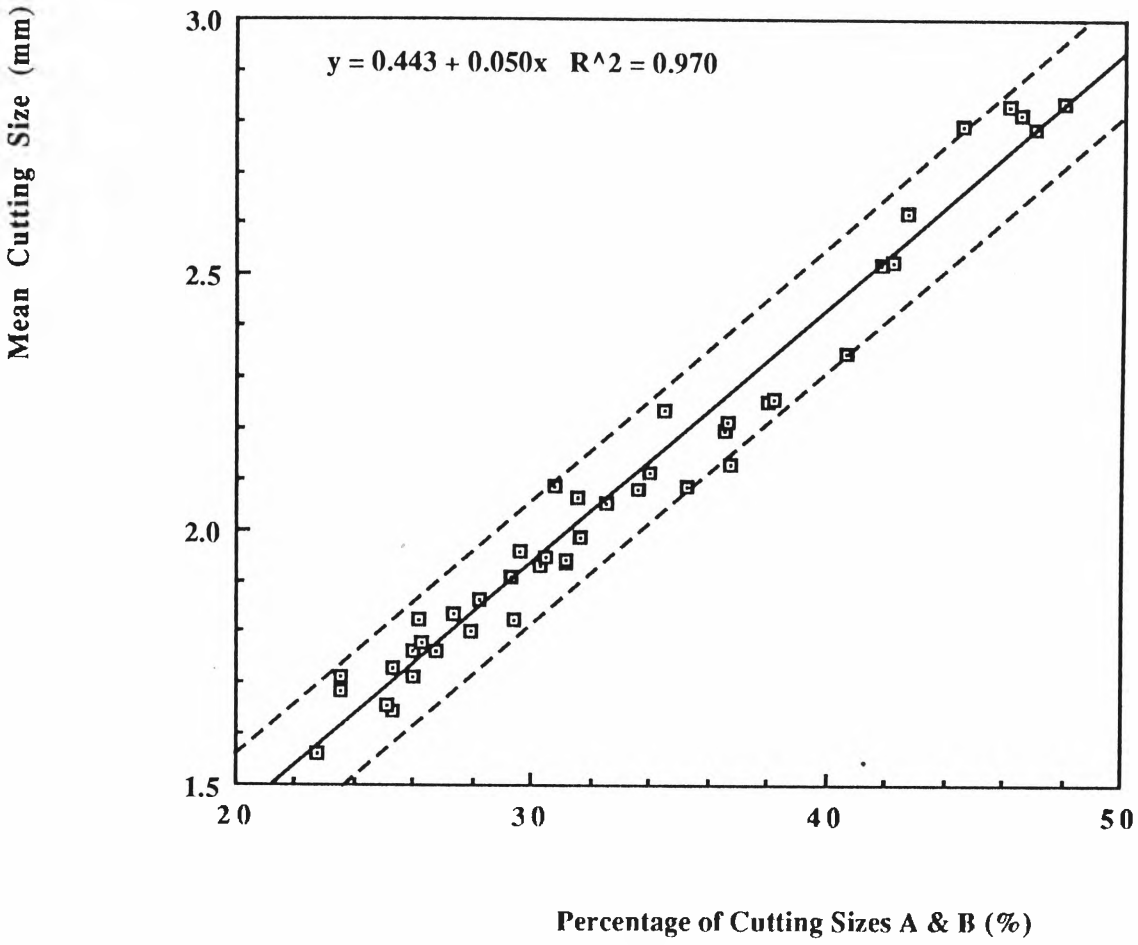

Fig. 6.43 Mean Cutting Size vs. Weight Percentage of Cuttings A & B

A linear regression line is fitted into the scatter diagram. All parameters calculated for the regression line are listed in Table 6.9.

Table 6.9 Parameters of Regression Line for Fig. 6.43

Symbol	**A**	**B**	**r**	**t**	$t_{0.00}$	**s**
Value	0.443	0.050	0.985	36.41	3.551	0.063255

Hence, the regression equation of the line is:

$$\mathbf{Y = 0.443 + 0.05x} \qquad \mathbf{(6.23)}$$

From Table 6.8, the following inequality exists:

$$t = 36.41 >> 3.551 = t_{0.001} \qquad \mathbf{(6.24)}$$

The inequality 6.25 implies that the correlation coefficient can be considered highly significant on the basis of the 0.1% level of significance.

Following the formulas 6.21 and 6.22, the prediction interval for **Y** on the basis of 95% and 99% confidence coefficients are respectively as:

$$\mathbf{Y \pm 2s = Y \pm 0.12651} \quad \text{when } (1 - \mathbf{a}) = 95\% \qquad \mathbf{(6.25)}$$

$$\mathbf{Y \pm 3s = Y \pm 0.18976} \quad \text{when } (1 - \mathbf{a}) = 99\% \qquad \mathbf{(6.26)}$$

The upper and lower prediction limits for the regression line on the basis of 95% confidence coefficient is plotted on the Fig. 6.43.

For practical use, the prediction for **Y** on a basis of the 95% confidence coefficient can be considered high precision. The prediction error for **Y** with a given **x** cannot be greater than 0.12651 based on a confidence coefficient of 95%. Comparing with the smallest mean cutting size, 1.562 mm, the greatest possible error 0.12651 mm from predicting a mean cutting size by the regression

equation 6.24, is only 8.1% of the mean cutting size based on a confidence coefficient of 95%. Even on the basis of the 99% confidence coefficient, the greatest possible error 0.18976 resulting from predicting a mean cutting size is only 12.1% of the value of the smallest mean cutting size. Consequently, the regression equation 6.24 has a high degree of usability in predicting mean cutting size from the weight percentage of cuttings A & B of a cutting sample.

6.6 Summary

By analysing the results of the experimental research the following conclusions can be drawn:

1. Bit performance or its penetration rate agrees well with the conditions of its cutting tip. A bit with less and/or minor chipping on its cutting tips usually performs better than a bits with more and/or severe chipping.

2. The tested sharp and aggressive new bits were prone to create some major chipping on their cutting tips, especially at the front point of a cutting tip. The cutting tips with major chipping might be further chipped and eventually develop fatal chipping which would lead to the failure of the bits, or might self-resharpen to a certain degree and form a rounded shape. The major chipping could result suddenly or from an accumulation of minor chips. It seems that a cutting tool with the major chipping caused suddenly tends to develop fatal chipping and fail in the due course of drilling. However, a cutting tool with major

chipping caused by an accumulation of minor chipping potentially self-resharpens and forms a rounded shape.

3. Major chipping on tips of a positive rake bit is likely to be created suddenly, while major chipping on tips of a negative rake bit is likely to be accumulated by minor chipping. This fact may explain why the much higher percent of positive rake bits fall into the prematurely-failed group

4. The life of a bit in a normal or high performance group is very much dependent on the lasting period of the re-sharpened round-shape tips. So, the longer the resharpened round shape cutting tips are maintained, the longer the bit life will be.

5. The specific energy responds to the cutting tool sharpness in a wide range and it is a useful parameter to predict the bit performance in an established drilling system. The result of the experiments conducted show that a higher specific energy period generally corresponds to a lower penetration rate period, and vice verse.

6. The main parameter of a drill bit, which can possibly affect the performance of the bit, is the rake angle. General speaking, a negative bit has a longer bit life and its penetration rate is improved with the increase of the rake angle, whereas a positive bit has a high initial performance in terms of its penetration rate and energy consumption, and its bit life is lengthened with reduction of its rake angle. The best performance bit in terms of number of holes drilled is bit N1 which had a bit life of more than 29 holes (about 24 m), and the

best performance bit in terms of the average penetration rate, bit P1, had a much higher average penetration rate (3.71 m/min) than any of the other test bits. The rake angle of a negative bit should not be smaller than -2.4° to reach a possibly high penetration rate, and the rake angle of a positive bit cannot be greater than 4° to avoid an extremely low bit life.

7. According to the analysis of the cutting size distribution by sieving, cuttings B (<6.70, ≥2.36 mm) in most cases take up the highest weight percentage of a sample (between 21-41%), while cuttings A (≥6.70 mm) or cuttings G (<0.15 mm) usually occupy the smallest fraction of the weight in a sample (between 1-11% and 3-13% respectively).

8. The value of the mean cutting size falls in the range of 1.5-2.9 mm. The mean cutting size mainly depends on the weight percentage of cutting sizes A and B, and maintains a good linear relation with it.

9. The mean cutting size correlates well with the cutting tip sharpness or the chipping patterns of the cutting tools, i.e. under the same drilling conditions, the sharper the cutting tools of a bit, the greater the mean cutting size will be produced.

Chapter Seven

Conclusions

Rockbolting is the primary roof support system in underground mining. It is not suitable for all strata conditions, but where it can be applied, it provides the most effective and most economical support system.

The Rapid Face Bolting System, taking a self-drilling bolt as its core, can be solution to the removal of the 'double handling' step of replacing the drill rod with the bolt, which is the practice in conventional rockbolting systems. The Rapid Bolting System therefore furnishes better productivity and greater safety.

The self-drilling bolt can be implemented by two different systems:

1) A round bar with slot or groove on the side, or with a hole at the centre to give the access of water/grout, and a conventional bolthole drag-bit.
2) A tube or a pipe, and a specially designed tubular roof bit.

The bolt in this system can be installed by existing techniques used for installation of grouted rockbolts.

The principal conclusions of the work presented in this thesis are as follows:

1. The tubular roof bit for the Rapid Face Bolting System is totally different from the core-bit for geological site investigation in terms of both the technical specifications and the design considerations. Aimed at low cost due to its special usage, a tubular roof bit should adopt comparatively cheap materials for its cutting tips, and keep a simplified configuration.

2. Generally speaking, tungsten carbide alloy (WC alloy) is chosen as the tip in order to drill a hole in hard rock formations, whereas high speed steel (HSS) is selected to drill a hole in soft rock formations. Basically then, two kinds of tubular roof bits have been designed respectively for the soft and hard rock formations. The suitability of the tubular roof bits to the rock formation may be determined by the trial-and-error method first, and later on modifications can be made to the bit design according to experience gathered from use.

3. Three dimensional finite element method is a convenient method to describe quantitatively the stress-strain condition of the top point of a cutting tip.

The currently used roof drag-bit employs the cutting tips with an obtuse angle in the front face. The result of the finite element analysis shows that the top point of this kind of cutting tip possesses a much greater stress concentration than any other parts of the tip, and is in a very adverse condition when load is imposed on the bit. The stress at the top point of the tip exceeds the critical stress even under the load applied in normal drilling conditions, and this part of the tip is likely to fail. With the increase of the loads, modelling severe drilling

conditions, the area with the stress reaching the critical stress is expanded, which implies that the failure region would be extended.

4. The performance of a bit is determined by the condition of the cutting tips of the bit. The specific energy generally corresponds to the bit performance.

5. The experimental results are in general agreement with the outcome of the finite element analysis. All new tested bits were prone to create major chipping at the top points of the cutting tips. There are two kinds of bit failure patterns in general for the tested bits, namely, early premature failure and gradual wearing-out failure. Positive rake bits showed a greater tendency to follow the early premature failure pattern than the negative bits tested.

6. An important phenomenon, called self-resharpening of cutting tips, is always observed in the gradually wearing-out failure. This self-resharpening process can resharpen cutting tips with some major chips into a round-shape on the front and side faces. As a result, the round-shape tips will bring a bit into a new relatively high performance period. It seems that a round shape is a more reasonable geometry for long life cutting tips than the currently-used sharp and aggressive tips, which have an obtuse angle in the front face and an acute angle in the side face.

7. A positive rake bit presents a high initial performance which can be maintained for a reasonable meterage if the rake angle is controlled under 4°. Therefore, the positive rake bit can be used in the rapid face bolting system as a

one-pass consumable bit, which is featured with a high penetration rate for a short period (approximately 2-3 metres). A negative bit demonstrates a very long life and is able to reach a fairly high average penetration rate if the rake angle has an absolute value smaller than 2.4°. Consequently it is favoured for the conventional bolting system to drill as many bolt holes as possible.

8. The mean cutting size is a very important index reflecting the characteristic of a cutting sample, and it indirectly correlates well with the performance of a bit. By comparing Figs. 6.13 to 6.15 with Figs. 6.32 to 6.34 respectively, it is clear that the variation of penetration rates of a tested bit follows the same pattern as the variation of mean cutting sizes, with the holes drilled under a specified drilling condition. This fact suggests that under the same drilling conditions, a bit produces a large mean size of cuttings when a high average penetration rate is reached.

The mean cutting size is determined by the weight percentage of cuttings A & B (cuttings with a size not smaller than 2.36 mm) in a sample following the regression equation 6.23:

$$Y = 0.443 + 0.05x \qquad (6.23)$$

where **x** weight percentage of cuttings A & B, i.e. cuttings with a size not smaller than 2.36 mm, in a cutting sample

Y the estimated mean cutting size (mm) of the sample.

This formula has a very high correlation coefficient r with a value of 98.5%, which implies that the formula 6.23 is precise enough in practice to predict the mean cutting size by the weight percentage of cuttings A & B, and therefore the performance of a bit.

Recommendations for Further Work

The following areas for further research are recommended:

1. Further experiments with the proposed tubular roof bits should be conducted in the laboratory, so as to evaluate their feasibility in practice and further to modify their configuration to improve their performance.

Resin or grouting method should be investigated in detail, especially in association with the tubular bit drilling method, as the success of the Rapid Face Bolting System largely depends on this incorporation.

2. The finite element analysis of the stress on a cutting tip should model the dynamic load imposed on the tip, as it is the real case in the process of rock drilling. A tip is more likely to fail under dynamic load rather than static load.

The finite element analysis should also be employed to design various tip configurations with features to suit requirements for different drilling purposes.

3. The drag-bit with tips of a rounded shape on the front face, which has been mentioned in Chapter 6, is worthy of investigation. As the bit is inclined to demonstrate a constant and high performance, and provides long service, it may be an effective and efficient substitute for the currently used drag-bit with its sharply pointed tips for conventional bolthole drilling.

References

Alder, H. L., 1977, *Introduction to Probability and Statistics*, 6th ed., W.H. Freeman and Company, San Francisco, 378 pp.

Allen, T., 1981, *Particle Size Measurement*, 3rd ed., Chapman and Hall, London.

Appl, F.C., and Rowley, D.S., (Given in Clark, 1982, page 8).

Aschan, I.J. et al., 1975, *Proc. 4th Nordic High Temp. Symp.*, Vol.1, pp. 227. (Given in Trent, 1984, page 125).

ASM Committee on Tool Steel, 1975, *Tool Steels, Properties and Selection of Tool Materials*, ASM, USA, pp. 1-36.

ASM Handbook Committee, 1985, *Metals Handbook, vol. 8: Mechanical Testing*, 9th ed., Amer. Soc. Metal, Ohio, pp. 69-114.

ASTM Commission on Standardization of Laboratory and Field Tests, 1977, *Suggested Methods for Determining Hardness and Abrasiveness of Rocks*, Int. J. Rock Mech. Min. Sci., vol. 15, pp. 89-97.

Atlas Copco, 1982, *Rock Reinforcement System, Swellex*, Promotion Brochure, 10 pp.

Beavis, F.C., 1985, *Engineering geology*, Blackwell Scientific Pub., Melbourne, pp. 47-52.

Bieniawski, Z.T., 1984, *Rock Mechanics Design in Mining and Tunneling*, Balkema, Rotterdam, pp. 40-51.

Bieniawski, Z.T., 1987, *Strata Control in Mineral Engineering*, Balkema, Rotterdam, pp. 1-35.

Biron, C. and Arioglu, E., 1980, *Supporting and Design of Supports in Mines*, Birsen Kitabevi, Istanbul, 232 pp.

Biron, C. and Arioglu, E., 1983, *Design of Supports in Mines*, John Wiley and Sons Inc., New York, pp. 89-123.

Black, P.H., 1961, *Theory of metal cutting*, McGraw-Hill, New York, pp. 1-10.

Blindheim, O.T., 1979, Drillability Predictions in Hard Rock Tunnelling, *Tunnelling'79*, Inst. Min. Metall., London, pp. 284-289.

Blomberry, R.I. et al., 1974, Abrasive Wear of Tungsten Carbide-cobalt Composites: I. Wear Mechanisms, *Metals Science and Engineering*, vol. 13, pp. 93-100.

Boyer, H.E., 1987, *Hardness Testing*, ASM International, Ohio, pp. 20-75.

Brown, E.T., Bray, J.W., Ladanyi, B. and Hoek, E., 1983, Ground Response Curves for Rock Tunnels', *J. geotech. Engng. (ASCE)*, vol. 109(1), pp. 15-31.

Burbank B.B., 1955, Measuring the Relative Abrasiveness of Rock Minerals and Ores', *Pit Quarry*, August, pp. 114-118

Carr, M.F., 1985, Case Studies of Roof Bolting Accidents', *Proc. 1985 Colliery Safety Symp.*, NSW, 7 pp.

Central Laboratory, 1979, *Drilling Technology*, (Gao, S. ed.), Geology Press, Beijing

Clark, G.B., 1982, Principles of Rock Drilling and Bit Wear, *Quart. Col. Sch. Min.*, vol. 77, no. 2, pp. 8-17.

Clark, I.E., 1987, Core Drilling with Syndax 3 Polycrystalline Diamond, *Drillex'87*, Aus. Inst. Min. Metall., Melbourne, pp. 126-137.

Collins, J.A., 1981, *Failure of Materials in Mechanical Design*, John Wiley & Sons Inc., New York, pp. 126-158

Cox, R.M., 1974, Why Some Bolted Mine Roofs Fail?, *Trans. Soc. Min. Eng., Amer. Inst. Min. Eng., 256*, June, pp.167-161.

Cutifani, M., 1983, Evaluation of Drill bits for Roof Drilling Applications, *Report*, Kembla Coal and Coke Pty. Ltd.

Das, B., 1974, Vicker's Hardness Concept in the Light of Vicker's impression, *Int. J. Rock Mech. Min. Sci. & Geomech. Abstr.*, vol. 11, pp. 85-89.

Daws, G., 1987, Coal Mine Roofbolting, *J. Min. Eng.*, Oct., pp. 147-154.

Deere, D.U. and Miller, R.P., 1966, Engineering Classification and Index Properties for Intact Rock, *Technical Report*, no. AFWL-TR-65-116, Kirtland Air Force Base, New Mexico.

Deere, D.U., Peck, R.B., Monsees, J.E. and Schmidt, B., 1970, Design of Tunnel Linings and Support Systems, *Highway Res. Rec. (Wash. D.C.)*, vol. 339, pp. 26-33.

Detourney, E. and Vardoulakis, I., 1985, Determination of the ground Reaction Curve Using the Holograph Method, *Int. J. Rock Mech. Min. Sci.*, vol, 22, pp. 173-176

Duklet, C.P. and Bates, T.R., 1981,Predicting Diamond Bit Drilling Rates, *World Oil*, vol 192, April, pp. 127-135.

Eagle and Globe Steel Ltd, 1981, More Hints on Steel, *Technical Services Department*, 1st ed.104 pp.

Engineers International Inc., 1979, Development and Testing of Self-drilling Roof Bolts, *Final Rep.*, submitted to US BurMines under contract no. H0272022, 225 pp.

Exner, H. D., 1970, A Review of Parameters Influencing Some Mechanical Properties of Tungsten Carbide-Cobalt Alloys, *J. Powder Metal.* vol. 13, pp. 13-31.

Fairhurt, C., 1964, Discussion of J. Furly, Strain Wave Behaviour in the Percussive Drilling Process, *Trans. Inst. Min. Metall.*, vol. 73, pp. 671-682.

Findlay, K., 1984, Roof Bolting Accidents When Using Hand Held Rotary Machines, *Joint Coal Board Rep.*, NSW, 22 pp.

Finnie, I., 1956, A Review of the Metal Cutting Analyses of the Past Hundred Years, *J. Mech. Eng.*, vol. 78, no. 8, pp. 715.

Fish, B.G. and Barker, J.S., 1956, Studies in Rotary Drilling, *National Coal Board, MRE Rep.* no. 209.

Fish, B.G., Guppy, G.A. and Robin, J.T., 1958, Studies in Rotary Drilling: the Abrasive Wear Effect, *National Coal Board, MRE Rep.* No. 2115.

Fish, B. G. et al., 1959, Abrasive Wear Effects in Rotary Rock Drilling, *Trans. Inst. Min. & Metall.*, vol. 68, p. 357.

Fowell, R. J., 1970, A Simple Method for Assessing the Machineability of Rocks, *J. Tunnels and Tunnelling*, vol. 4, pp. 251-253

Fritzlen, G.A. and Elbaum, J.K., 1975, Cabalt-Chromium-Tungsten-Molybdenum Wear-Resistant Alloys, Properties and Selection of Tool Materials, *ASM press*, Ohio, pp. 67-72.

Furby, J., 1964, Tests for Rock Drillability, *Mine Quarry Eng.*, July.

Gale, W. J. and Fabjanczyk, M. W., Application of Field Measurement Techniques to the Design of Roof Reinforcement Systems in Underground Coal Mines, *Ground Movement and Control Related to Coal Mining Symposium*, The AusIMM Illawarra Branch.

Gao, S., 1979, *Drilling Technology*, Geology Press, Beijing.

Goldschmidt, H.J., 1967, *Interstitial Alloys*, Butterworths, London, 632 pp.

Goodrich, R.H., 1956, High Pressure Rotary Drilling Machines, *Proc. 2nd Ann. Symp. on Min. Res.*, Univ. of Missouri, pp. 25.

Goodrich, R.H., 1961, Drag Bits and Machines, *Colo. Sch. Mines Q.* 56, no. 1, pp. 1-21

Gray, K.E., Armstrong, F. and Gatlin, C., 1962, Two Dimensional Study of Rock Breakage in Drag Bit Drilling at Atmospheric Pressure, *J. Petrol. Tech.*, vol. 6, p. 93.

Hartman, H.L., 1959, Basic Studies of Percussion Drilling, *Min. Eng.*, New York, vol. 11, Jan., pp. 68-75

Heywood, H., 1970, *Proc. Particl Size Analysis Conf.*, Soc. Analyt. Chem., London.

Hidon, A. et al., 1967, *Mechanics of Materials*, John Willey & sons, Inc., New York, 2nd ed., pp.415-417.

Hii, J. K. L., 1985, *Application of Rock Bolting in Modern Mines*, B.E. thesis, Dept. of Civl. & .Min. Eng., Univ. of Wollongong, 142 pp.

Hill, J.R.M. and Hay, K.E., 1983, New Developments in Ground Support Installation Systems, *Mini. Symp. on Rock Reinforcement*, Soc. Min. Eng. AIME, Atlanta, GA, Mar., pp 11-13.

Hoek, E., 1982, Geotechnical Considerations in Tunnel Design and Contract Preparation, *Trans. Inst. Min. Metall.*, London, vol. 91: A101- A109.

Hoerndlein, K.R., 1985, Roof Bolting with Safety, *Proc. 1985 Colliery Safety Symp.*, NSW, 7 pp.

Howarth, D.F., 1986, Review of Rock Drillability and Borability Assessment Methods, *Trans. Inst. Min. Metall. (A)*, vol. 95, Oct.

Industrial Diamond Review, 1986, 5/41, No.6, De Beers Industrial Diamond Division, London, pp. 42-47.

Int. Soc. for Rock Mechanics, 1978, Suggested Methods for Determining Hardness and Abrasiveness of Rocks, *Int. J. Rock Mech. Min. Sci.& Geomech. Abstr.* vol. 15, pp 89-97.

Jackson, I.F. et al., 1962, An Investigation of Hard Metal Inserts for Cutting Slates, *Trans. Amer. Inst. Min. Metall. & Petro. Eng. Soc.*, vol. 233.

Jumikis, A.R., 1983, *Rock Mechanics*, 2nd ed., Trans Tech Pub., Rockport, pp. 177-194.

Karabin G.J. and Debevec, L., 1976, Comparative Evaluation of Conventional and Resin Bolting Systems, U.S. Department of Interior, *MSHA*, IR 1033, 22 pp.

Kennedy, R.G., Marrotte, N W. and Brezina, E.Z., 1975, *Selection of Material for Drills: Properties and Selection of Tool Material*, ASM, USA, pp 94-97.

Lang, T.A., etc, 1979, A Program Plan for Determining Optimum Roof Bolt Tension: Theory and Application of Rock Reinforcement Systems in Coal Mines, *A Final Report* submitted to U.S. Bureau of Mines by Leeds, Hill and Jewett, Inc., March, Vol. 1.

Larsen-Basse, J., 1973, Wear of Hard Metals in Rock Drilling: A Survey of the Literature, *Powder Metallurgy*, Vol. 16, pp. 1-32.

Leschonski, K., 1977, *Proc. Particle Size Analysis Conf.*, Chem. Soc. Analyt. Div., London.

McGregor, K., 1967, *The Drilling of Rock*, C.R. Books Ltd., A. MacLaren Co., London, pp. 24-36.

Maurer, W.C., 1967, Fracture Breakage of Rock, *Amer. Inst. Min. Metall. & Petro. Eng.*, pp. 355-369.

Maurer, W.C., 1980, *Advanced Drilling Techniques*, Petro. Pub. Co., Tulsa, pp. 1-14.

Mendenhall, W., 1983, *Introduction to Probability and Statistics*, 6ed., Duxbury Press, Boston, 646 pp.

Miyoshi, A. and Hara, A., 1965, *J. Japan Soc. Powder and Powder Met.*, Vol 12, pp. 78-84.

Nevill, H.F.C. et al., 1962, Wear of Rotary Drag Bits in Granitic Rock, *Trans. Inst. Min. & Metall.*, vol. 121, pp. 249-256.

Obert, L., Windes, S.L. and Duval, W.I., 1946, Standardized Test for Determining the Physical Properties of Mine Rock, *U.S. Bur. Mines Rep. Invest.*, RI 3891.

Obert, L. & Duvall, W. I., 1967, *Rock Mechanics and the Design of Structures in Rocks*, John Wiley and Sons, New York, pp. 609-630.

Pacher, F., 1977, Underground Openings and Tunnels, *Proc. of 16th US Symp. on Rock Mechanics*, ASCE, New York, pp. 223-234.

Panek, L.A., 1961, Use of Vertical Roof Bolts to Reinforce an Arbitrary Sequence of Beds, *Proc. Int. Sym. on Mining Research*, University of Missouri, vol. 2, pp. 499-508.

Panek, L.A., 1962, The Effect of Suspension in Bolting Bedded Mine Roof, U.S. Bureau of Mines, *RI 6138*, 59 pp.

Panek, L.A., 1964, Design for Bolting Stratified Roof, *Trans. Soc. Min. Eng., Amer. Inst. Min. Eng.*, June, pp.113-119.

Panek, L.A., 1973, *Rockbolting, SME Mining Engineering Handbook*, vol. 1, Section 13, AIME, New York, pp. 125-145.

Peng, S.S. and Tang, H.Y., 1985, Stress Analysis of Fully Grouted Resin Bolts in Pullout Tests, *Technical Report*, Uni. West Virg., 25 pp.

Peng, S.S., 1986, *Coal Mine Ground Control*, John Wiley & Sons, New York, 2nd ed., 491 pp.

Rabcewicz, L., 1964, The New Austrian Tunneling Method,*J. Water Power*, November , pp 453-457.

RG Cram and Sons, 1985, *Wombat Roof Rig*, Commercial Brochure, 16 pp.

Robertson, R. et al., 1986, *Professional Users Handbook for Rock Bolting*, Trans Tech, FRG, 145 pp.

Roberts, A., 1981, *Applied Geotechnology*, Pergamon, London, 344 pp.

Roxborough, F.F., 1981, Applied Rock and Coal Cutting Mechanics, *Workshop course 156/81*, Aus. Miner. Found., 40 pp.

Roxborough, F.F., 1986, A Review of Research Progress in Coal and Rock Cutting, *J. Coal*, no. 13, pp. 37-48.

Schmidt, L.C., Aziz, N.I. and Guo, H., 1988, Mechanics of Rock Drilling, Cutting and Future Developments, *Proc. 21st Cent. Higher Prod. Coal Min. Systm.*, Wollongong, pp. 221-231.

Schwarzkopf, P. and Kieffer, R., 1960, Refractory Hard Metals, MacMillan, New York, pp. 20-31.

Scott, J.J., 1977, Friction Rock Stabilizers, a New Rock Reinforcement Method, *Proc. SME-AIME Annual Meeting*, Atlanta, GA.

Scott, J.J., 1983, Friction Rock Stabilizer Impact upon Anchor Design and Ground Control Practices, *Proc. Int. Symp. on Rock Bolting*, Abisko, pp. 407-417.

Seco-Titan, 1988, *Rotary Drilling Bits*, Commercial Brochure, 8 pp.

Selmer-Olsen, R. and Blindheim, O.T., 1970, On the Drillability of Rock by Percussive Drilling, *Porc. 2nd Congr. Int. Soc. Rock Mech.*, Beograd.

Shaw, M. C., 1989, *Metal Cutting Principles*, Clarndon Press, Oxford, pp. 333-367.

Singh, R.N., Daws, G., and Dhar, B.B., 1984, Status of Roofbolting as a Sole Means of Support in Coal Mines, *Proc. 12th Wld. Min. Cong.*, New Delhi, vol. 3, pp 3.11.1-3.11.16.

Smelser, T.W. et al., 1982, Modeling and Field Verification of Roof-bolt Systems, presented at the SME-AIME Annual Meeting, Dalas, TX, Preprint, no. 82-121, 11 pp.

Soloman, B.A. and Rich, T.R., 1983, Chemical Modification of Pumpable Bolt Resin, *Final Report* submitted to US Bur. Min. under contract no. H0282012, 165 pp.

Stillborg, B., 1986, *Professional users handbook for rock bolting*, Trans Tech, FRG, 145 pp.

Stjernberg, D.G. et al. 1975, Wear Mechanisms due to Different Rock Drilling Conditions, *Powder Metallurgy*, vol 18, pp. 89-106.

G+D Cmputing Pty. Ltd, 1988, *STRAND5 User Guide Reference Manual*, Ultimo, pp.387.

Teale, R., 1965, The Concept of Specific Energy in Rock Drilling, *Int. J. Rock Mech. Min. Sci.*, vol. 2, pp.57-73.

Trent, E.M., 1968, *Pro. Int. Conf., M.T.D.R.*, Manchester, p. 629 (Given in Trent, 1984, p. 157)

Trent, E.M., 1984, *Metal Cutting*, Butterworths, London, 2nd ed., pp.81-142.

Tsoutrelis C.E., 1969, Determination of the Compressive Strength of Rock in-situ or in Test Block Using a Diamond Drill, Int. J. Rock Mech. Min. Sci., vol. 6, pp. 311-321.

Warren T.M., 1981, Drilling Model for Soft-formation bits, *J. Petrol. Tech.*, vol. 33, June, pp. 963-969

Weigel, W.W., 1943, Channel Irons for Roof Control, *Engng. & Min. J.*, 144 (5), pp. 70-72.

White, C.G., 1969, A Rock Drillability Index, *Colo. Sch. Mines Q.* 64, No. 2, 1-92

Winchell, H., 1946, Observations on Orientation and Hardness Variations, *Am. Miner.*, vol. 31, pp. 149-152.

Yang, X., 1979, *Drilling Technology*, (Gao, S. ed.), Geology Press, Beijing.

Yamaguchi, V., 1970, The Number of Test-pieces Required to Determine the Strength of Rock, *Int. J. Rock Mech. Min. Sci.* Vol. 7, pp. 209-277.

Commercial reports used as reference material, but still remain confidential

A1 Standish, P. N., 1987, *Rapid Face Bolting Interim Report No. 1, Proposed Trial systems*, Department of Civil and Mining Engineering, The University of Wollongong.

A2 Standish, P. N., 1988, *Rapid Face Bolting, Interim Report No. 2, Trial Systems Performance, and Prototype Directions*, Mining Research Centre, The University of Wollongong.

A3 Standish, P. N., 1988, *Rapid Face Bolting, Interim Report No. 3, Prototype Preparations and Completion Directions*, Mining Research Centre, The University of Wollongong.

A4 Standish, P. N., 1989, *Rapid Face Bolting, Interim Report No. 4*, Mining Research Centre, The University of Wollongong.

A5 Upfold, R. W., Standish, P. N., 1989, Stress and Failure Pattern Analysis of Seco Ten Roof Bits, *Contract Report for Sandvik Aust. P/L (Order No. 18790)*, Mining Research Centre, The University of Wollongong.